

# **INVESTIGATION OF SUBSTITUTED THIAZOLIDINEDIONES AS CORROSION INHIBITORS ON DIFFERENT METALS IN ACIDIC MEDIA**

**TSHIKHUDO FULUFHELO**

**(14001862)**

A dissertation submitted in the fulfilment of the requirements of the Master of Science in  
the

**Department of Chemistry**

School of Mathematical and Natural Science

**University of Venda**

Supervisor: Dr L.C Murulana, PhD

Co-supervisor: Dr S.S Mnyakeni-Moleele, PhD

**March 2021**

## DECLARATION

I hereby declare that the work in this dissertation is my own with the assistant of my supervisor Dr. Lutendo Chester Murulana and Dr. Simon Mnyakeni-Moleele as my co-supervisor. The information derived from the literature has been duly acknowledged in the text and a list of references provided. This work is being submitted for the qualification of master's in chemistry at the University of Venda and has not been submitted before for any degree or examination at any university.

Signature:  \_\_\_\_\_

Date: 16 March 2023

# TABLE OF CONTENTS


<u>Contents</u>	<u>Pages</u>
DECLARATION.....	i
ACKNOWLEDGEMENTS.....	v
ABSTRACT .....	vi
LIST OF ABBREVIATIONS .....	vii
LIST OF FIGURES.....	viii
LIST OF TABLES .....	xiii
LIST OF SCHEMES .....	xv
<b>CHAPTER 1</b> .....	<b>1</b>
<b>INTRODUCTION</b> .....	<b>1</b>
1.1. Introduction .....	2
2.1. Significance of the study .....	4
2.2. Aims and objectives of the study.....	4
<b>CHAPTER 2</b> .....	<b>6</b>
<b>LITERATURE REVIEW</b> .....	<b>6</b>
2.1. Definition of corrosion .....	7
2.2. Theory of corrosion .....	7
2.2.1. Acid theory .....	7
2.2.2. Chemical theory .....	7
2.2.3. Wet or electrochemical theory of corrosion .....	8
2.3. Types of corrosion .....	10
2.3.1. General corrosion.....	10
2.3.2. Localized corrosion .....	13
2.4. Cost and consequences of corrosion.....	15
2.4. Rate of corrosion and factors that affect the rate of corrosion .....	16
2.4.1. Rate of corrosion .....	16

2.4.2. Factors that affect the rate of corrosion.....	17
2.5. Corrosion of metals.....	19
2.5.1. Aluminum metal.....	19
2.5.2. Zinc metal.....	19
2.6. Methods of corrosion protection.....	20
2.6.1. Coating the metal.....	20
2.6.2. Cathodic protection.....	21
2.6.3. Corrosion inhibitors.....	22
2.7. Organic compounds used as corrosion inhibitors.....	24
2.8. Thiazolidinediones (TZD).....	25
<b>CHAPTER 3.....</b>	<b>27</b>
<b>Experimental Procedures:.....</b>	<b>27</b>
3.1. Introduction.....	28
3.2. Synthesis procedure of inhibitors.....	28
3.2.1. Synthesis of Thiazolidine-2,4-dione.....	28
3.2.2. Synthesis of ethyl (2,4-dioxo-1,3-thiazolidin-3-yl)acetate.....	29
3.2.4. Ethyl (2-(5-(benzo[d][1,3]dioxol-5-ylmethylene)-2,4-dioxothiazolidin-3-yl)acetyl)glycinate (EBDMDG).....	30
3.3. Preparation of inhibitors.....	30
3.4. Metal specimen.....	31
3.5. Gravimetric analysis.....	31
3.4. Electrochemical studies.....	32
3.4.1. Potentiodynamic polarization (PDP).....	32
3.4.2. Electrochemical Impedance Spectroscopy (EIS).....	33
<b>CHAPTER 4.....</b>	<b>34</b>
<b>RESULTS AND DISCUSSION.....</b>	<b>34</b>
4.0. RESULTS AND DISCUSSION.....	35
4.1. Characterization of synthesized compounds.....	35

4.1.1. Synthesis of glitazone (2,4-thiazolidinediones).....	35
4.1.2. Synthesis of ethyl (2,4-dioxo-1,3-thiazolidin-3-yl) acetate. ....	37
4.1.3. Synthesis of ethyl 2-(5-(substituted benzylidene)-2,4- dioxothiazolidin-3-yl) acetates. ....	39
4.1.4. Ethyl 2-(2-(5-(Benzo[d][1,3] dioxol-5-ylmethylene)-2,4- dioxothiazolidin-3-yl)acetamido)acetate.....	49
4.2. Gravimetric Analysis .....	53
4.2.1. Effect of temperature.....	57
4.2.2. Effect of inhibitor concentration .....	64
4.2.3. Effects of molecular structures .....	69
4.3. Adsorption Isotherm and Thermodynamic Parameters for zinc and aluminium ...	72
4.4. Thermodynamic and a Kinetic models.....	79
4.4.1. Zinc metal.....	80
4.4.2. Aluminium metal.....	86
4.4. Electrochemical Impedance Spectroscopy (EIS) .....	91
4.5. Potentiodynamic Polarization (PDP) .....	104
CHAPTER 5 .....	111
CONCLUSIONS .....	111
5.1. Conclusions .....	112
5.2. RECOMMENDATIONS.....	113
REFERENCES.....	114

## ACKNOWLEDGEMENTS

Firstly, I would love to thank the giver of life (God) because if it was not for the strength and wisdom He gave me I don't think I would have completed this research.

I would also love to express my deepest appreciation and gratitude to my supervisor Dr. L.C Murulana, for achieving this outcome on my research. His support, **patience**  **guidance**, and inspiration throughout the research. Your words have successfully transformed me into a better person in life and also in academia, I am so grateful.

I would also like to thank my co-supervisor Dr. S.S Mnyakeni-Moleele who is also the head of the department of chemistry, for helping me with the synthesis and analysis of my compounds that I used in the research and his motivation.

I extend my gratitude to Mr. N.R Tshiluka for helping with the organic synthesis and his support throughout the research. He was so helpful, thank you.

This work would have adopted a different shape than it is if it was not for my colleagues, thank you for all the scientific discussions.

Finally, I would like to thank my lovely parents and my whole family at large for their support, understanding, and mostly their words of encouragements that gave me hope.

## ABSTRACT

This study is based on the synthesis of four Thiazolidinediones (TZD) derivatives which are Ethyl 2-(5-(4-methoxybenzylidene)-2,4-dioxothiazolidin-3-yl)acetate (EMDA), Ethyl 2-(5-(Benzo[d][1.3]dioxol-5-ylmethylene)-2,4-dioxothiazolidin-3-yl)acetate (EBMDA), Ethyl 2-(5-(substituted benzylidene)-2,4-dioxothiazolidin-3-yl) acetates (EBDA) and Ethyl 2-(2-(5-(Benzo[d][1.3]dioxol-5-ylmethylene)-2,4-dioxothiazolidin-3-yl)acetamido)glycinate (EBDMDG) as corrosion inhibitors for two different metals (zinc and aluminium) in 1.5M hydrochloric acid solution at various temperatures. The corrosion inhibition characteristics including corrosion inhibition efficiencies and inhibitor-metal adsorption/desorption behaviour were studied using electrochemical impedance spectroscopy, potentiodynamic polarization, and gravimetric analysis. The results obtained from the gravimetric analysis indicate that the corrosion inhibition efficiency of zinc and aluminium metal in an acidic environment increased with an increase in the concentration of the inhibitors. The inhibition efficiency of EBMDA, EBDA, and EBDMDG inhibitors for zinc metal is directly proportional to temperature whereas inhibition efficiency for aluminium metal is inversely proportional. The inhibition efficiency of EMDA inhibitor for zinc is inversely proportional to temperature and directly proportional to temperature for aluminium metal. Both inhibitors obeyed Langmuir adsorption.

Electrochemical studies have been carried out using PDP and EIS. PDP was used to obtain corrosion parameters while EIS was applied to determine the charge transfer during corrosion. The result indicates that all four compounds are mixed type inhibitors also when the concentration of inhibitor increase the charge transfer resistance during corrosion increased.

Keywords: Thiazolidinedione, Corrosion inhibition efficiency, electrochemical.

## LIST OF ABBREVIATIONS

Abbreviations	Full name
HCl	Hydrochloric acid
Zn	Zinc
Al	Aluminium
TZD	Thiazolidinediones
EMDA	Ethyl 2-(5-(4- methoxybenzylidene)-2,4-dioxothiazolidin-3-yl) acetate.
EBMDA	Ethyl 2-(5-(Benzo[d][1,3] dioxol-5 ylmethylene)-2,4dioxothiazolidin-3-yl) acetate
EBDA	Ethyl 2-(5(substituted benzylidene)-2,4-dioxothiazolidin-3-yl)acetates
EBDMDG	Ethyl 2-(2-(5-(Benzo[d][1,3] dioxol-5-ylmethylene)-2,4- dioxothiazolidin-3-yl)acetamido)glycinate.
CR	Corrosion rate
IE	Inhibition efficiency
FT-IR	Fourier transform infrared
NMR	Nuclear magnetic resonance
DMSO	Dimethyl <b>Suphoxide</b>
PDP	Pontentiodynamic Polaristion
EIS	Electrochemical Impedance Spectroscopy



## LIST OF FIGURES

<b>Figure 2. 1:</b> Galvanic corrosion of steel pipe connected to copper connecter .....	11
<b>Figure 2. 2:</b> Erosion corrosion inside the pipe. ....	12
<b>Figure 2. 3:</b> Stages of crevice corrosion .....	14
<b>Figure 2. 4:</b> Pit Propagation due to Particle Deposition. ....	15
<b>Figure 2. 5:</b> Iron protected with ICCP .....	21
<b>Figure 2. 6:</b> Iron protected with SACP .....	22
<b>Figure 2. 7:</b> Classification of inhibitors .....	23
<b>Figure 2. 8:</b> Thiazolidinediones.....	25
<b>Figure 2. 9:</b> Rosiglitazone/Pioglitazone .....	25
<b>Figure 4. 1:</b> <sup>13</sup> C NMR spectra of synthesized Glitazone .....	35
<b>Figure 4. 2:</b> <sup>1</sup> H NMR spectra of synthesized glitazone .....	36
<b>Figure 4. 3:</b> <sup>13</sup> C NMR spectra of synthesis of ethyl (2,4-dioxo-1,3-thiazolidin-3-yl) acetate .....	37
<b>Figure 4. 4:</b> <sup>1</sup> H NMR spectra of ethyl (2,4-dioxo-1,3-thiazolidin-3-yl) acetate .....	38
<b>Figure 4. 5:</b> <sup>1</sup> H NMR spectra (aliphatic expansion) of Ethyl 2-(5(substituted benzylidene)-2,4-dioxothiazolidin-3-yl)acetates.....	40
<b>Figure 4. 6:</b> <sup>1</sup> H NMR spectra (aromatic expansion) of Ethyl 2-(5(substituted benzylidene)-2,4-dioxothiazolidin-3-yl)acetates.....	41
<b>Figure 4. 7:</b> <sup>13</sup> C NMR spectra of Ethyl 2-(5(substituted benzylidene)-2,4-dioxothiazolidin-3-yl)acetates.....	41
<b>Figure 4. 8:</b> IR spectrum of ethyl 2-(5(substituted benzylidene)-2,4-dioxothiazolidin-3-yl)acetates.....	42
<b>Figure 4. 9:</b> <sup>1</sup> H NMR spectra (aliphatic expansion) of Ethyl 2-(5-(Benzo[d][1,3] dioxol-5-ylmethylene)-2,4dioxothiazolidin-3-yl) acetate. ....	43
<b>Figure 4. 10:</b> <sup>1</sup> H NMR spectra (aromatic expansion) of Ethyl 2-(5-(Benzo[d][1,3] dioxol-5-ylmethylene)-2,4dioxothiazolidin-3-yl) acetate. ....	44
<b>Figure 4. 11:</b> <sup>13</sup> C NMR spectra of Ethyl 2-(5-(Benzo[d][1,3] dioxol-5-ylmethylene)-2,4dioxothiazolidin-3-yl) acetate.....	44
<b>Figure 4. 12:</b> IR spectra of Ethyl 2-(5-(Benzo[d][1,3] dioxol-5-ylmethylene)-2,4dioxothiazolidin-3-yl) acetate.....	45

<b>Figure 4. 13:</b> <sup>1</sup> H NMR spectra of ethyl 2-(5-(4- methoxybenzylidene)-2,4-dioxothiazolidin-3-yl) acetate. ....	46
<b>Figure 4. 14:</b> <sup>1</sup> H NMR spectra of ethyl 2-(5-(4- methoxybenzylidene)-2,4-dioxothiazolidin-3-yl) acetate. ....	47
<b>Figure 4. 15:</b> <sup>13</sup> C NMR spectra of ethyl 2-(5-(4- methoxybenzylidene)-2,4-dioxothiazolidin-3-yl) acetate.....	47
<b>Figure 4. 16:</b> FT-IR spectra of ethyl 2-(5-(4- methoxybenzylidene)-2,4-dioxothiazolidin-3-yl) acetate.....	48
<b>Figure 4. 17:</b> <sup>1</sup> H NMR spectra of Ethyl 2-(2-(5-(Benzo[d][1,3] dioxol-5-ylmethylene)-2,4-dioxothiazolidin-3-yl)acetamido)acetate. ....	49
<b>Figure 4. 18:</b> <sup>1</sup> H NMR spectra ( aromatic expansion) of Ethyl 2-(2-(5-(Benzo[d][1,3] dioxol-5-ylmethylene)-2,4- dioxothiazolidin-3-yl)acetamido)acetate.....	50
<b>Figure 4.19:</b> <sup>13</sup> C NMR spectrum of Ethyl 2-(2-(5-(Benzo[d][1,3] dioxol-5-acetate.ylmethylene)-2,4- dioxothiazolidin-3-yl)acetamido).....	50
<b>Figure 4. 20:</b> FT-IR spectra of Ethyl 2-(2-(5-(Benzo[d][1,3] dioxol-5-ylmethylene)-2,4-dioxothiazolidin-3-yl)acetamido)acetate. ....	51
<b>Figure 4.21:</b> The graph of inhibition efficiency using EMDA at different temperature ....	64
<b>Figure 4.22:</b> The graph of inhibition efficiency using EBMDA at different temperature ..	65
<b>Figure 4.23:</b> Graph of inhibition efficiency using EBDA at different temperature .....	65
<b>Figure 4.24:</b> Graph of inhibition efficiency using EBDMDG at different temperature .....	66
<b>Figure 4.25:</b> The graph of inhibition efficiency on aluminium using EMDA at different temperatures. ....	67
<b>Figure 4.26:</b> The graph of inhibition efficiency on aluminium using EBMDA at different temperatures. ....	67
<b>Figure 4.27:</b> The graph of inhibition efficiency on aluminium using EBDA at different temperatures. ....	68
<b>Figure 4.28:</b> The graph of inhibition efficiency on aluminium using EBDA at different temperatures. ....	68
<b>Figure 4. 29:</b> Graph of inhibition efficiency using EMDA and EBMDA as a corrosion inhibitor at 60°C. ....	71
<b>Figure 4. 30:</b> Graph of inhibition efficiency on aluminium metal using EMDA and EBMDA inhibitor at 60°C .....	71
<b>Figure 4.31:</b> Graph of inhibition efficiency on zinc metal using EBDA and EBDMDG inhibitor at 60°C. ....	71

**Figure 4.32:** Graph of inhibition efficiency on aluminium metal EBDA and EBDMDG inhibitor at 60°C.....72

**Figure 4. 33:** Langmuir adsorption isotherm for the adsorption of EMDA on zinc metal. ....74

**Figure 4. 34:** Langmuir adsorption isotherm for the adsorption of EBMDA on zinc metal. ....74

**Figure 4. 35:** Langmuir adsorption isotherm for the adsorption of EBDA on zinc metal.75

**Figure 4. 36:** Langmuir adsorption isotherm for the adsorption of EBDMDG on zinc metal. ....75

**Figure 4. 37:** Langmuir adsorption isotherm for the adsorption of EMDA on aluminium metal. ....77

**Figure 4. 38:** Langmuir adsorption isotherm for the adsorption of EBMDA on aluminium metal. ....77

**Figure 4. 39:** Langmuir adsorption isotherm for the adsorption of EBDA on aluminium metal. ....78

**Figure 4. 40:** Langmuir adsorption isotherm for the adsorption of EBDMDG on aluminium metal. ....78

**Figure 4. 41:** Arrhenius plots for zinc metal corrosion in 1.5 M HCl solution in the absence and presence of a different concentration of EMDA as an inhibitor.....81

**Figure 4. 42:** Arrhenius plots for zinc metal corrosion in 1.5 M HCl solution in the absence and presence of a different concentration of EBMDA as an inhibitor .....81

**Figure 4. 43:** Arrhenius plots for zinc metal corrosion in 1.5 M HCl solution in the absence and presence of a different concentration of EBDA as an inhibitor .....81

**Figure 4. 44:** Arrhenius plots for zinc metal corrosion in 1.5 M HCl solution in the absence and presence of a different concentration of EBDMDG as an inhibitor .....82

**Figure 4. 45:** Transition state plots at different concentration of EMDA .....84

**Figure 4. 46:** Transition state plots at different concentration of EBMDA .....84

**Figure 4. 47:** Transition state plots at different concentration of EBDA .....85

**Figure 4. 48:** Transition state plots at different concentration of EBDMDG .....85

**Figure 4. 49:** Arrhenius plots for aluminium metal corrosion in 1.5 M HCl solution in the absence and presence of a different concentration of EMDA as an inhibitor .....86

**Figure 4. 50:** Arrhenius plots for aluminium metal corrosion in 1.5 M HCl solution in the absence and presence of a different concentration of EBMDA as an inhibitor.....87

**Figure 4. 51:** Arrhenius plots for aluminium metal corrosion in 1.5 M HCl solution in the absence and presence of a different concentration of EBDA as an inhibitor .....87

<b>Figure 4. 52:</b> Arrhenius plots for aluminium metal corrosion in 1.5 M HCl solution in the absence and presence of a different concentration of EBDMDG as an inhibitor .....	88
<b>Figure 4. 53:</b> Transition state plots at different concentration of EMDA.....	89
<b>Figure 4. 54:</b> Transition state plots at different concentration of EBMDA .....	90
<b>Figure 4. 55:</b> Transition state plots at different concentration of EBDA .....	90
<b>Figure 4. 56:</b> Transition state plots at different concentration of EBDMDG .....	91
<b>Figure 4. 57:</b> Nyquist plot of zinc in 1.5M HCl in the absence and presence of different concentrations of EMDA.....	92
<b>Figure 4. 58:</b> Bode plots of mild steel in 1.5M HCl in the absence and presence of different concentrations of EMDA.....	92
<b>Figure 4. 59:</b> Nyquist plot of zinc in 1.5M HCl in the absence and presence of different concentrations of EBMDA .....	93
<b>Figure 4. 60:</b> Bode plots of mild steel in 1.5M HCl in the absence and presence of different concentrations of EBMDA .....	93
<b>Figure 4. 61:</b> Nyquist plot of zinc in 1.5M HCl in the absence and presence of different concentrations of EBDA .....	94
<b>Figure 4. 62:</b> Bode plots of mild steel in 1.5M HCl in the absence and presence of different concentrations of EBDA .....	94
<b>Figure 4. 63:</b> Nyquist plot of zinc in 1.5M HCl in the absence and presence of different concentrations of EBDMDG .....	95
<b>Figure 4. 64:</b> Bode plots of mild steel in 1.5M HCl in the absence and presence of different concentrations of EBDMDG. ....	95
<b>Figure 4. 65:</b> Nyquist plot of zinc in 1.5M HCl in the absence and presence of different concentrations of EBDMDG. ....	96
<b>Figure 4. 66:</b> Bode plots of zinc in 1.5M HCl in the absence and presence of different concentrations of EBDMDG. ....	96
<b>Figure 4. 67:</b> Nyquist plot of aluminium in 1.5M HCl in the absence and presence of different concentrations of EMDA.....	97
<b>Figure 4. 68:</b> Bode plots of aluminium in 1.5M HCl in the absence and presence of different concentrations of EMDA.....	97
<b>Figure 4. 69:</b> Nyquist plot of aluminium in 1.5M HCl in the absence and presence of different concentrations of EBMDA. ....	98
<b>Figure 4. 70:</b> Bode plots of aluminium in 1.5M HCl in the absence and presence of different concentrations of EBMDA. ....	98

<b>Figure 4. 71:</b> Nyquist plot of aluminium in 1.5M HCl in the absence and presence of different concentrations of EBDA. ....	99
<b>Figure 4. 72:</b> Bode plots of aluminium in 1.5M HCl in the absence and presence of different concentrations of EBDA. ....	99
<b>Figure 4. 73:</b> Nyquist plot of aluminium in 1.5M HCl in the absence and presence of different concentrations of EBDMDG. ....	100
<b>Figure 4. 74:</b> Bode plots of aluminium in 1.5M HCl in the absence and presence of different concentrations of EBDMDG. ....	100
<b>Figure 4. 75:</b> Equivalent circuit used to fit the impedance spectra obtained for zinc corrosion in 1.5 M HCl in the absence and presence of EMDA, EBMDA, and EBDMDG. ....	101
<b>Figure 4. 76:</b> Equivalent circuit used to fit the impedance spectra obtained for zinc corrosion in 1.5 M HCl in the presence of EBDA.....	101
<b>Figure 4. 77:</b> Equivalent circuit used to fit the impedance spectra obtained for aluminium corrosion in 1.5 M HCl in the absence of inhibitor. ....	101
<b>Figure 4. 78:</b> Equivalent circuit used to fit the impedance spectra obtained for aluminium corrosion in 1.5 M HCl in the presence of inhibitors. ....	102
<b>Figure 4. 79:</b> Tafel plots for zinc in 1.5 M HCl in the absence and presence of different concentrations of EMDA.....	104
<b>Figure 4. 80:</b> Tafel plots for zinc in 1.5 M HCl in the absence and presence of different concentrations of EBMDA .....	105
<b>Figure 4. 81:</b> Tafel plots for zinc in 1.5 M HCl in the absence and presence of different concentrations of EBDA .....	105
<b>Figure 4. 82:</b> Tafel plots for zinc in 1.5 M HCl in the absence and presence of different concentrations of EBDMDG .....	105
<b>Figure 4. 83:</b> Tafel plots for aluminium in 1.5 M HCl in the absence and presence of different concentrations of EMDA.....	106
<b>Figure 4. 84:</b> Tafel plots for aluminium in 1.5 M HCl in the absence and presence of different concentrations of EBMDA .....	106
<b>Figure 4. 85:</b> Tafel plots for aluminium in 1.5 M HCl in the absence and presence of different concentrations of EBDA .....	107
<b>Figure 4. 86:</b> Tafel plots for aluminium in 1.5 M HCl in the absence and presence of different concentrations of EBDMDG .....	107

## LIST OF TABLES

<b>Table 4. 1:</b> Weight loss measurements on zinc metal in the presence of EMDA and EBMDA as the corrosion inhibitor.....	53
<b>Table 4. 2:</b> Weight loss measurements on zinc metal in the presence of EBDA and EBDMDG as the corrosion inhibitor.....	54
<b>Table 4. 3:</b> Weight loss measurements on aluminium metal in the presence of EMDA and EBMDA as the corrosion inhibitor. ....	55
<b>Table 4. 4:</b> Weight loss measurements on aluminium metal in the presence of EBDA and EBDMDG as the corrosion inhibitor.....	56
<b>Table 4. 5:</b> Corrosion parameters for zinc in an aqueous solution of 1.5M HCl in the absence and presence of different concentrations of EMDA and EBMDA from weight loss of different temperature: .....	58
<b>Table 4.6:</b> The corrosion parameters for zinc in an aqueous solution of .5M HCl in the absence and presence of different concentrations of EBDA and EBDMDG from weight loss at different temperatures.....	59
<b>Table 4. 7:</b> Corrosion parameters for aluminium in an aqueous solution of 1.5M HCl in the absence and presence of different concentrations of EMDA and EBMDA from weight loss of different temperature .....	61
<b>Table 4. 8:</b> Corrosion parameters for aluminium in an aqueous solution of 1.5M HCl in the absence and presence of different concentrations of EBDA and EBDMDG from weight loss of different temperature.....	62
<b>Table 4. 9:</b> The abbreviations and molecular structures of the acetate and glycinate compounds.....	69
<b>Table 4. 10:</b> Adsorption parameters from Langmuir Adsorption Isotherm plots for EMDA, EBMDA, EBDA, and EBDMDG on Zinc metal.....	76
<b>Table 4. 11:</b> Adsorption parameters from Langmuir Adsorption Isotherm plots for EMDA, EBMDA, EBDA, and EBDMDG on Aluminium metal.....	79
<b>Table 4.12:</b> Arrhenius and transition parameters for the adsorption of different concentration of EMDA, EBMDA, EBDA, and EBDMDG in 1.5M HCl on zinc metal.....	83
<b>Table 4.13:</b> Arrhenius and transition parameters for the adsorption of different concentrations of EMDA, EBMDA, EBDA and EBDMDG in 1.5M HCl on aluminium metal. ....	88
<b>Table 4. 14:</b> Corrosion inhibition efficiencies calculated from EIS data for zinc. ....	102
<b>Table 4. 15:</b> Corrosion inhibition efficiencies calculated from EIS data for aluminium. ....	103

**Table 4. 16:** Potentiodynamic polarization (PDP) parameters such as corrosion potential ( $E_{\text{corr}}$ ), corrosion current density ( $i_{\text{corr}}$ ), and anodic and cathodic Tafel slopes ( $b_a$  and  $b_c$ ) using different inhibitors on zinc metal. ....108

**Table 4. 17:** Potentiodynamic polarization (PDP) parameters such as corrosion potential ( $E_{\text{corr}}$ ), corrosion current density ( $i_{\text{corr}}$ ), and anodic and cathodic Tafel slopes ( $b_a$  and  $b_c$ ) using different inhibitors on Aluminium metal. ....109

## LIST OF SCHEMES

<b>Scheme 1:</b> Synthesis of thiazolidine-2,4-dione/glitazone:.....	35
<b>Scheme 2:</b> Synthesis of ethyl (2,4-dioxo-1,3-thiazolidin-3-yl) acetate:.....	37
<b>Scheme 3:</b> synthesis of acetates. ....	39
<b>Scheme 4:</b> Synthesis of ethyl 2-(5(substituted benzylidene)-2,4-dioxothiazolidin-3-yl)acetates:.....	40
<b>Scheme 5:</b> synthesis of Ethyl 2-(5-(Benzo[d][1,3] dioxol-5-ylmethylene)-2,4dioxothiazolidin-3-yl) acetate:.....	43
<b>Scheme 6:</b> Synthesis of ethyl 2-(5-(4- methoxybenzylidene)-2,4-dioxothiazolidin-3-yl) acetate. ....	46
<b>Scheme 7:</b> Ethyl 2-(2-(5-(Benzo[d][1,3] dioxol-5-ylmethylene)-2,4- dioxothiazolidin-3-yl)acetamido)glycinate.....	49



# CHAPTER 1

## INTRODUCTION

## 1.1. Introduction

All that encompasses this world is in a chemical shape and is composed of a common or manufactured chemical compound. A few compounds are intense; a few of them are less stable. All those chemical compounds experience the interaction with the environment which at that point influences the execution of the structure, counting unwavering quality over time that falls beneath the common heading of corrosion<sup>1</sup>. When items are made out of zinc, aluminum, or other metals, it is normal for them to return to their unique state. Since corrosion may be a normal activity, metals began to discharge vitality by responding with oxygen<sup>2</sup>.

Numerous metals like zinc, mild steel, aluminum, etc., are utilized broadly in industry, owing to their amazing thermal conductivity and mechanical properties. All things considered, these metals respond rapidly with their encompassing situations containing oxygen. Acidic arrangements are broadly utilized for different purposes like corrosive pickling, mechanical corrosive cleaning, acid-descaling, and oiler; such acids tend to make contact with metals, and as result metals are vulnerable to corrode<sup>3</sup>. Corrosion within the agriculture industry is caused by chemicals that are utilized in cultivating fertilizer, grain, and silage additive chemicals for weed control and restrictive corrosive arrangement for cleaning acids<sup>4,5</sup>.

The chemicals which cause corrosion are the ones which are connected through the soil or flounder showering for plant development. If the chloride ions are present in the process of ammonia or hydrogen sulphide when the fertilizers decomposed, they lead to an increase of corrosion via hydrolysis acids<sup>5</sup>. The corrosion wonder impacts our society every day; it has various consequences on industrial components such as automobiles, foundation, electric appliances, and vitality dispersion frameworks. The corrosion of such components influences the economy and the environment.

Corrosion forms consume billions of Rands every year in upkeep and repair. In 2016, a study conducted by the National Association of Corrosion Engineers (NACE) and sketched out in their distribution “the International Measures of Prevention, Application, and Economics of Corrosion Technology (IMPACT),” appears that corrosion incites a worldwide taken toll of \$US 2.5 trillion dollars which is identical to 3.4%<sup>6</sup>. While the direct cost of corrosion is assessed to be around R130-billion in South Africa<sup>7</sup>.

Corrosion is made up of chemical reactions and may occur through many different mechanisms that depend on the environment and its surrounding. This gives rise to the various classifications of corrosion, such as atmospheric, galvanic, uniform, erosion-corrosion, etc<sup>8</sup>. Corrosion is not something new or something that can be eliminated from occurring since it occurs naturally. However, it is possible to manage corrosion using different techniques such as anodizing, painting, conversion coating, and corrosion inhibitors for the equipment to perform their required tasks successfully for the estimated period that they were constructed for. The use of inhibitors has become one of the most economical and practical methods of reducing corrosive attacks on metal<sup>9,10</sup>.

It was evaluated that the request for corrosion inhibitors in the U.S. assessed that rise 4.1% p.a. to USD\$ 2.5 billion in 2017. In 2012, it was moreover assessed that the showcase request of inhibitors was isolated on 26.6% to refining petroleum, 16.9% utilities, 16.7% for gas and oil generation, 15.3% chemical, 9.5% metals, 7.1% mash and paper, and 8.0% other<sup>11</sup>. Corrosion inhibitors are chemical compounds made of a particular frame of substance (such as a natural compound). To get a handle on the component included between a metal and an Inhibitor, a few components must be taken into thought.

Such components incorporate the thought of the geometric (size, shape etc.) additionally the electronic properties of the compound when selecting a fitting corrosion inhibitor compound. Reason being that these variables impact the control of the compound to cover up the metal surface and its capacity to respond with the metal surface<sup>12,13</sup>. Other considers appeared that the best compounds are the one with planar geometry than the one with less planar geometry. The inclination of planar geometry compounds is since they have the propensity to have more particles in-tuned with the metal surface. The electronic properties are impacted by the kind of utilitarian gathering the compound has<sup>14</sup>.

The ideal corrosion inhibitors are compounds with utilitarian bunches containing high electron density, since the adsorption handle between corrosion inhibitor on the metal surface requires the electrons that are given from inhibitors to the mostly filled of the metal surface shaping the bond between metal and inhibitor. Inhibitors that comprise heteroatoms (such as O, S, N, etc.), as well as a fragrant ring in their structures, are moreover favoured as corrosion inhibitors<sup>15</sup>.

## 2.1. Significance of the study

Corrosion is the major issue that causes the disappointments of development structures (building, bridge, and pipeline) which are exceptionally vital in our lives. This comes about in challenges with the metals which don't stay in their unique state after they are uncovered to the atmospheric environment. These metals cannot stand up to the assaults by different acids and bases as corrosion happens normally. When the human body is influenced by the malady such as cancer if the illness isn't controlled it spread quickly and the individual passes on after a few times.

Essentially, when metals are influenced by corrosion, the building may collapse with time, in case corrosion isn't controlled within the starting. Be that as it may, corrosion will be overseen for types of gear to perform their required errands effectively for an anticipated length of time. This could be accomplished utilizing corrosion inhibitors and other diverse methods<sup>16</sup>. This extend is of fundamental significance since of the effect that corrosion has on the worldwide economy, with the reports from the corrosion organized of Southern Africa appearing that the evaluated fetched of corrosion is roughly R154 billion per annum<sup>7</sup>. Therefore, using inhibitors will diminish the rate at which corrosion takes put, coming about within the decrease of misfortune due to corrosion the economy of a nation.

Corrosion too influences the wellbeing of human creatures. For occasion, iron can be changed into an iron oxide that's harmful and unsafe towards human creatures. By ensuring the fabric from rusting, numerous lives will be spared<sup>17,18</sup>. For civil and structural engineers, in case appropriate corrosion control measures are not carried out on buildings, bridges, gear, and pipelines. A few harms may happen due to corrosion in this way utilizing corrosion inhibitors is prescribed to dodge having corroded structures, which is able at that point decreased the taken a toll that can be brought about from supplanting the corroded structures<sup>19</sup>.

## 2.2. Aims and objectives of the study

The study aims are to investigate the inhibiting behavior of thiazolidinediones (TZD) derivatives on corrosion of zinc and aluminium metals in 1.5M of hydrochloric acid.

**The specific objectives are to:**

- Synthesize three series of TZD (acetates, glycinate, alaninates).

- Purify the synthesized compounds, using column chromatography and other purification techniques.
- Characterize the final target compound using NMR, FTIR spectroscopy techniques.
- Evaluate inhibition efficiency of inhibitor on zinc and aluminum within the aggressive aqueous environment by gravimetric weight loss analysis at different temperatures, the concentration of the inhibitor, and the time of exposure.
- Investigate the inhibition efficiency of TZD derivatives compounds using thermodynamics, kinetics, and adsorption principles.
- Propose the possible inhibition mechanism type of adsorption, and the adsorption isotherm for corrosion inhibition.
- Study the inhibiting effect of the TZD compounds on the corrosion of zinc and aluminium metals in 1.5M hydrochloric acid solution using electrochemical techniques such as electrochemical impedance spectroscopy (EIS) and potentiodynamic polarization (PDP).

# CHAPTER 2

## LITERATURE REVIEW

## 2.1. Definition of corrosion

Corrosion is viewed as a rare universal occurrence, omnipresent, and omnipotent. Furthermore, it is within the water, soil, and in each environment. Everything that encompasses this world is in a chemical frame is composed of normal or manufactured chemical compounds<sup>20,21</sup>.

Corrosion brings an entire change within the properties of the material; therefore, corrosion is mentioned as an electrochemical process and chemical reaction. For instance, when mild steel metal is subjected to the interaction with the environment, mild steel changes entirely from its form to rust. Rust is the primary cause of corrosion<sup>22</sup>.

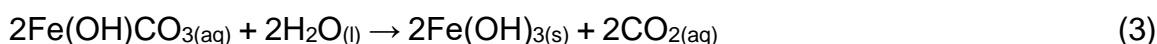
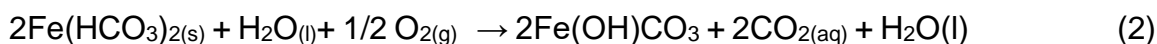
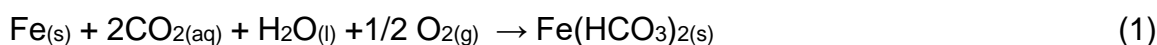
Corrosion can be define as the decomposition of materials by chemical associate with their environment. As corrosion occurs natural, metals return to their natural state; e.g., iron in the presence of moist air will revert to its natural state, iron oxide<sup>20</sup>.

## 2.2. Theory of corrosion

Acid theory, dry or chemical corrosion, and electrochemical or wet corrosion are three theories of corrosion.

### 2.2.1. Acid theory

Acid theory proposed corrosion of a metal (iron) happen due to the presence of acids around it. According to this theory, iron corrode by atmospheric carbon dioxide, moisture, and oxygen. The chemical reactions of this theory are given below:



The examination of rust that gives the test of  $\text{CO}_3^-$  ion is the supporting information of acid theory<sup>23</sup>.

### 2.2.2. Chemical theory

There are numerous chemical theories of corrosion on the surface of the metals one of them states that gasses like oxygen, incandescent light, oxides of sulphur oxides of nitrogen, hydrogen sulphide, and fumes of chemicals with the metal, has a direct

reaction influence on the surface of that metals. The fascination of chemical fondness of the metal towards receptive gas depends on the interface scope of corrosion of a specific metal. Among these gasses oxygen is the one which plays a major part for the corrosion of most metallic substance<sup>23,24</sup>. These theories mentioned above amongst them are liquid metal corrosion, oxidation corrosion and corrosion by other gases.

### **I. Liquid metal corrosion**

This sort of chemical hypothesis happens generally in a few businesses; liquid metal passes through metallic channels and corrosion is caused by disintegration or inside infiltration. For illustration, fluid metal mercury breaks up most metals by shaping amalgams, subsequently eroding the metal<sup>24</sup>.

### **II. Oxidation corrosion**

Oxidation corrosion occurs when metals directly reacting with oxygen in the absence of moisture. Alkali and alkaline earth metals form corresponding oxides when they react with oxygen<sup>23-25</sup>.

### **III. Corrosion by other gases (Cl<sub>2</sub>, SO<sub>2</sub>, H<sub>2</sub>S, NO<sub>x</sub>)**

These gases react with metal and form corrosion products in the dry atmosphere which may be protective or non-protective. Dry dichloride reacts with silver and forms silver chloride which is considered as a protective layer. Hydrogen sulphide (H<sub>2</sub>S) attacks steel forming ferrous sulphide scale which is porous and inhibits normal operations; this happens in petroleum industries at high temperatures<sup>26</sup>.

### **2.2.3. Wet or electrochemical theory of corrosion**

Wet theory corrosion it's a standard sort of corrosion metal in a watery environment. This sort of corrosion happens when the metal comes in reality with conducting fluid or when two distinctive metals are plunged in an arrangement. On the surface of the metal concurring to the electrochemical hypothesis, there is the arrangement of a galvanic cell, where metal in address acts as the node and for the most part loses useful steadiness. There are four prerequisites of electrochemical corrosion. When one of the underneath prerequisites is dispensed with, corrosion will not occur<sup>27</sup>.

- Oxidation half-reaction: it also known as an anodic electrode where corrosion process take place.



- Electrolyte connection between anode and cathode (wire, metal wall, etc.)
- Reduction half-reaction: it also known as cathode electrode where the corrosion process does not take place.
- Electrolyte (Soil, Water, Moisture, etc.)

The real truth that corrosion comprises of a least of one oxidation response and one lessening response that does not make a completely apparent because both reactions are usually joined in one piece of metal. For occurrence, when iron corrodes, iron particles embrace oxidation to make particles at that point provide absent electrons, whose negative charge would rapidly construct up inside the metal and halt further anodic response or corrosion. The method will as it has proceeded in case electrons discharged can pass to the location of the metal surface where a cathode response happen<sup>28</sup>.

At the cathode location, the electrons respond with a few reducible components of the electrolyte and are evacuated from the metal. Faraday's laws states that the rate of anode and cathode responses must be proportionate and is decided by corrosion current which is the whole stream of electrons from anodes to cathodes. Since anodic and cathode responses continue at the same time on the metal surface, the corroding piece of metal is described as a "mixed electrode" which may be a total electrochemical cell on the metal surface<sup>29</sup>. The most common and fundamental electrochemical responses amid the corrosions of the press are appeared in responses (4) to (7) below:

Iron is oxidized first into ferrous ions; this kind of reaction is known as an anodic reaction;



It can oxidize into ferric iron depending on the potential;



The main reaction at the cathode is hydrogen evolution which is reaction 6.



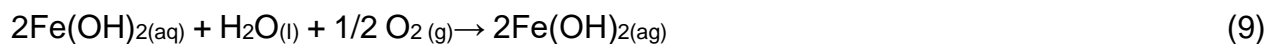
Oxygen reduction is the most important reaction, as shown in reaction (7). In this case, corrosion is usually accompanied by the formation of solid corrosion debris from the reaction between the anodic and cathodic products.



Pure iron (II) hydroxide is white in colour, because of partial oxidation in the air the material produced by corrosion is normally greenish in colour.



The reddish rust that eventually forms is a complex mixture whose form depends on other trace elements that are present. This is caused by further hydration and oxidation reaction occurrence. Because rust is precipitated, this becomes the result of secondary reactions, it is porous and absorbent and tends to act as sort of harmful poultice which encourages further corrosion<sup>23</sup>.



## 2.3. Types of corrosion

Corrosion consists of a series of usually complex chemical reactions and may be initiated by several different mechanisms that are dependent on the surrounding environment. This has given rise to the various classifications of corrosion. Corrosion can occur in two general ways, over the entire surface of the metal (Generalized Corrosion), or in local spots or areas (Localized Corrosion).

### 2.3.1. General corrosion

General corrosion also refers to as uniform attack corrosion, and general corrosion is the type of corrosion that is caused by a chemical or electrochemical reaction, where the entire exposed metal resulting in the deterioration<sup>30</sup>. However, the general corrosion is predictable and manageable is considered a safe form of corrosion. Some of the examples of general corrosion are shown below:

#### 2.3.1.1. Galvanic corrosion

Galvanic corrosion is additionally known as electrolysis, within the marine environment is considered one of the foremost common shapes of erosion. Galvanic corrosion includes two electrochemically heterogeneous metals and electrolytes to carry an

electric current<sup>31</sup>. The two distinctive metals in dampness make a cell, for a case, copper coupled with aluminum. The aluminum metal act as the anode whereas copper acts as a cathode.



From the condition underneath, it appears that amid galvanic erosion cathode is ensure from erosion because it can be seen by the item of response  $\text{Al}^{3+}$  and strong copper.



The quickened weakening of one metal characterizes this sort of erosion whereas others stay unaffected, as shown in figure 2.1. Since galvanic erosion included two electrochemically heterogeneous metals subsequently the rate of erosion at the anode is higher when the metals are encourage separated in a galvanic arrangement. For illustration, the erosion of tin joins with aluminum will be more as compared to copper connect with aluminum. Galvanic erosion can be anticipated by the electromotive constrain or standard potential arrangement for metal reduction<sup>31, 32</sup>.



**Figure 2. 1:** Galvanic corrosion of steel pipe connected to copper connector<sup>33</sup>

### 2.3.1.2. Erosion corrosion

Erosion corrosion occurs through the interaction of erosion and the corrosion process. Where erosion is the removal of a small number of materials due to the effects of particles on the surface<sup>34</sup>. Furthermore, after high mechanical interaction between the

surface and multiphase fluid passing across it, can be enough to cause a functional failure in other material like brittle their crack is formed by countless impacts.

When those cracks are joined together to allow the broken material to be removed. Erosion corrosion is classified as the 5<sup>th</sup> common degradation issue in fluid handling systems such as pumps, piping systems in offshore oil/gas facilities. Erosion corrosion is when the material is removed by the mechanical process of erosion coupled with the electrochemical process of corrosion. Erosion corrosion depends on the rate of the movement, abrasion that takes place<sup>35,36</sup>.



**Figure 2. 2:** Erosion corrosion inside the pipe<sup>33</sup>.

### **2.3.1.3. Intergranular corrosion**

Intergranular corrosion is the frame of corrosion that happens when metal from an anode pick up boundaries and the interior of the pick-up which acts as the cathode, this leads to the grains falling separated. Intergranular corrosion gets to be an issue with stainless steel. In stainless steel, this happens when metal is warmed at the next temperature which at that point causes chromium to respond with carbon and shape particles of chromium carbide at the grain boundaries. The grain boundaries now represent a path of high corrosion vulnerability<sup>37</sup>.

### 2.3.2. Localized corrosion

Localized corrosion refers to the hastened attack of passive metals in corrosive environments. It is characterized by an intense attack at confined areas on surface components, while the remaining area of the surface corrodes at a much slower rate.

This can be due to environmental effects or the component material's inherent properties, like in the creation of protective film oxide. In localized corrosion, the material's surface may be fundamentally under suitable corrosion control, with the corrosion confined at localized sites where the corrosion protection has stopped working<sup>38,39</sup>. Some examples of localized corrosion are shown below:

#### 2.3.2.1. Crevice corrosion

Crevice corrosion occurs on any metals and in any corrosive environment. However, metals that depend on their surface oxide film for corrosion resistance like aluminum and stainless steel are particularly prone to crevice corrosion, especially in an environment such as seawater that contains chloride ions. The oxygen level in the crevice is very low, while on the surface, it is much higher<sup>40</sup>.

Figure 2.3 illustrates the stages which happened in an oxygenated environment. Where there is a reduction of oxygen in the crevice which leads to the increase in acidity and anion content e.g.  $\text{Cl}^-$  of the crevice solution. After that, there's a permanent breakdown of the passive film and the initiation of rapid corrosion, final there is a spreading of a single chemical reaction of crevice corrosion<sup>32</sup>. Figure 2.4 illustrates the crevice corrosion of mild steel.

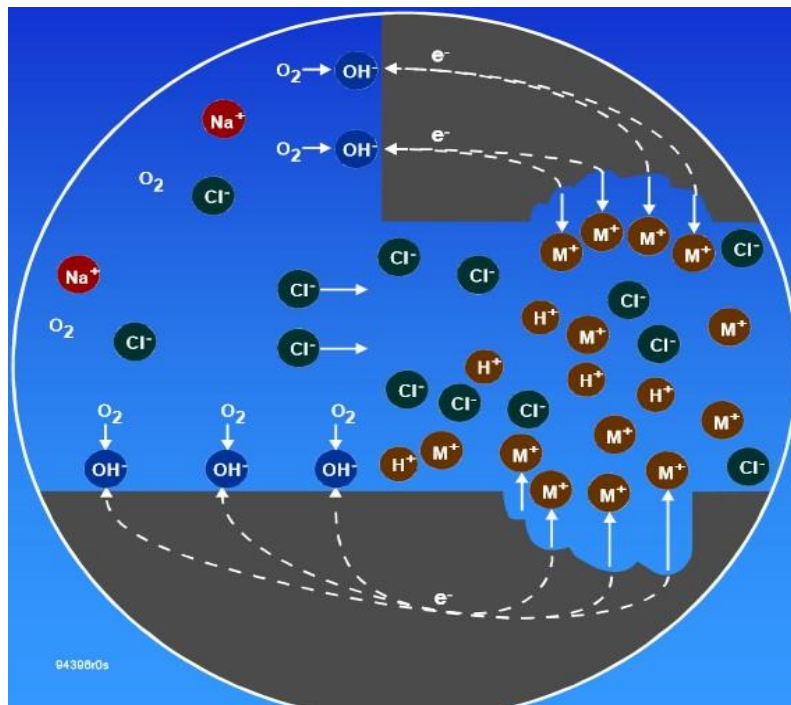


**Figure 2. 3:** Stages of crevice corrosion<sup>41</sup>

### 2.3.2.2. Pitting corrosion

The fact that a surface of metals appears “pitted” does not mean that the corrosion degradation mechanism is that of pitting corrosion. Pitting corrosion is like crevice corrosion, it creates small anodes that increase in size with further corrosion as is illustrated in figure 2.5. This type of corrosion is difficult to detect in the laboratory because they are tiny and it takes time for visual detection of pitting corrosion attack to depend primarily on the chloride content, the pH value, and the temperature<sup>35</sup>. Pitting corrosion is generally initiated due to some chemical or physical heterogeneity at the surface such as second phase particles, inclusions, flaws, mechanical damage, or dislocations. Pitting corrosion results in the breakdown of protecting film. This type of corrosion affects the integrity of many materials and structures in civil, nuclear, and aerospace engineering<sup>41,42</sup>.



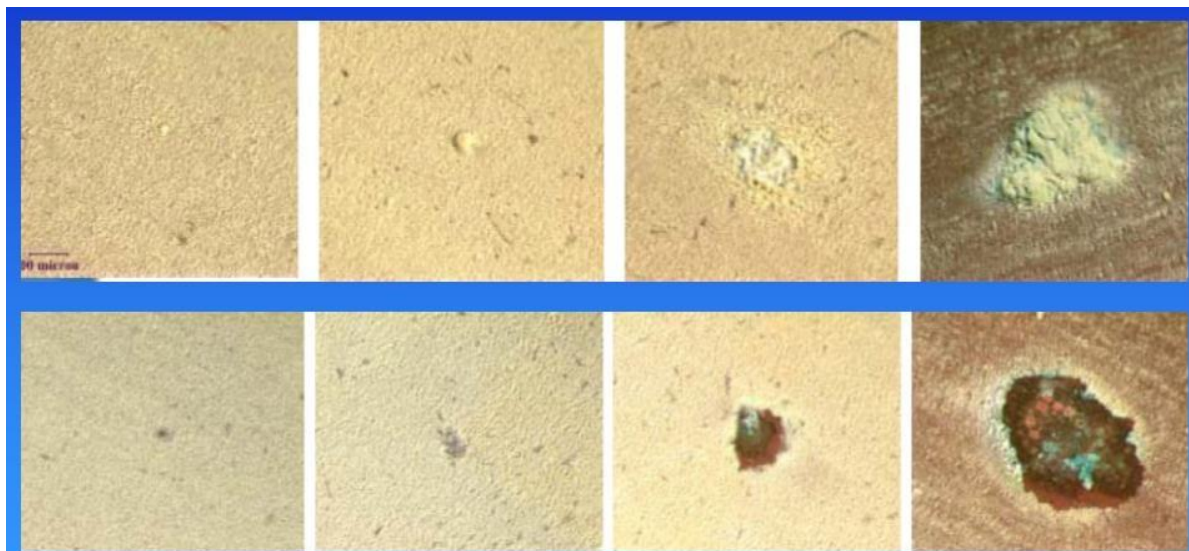


**Figure 2. 4:** Pit Propagation due to Particle Deposition<sup>41</sup>.

#### **2.4. Cost and consequences of corrosion**

Corrosion has a significant economic impact on the industry and the community. It is estimated that governments spend billions of dollars every year on repairing corrosion damages. Corrosion causes crashes of airplanes, bridges, and buildings collapse, and refineries and factories experience explosions. Half of all unplanned power outages are caused by corrosion according to the study conducted by the Electric power Research Institute of the US (EPRI). Studies in different countries indicated between 25% to 30% of water supply are lost in the supply chain due to corrosion<sup>43, 44</sup>.

According to the study that was conducted by Council for Mineral Technology (MINTEK) the economic loss of corrosion worldwide is estimated to be higher than the US \$1.8 trillion per year for American industry, while in South Africa, the direct cost of corrosion is estimated to be around R130 billion<sup>7</sup>. Economic losses are divided into direct losses and indirect losses below.

##### **Direct losses**

- Include the costs of replacing corroded structures and their components.
- Over design to allow for corrosion.
- Cost of anti-corrosive painting or other protection methods.
- The inability to use otherwise desirable materials.

## Indirect losses

- Loss of product.
- Contamination of the product.
- Loss of valuable product from a container that corroded.

Corrosion in buildings structures can diminish the overall value of various buildings because it can result in the thinning of metals used, leading to loss of mechanical strength, damages, and ultimately a failure and a collapsing bridge can have severe consequences for so many lives. For environmental damage, Corrosion also affects domestic water supplies. The chemical process slowly dissolves metal causing water supplies to deteriorate and fail. Corrosion often reduces water flow through supply lines and destroys water valves cause leaks inside and outside the valves. Fuel tanks and vessels can grave consequences on public health and the entire ecosystem<sup>45,46</sup>.

## 2.4. Rate of corrosion and factors that affect the rate of corrosion

### 2.4.1. Rate of corrosion

The rate of corrosion is the speed at which any given metal deteriorates in a specific environment. The rate of corrosion depends upon environmental conditions as well as the type and condition of the metal. To calculate the rate of corrosion, weight loss density, surface area, and time data must be collected. The rate of corrosion determines the maintenance requirement for structure<sup>47</sup>.

$$C_R = \frac{\Delta W}{St} \quad (13)$$

where:  $C_R$  = Corrosion rate ( $\text{g}\cdot\text{cm}^{-2}\cdot\text{h}^{-1}$ )

$W$  = Weight loss of metal (g)

$S$  = the total surface area ( $\text{cm}^2$ )

$t$  = the total immersion time (h)



The rate of corrosion can also be calculated using equation (14)

$$C_R = \frac{\Delta W}{PA t} \quad (14)$$

where:  $C_R$  = Corrosion rate ( $\text{g}\cdot\text{cm}^{-2}\cdot\text{h}^{-1}$ )

$W$  = is the total weight lost

$T$  = is the time taken for the loss of metal

$A$  = is the surface area of the exposed metal

$P$  = is the metal density ( $\text{g}/\text{cm}^{-3}$ )

#### **2.4.2. Factors that affect the rate of corrosion**

For corrosion to occur four elements (anode, cathode, metallic conductor, and electrolyte) are need to be present and are referred to as corrosion cells. The rate of corrosion is affected by the electrolyte change. Several factors influence the change of electrolyte which then affect the rate of corrosion including the nature of metal, the surface of the metal, nature of the corrosion product, pH of the medium, temperature, humidity, and polarization at the anodic and cathodic area<sup>48</sup>. Those factors are explained below.

##### **2.4.2.1. Nature of the metal**

Metals with high electrode potential do not corrode easily, which are noble metals like gold, platinum, and silver. Metals with lower electrode potentials undergo corrosion, for example, zinc, magnesium, aluminum. When two metals are associating with each other, the higher the difference in electrode potentials more enormous is the corrosion. For example, the potential difference between iron and copper is 0.78V which is more than that between iron and tin (0.3V). Therefore, iron corrodes faster when in contact with copper than that with tin<sup>48</sup>.

#### **2.4.2.2. The surface state of the metal**

The larger the surface area of the metal, the more will be the corrosion. The corrosion rate is very high when the metal has a small anode and large cathodic region. As the ratio decreases, the corrosion rate further increases. This is because the anode electrons are released. If the cathodic area is larger, the released electrons are rapidly consumed at the cathode. This further enhances the anodic reaction leading to an increase in the overall rate of corrosion<sup>49, 50</sup>.

#### **2.4.2.3. Nature of the corrosion product**

If the corrosion product is insoluble, stable, uniform, and nonporous, it acts as a protective film preventing any further corrosion by acting as a barrier between the metal surface and corrosion medium. If the corrosion product is unstable, porous, and soluble, it further enhances corrosion<sup>51, 52</sup>.

#### **2.4.2.4. The pH of the medium**

The pH is a measure of acidity or alkalinity on a scale of 1 to 14. There is a greater quantity of hydrogen ions than hydroxyl ions present in the solution when the environment is more acidic and the pH is closer to 1. When both hydrogen ions and hydrogen gas can diffuse very rapidly the steel tends to corrode faster. However, steel cannot corrode under alkaline conditions where there is an excess of hydroxyl ions and the pH tend towards 14<sup>53, 54</sup>.

#### **2.4.2.5. Temperature**

When temperature increases, the conductance of the aqueous medium increases; as a result, the rate of diffusion also increases, and this causes the rate of corrosion to increase because electrochemical reactions generally occur faster at high temperatures. The temperature increase adds energy to the reactions which then increases the rate of corrosion<sup>51, 55</sup>. This means corrosion proceeds faster in warmer environments than in cooler ones.

#### **2.4.2.6. Humidity**

Humidity and time-of-wetness play a large role in promoting and accelerating the corrosion rate. Humidity provides the conducting medium which helps in the formation of electrochemical cells on the surface of the metal. The metal corrodes faster in a

humid atmosphere than in dry air due to the presence of an electrochemical cell which the humidity forms<sup>56</sup>.

#### **2.4.2.7. Polarization at anodic and cathodic area**

The polarization of anodic and cathodic decreases the rate of corrosion. The metal that undergoes oxidation decrease the dissolution of metal. Because the anodic polarization takes place due to some reaction, the cathodic polarization decreases the cathodic reaction and then hindering the combination of the cathode reactant and the electron<sup>54</sup>.

### **2.5. Corrosion of metals**

This study is dealing with two metals (zinc and aluminum). Corrosion of zinc and aluminum was studied quite intensively in the 1970s and early 1980s. The studies were limited to the assessment of the hydrogen production potential in a case of a large pipe break, which formed the design basis for reactor containments<sup>57</sup>.

#### **2.5.1. Aluminum metal**

Aluminum is made from bauxite mineral that is mined from the earth to make usable aluminum. Because of aluminum characteristics which are (lightweight, strength, and corrosion resistance is due to the inert and protective character aluminum oxide film which forms on the metal surface<sup>58</sup>. The rate of corrosion of aluminum is reduced rapidly with time. The stability of the oxide film determines the corrosion resistance of the aluminum. Since the stability depends upon the pH of the environment, when the pH range below 4 acid dissolution yields  $Al^{3+}$  ions and when the pH is above 8 the alkaline dissolution leads to the formation of  $Al(OH)$  ions<sup>59,60</sup>.

#### **2.5.2. Zinc metal**

Zinc is a generous metal found in the earth's crust with a multitude of industrial and biological uses. Zinc is currently the fourth most important among metals in worldwide production and consumption after iron, aluminum, and copper. Zinc is also strong anti-corrosive properties and bonds well with other metals. Zinc is used in different categories such as zinc galvanizing which happened by adding a thin layer of zinc to iron to prevent rusting, the alloy is when zinc combines with copper and with other metals to form materials that are used in automobiles, electrical components, and

household fixtures. Zinc is also used in the production of zinc oxide which is used to protect skin ointment<sup>61</sup>.

Compared to mild steel zinc, suffer the slightest from corrosion due to the fact of forming insoluble basic carbonate. That layer has protective properties which then reduce the rate of corrosion. Zinc corrosion depends upon the type of environment. Zinc will exhibit active corrosion under acidic conditions ranging from reducing through highly oxidizing and in strongly acidic up through neutral environments<sup>62</sup>. Zinc also sustains an attack and forms soluble corrosion products under strongly alkaline conditions. Zinc resists corrosion in mildly alkaline conditions due to the formation of passive films. Zinc is not used for structural purposes under strongly acidic or strongly alkaline conditions<sup>63</sup>.

## **2.6. Methods of corrosion protection**

Several methods can be used to protect metals from corrosion. The type of methods to be used depends on different parameters such as the type of corrosion and the place where it occurs, amongst others. The following are some of the methods that can be used to control corrosion:

### **2.6.1. Coating the metal**

The selection of the coating process depends on several factors like the corrosion resistance that is required, the anticipated lifetime of the coated material, the number of parts being produced, the production rate that is needed, and the environmental considerations<sup>64</sup>. Metal coatings are applied by some of the following methods.

- **Dipping**

Dipping is carried out by saturating the metal on which the coating is to be applied. Furthermore, dipping is a continuous process as in the galvanizing steel sheet<sup>59</sup>.

- **Spraying**

Thermal spraying of the metal coating process occurs when a gun is used that simultaneously melts and propels small droplets of metal onto the surface to be coated. There are several types of spraying, and each contains three main variables including the temperature of the flame, the velocity of the particles that are sprayed onto the

substrate to form the coating, and the nature of the material that is to form the coating for example powder, wire, etc.<sup>65,66</sup>.

- **Cementation**

Cementation consists of tumbling the work in a mixture of metal powder and flux at elevated temperatures. Allowing the metal to diffuse into the base metal<sup>67</sup>.

### 2.6.2. Cathodic protection

Cathodic security control corrosion by constraining the potential to a negative locale where metal is altogether stable<sup>68</sup>. Corrosion is diminished drastically to zero in utilizing a remotely connected electric current. Awed current cathodic assurance (ICCP) and conciliatory anode are two sorts of cathodic protection. Impressed current cathodic render protection melts from erosion by interfacing the negative terminal of DC control source to the press structure, to total electrical circuit positive terminal which is connected to an assistant anode have to be included. Due to the voltage that is given from a DC source anode does not oxidize. For the most part, the ICCP is utilized on all pipelines because it isn't persistently monitored<sup>69</sup>.

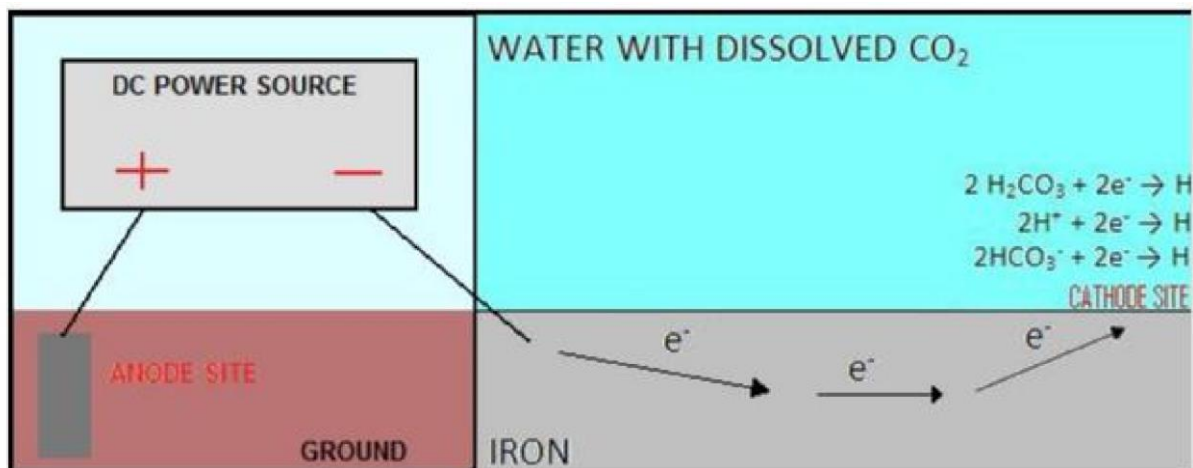


**Figure 2. 5:** Iron protected with ICCP <sup>70</sup>

Conciliatory anode cathodic assurance (SACP) is when both metals are associated with a framework and got a higher potential to cause oxidization sometime recently press. When those metals are associated to press structures, electrons will move from the conciliatory anode through the press structure and decrease location because it appeared in figure 2.7 below<sup>70</sup>. When the anode is utilized up the metal begins to erode,

that's why the conciliatory anode is utilized to ensure pipeline which is temporary or where there's no get to for a controlled supply.

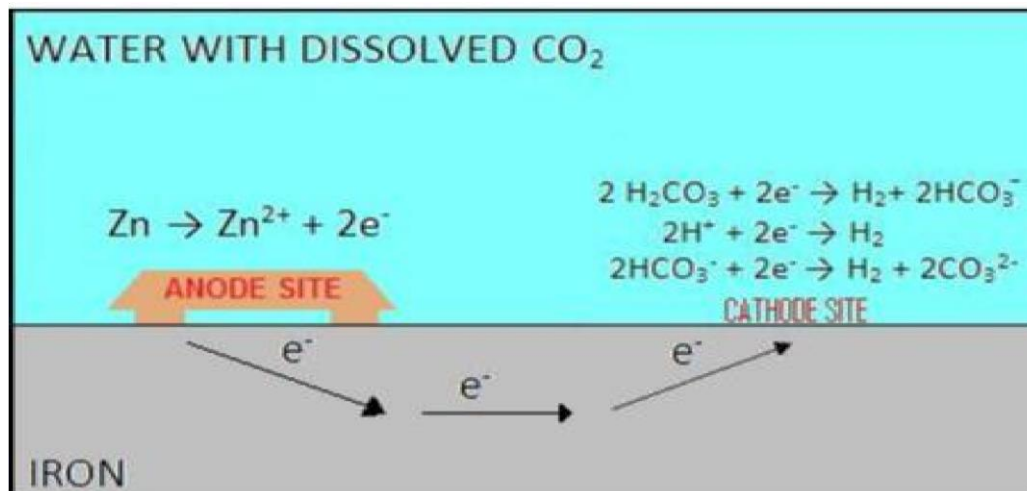


**Figure 2. 6:** Iron protected with SACP<sup>70</sup>

### 2.6.3. Corrosion inhibitors

Corrosion inhibitors are one of the foremost temperate and common-sense strategies of decreasing the destructive assault on the metals. Corrosion inhibitors moderate down the rate of corrosion by the addition of little concentration of the chemical compound to a destructive environment<sup>65</sup>. Corrosion Inhibitors cause the metal to make its defensive film of metal oxide by expanding resistance. Corrosion inhibitors are for the most part connected in the contribution of pipelines and vessels. Corrosion inhibitors can be chemicals either engineered or common a may well be classified by the chemical nature as either natural or inorganic. Component of activity of inhibitor can be anodic, cathodic, or an anodic-cathodic mix-type adsorption activity, or as oxidants or non-oxidant<sup>71</sup>. In common, inorganic inhibitors have a cathodic or anodic response. Natural inhibitors have both activities, cathodic and anodic, secure metal through the arrangement of an adsorption film<sup>46</sup>. Underneath diagram show the classification of erosion inhibitors:

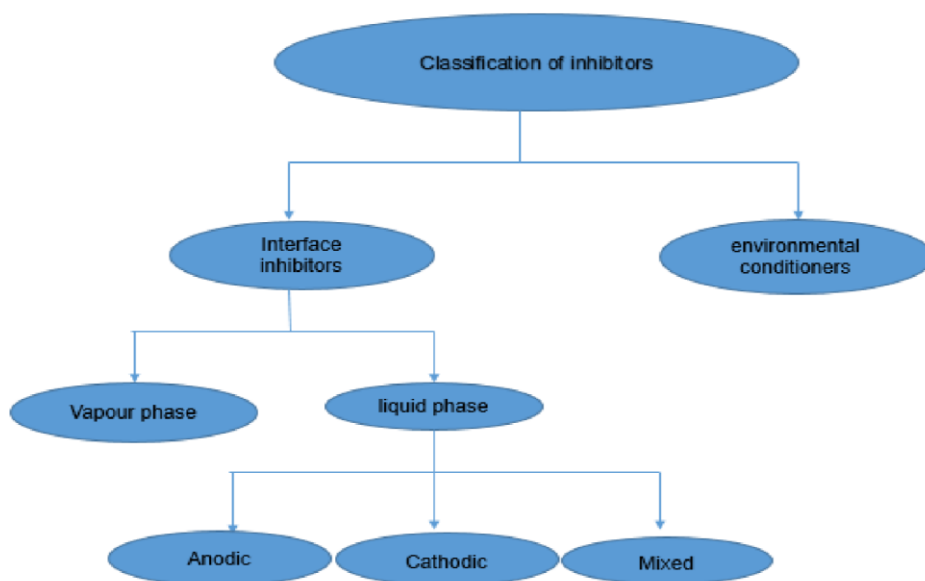


**Figure 2. 7:** Classification of inhibitors<sup>72</sup>

### 2.6.3.1. Environmental conditioners

Natural conditioners which are also known as foragers where inhibitors that diminish corrosively of the medium by rummaging the forceful substances. This sort of inhibitor control corrosion, by diminishing the oxygen substance utilizing foragers since, in near-neutral and antacid circumstances, oxygen decrease may be a common cathodic reaction<sup>72</sup>.

### 2.6.3.2. Interface inhibitors

Interface inhibitors control corrosion by forming a protective film at the metals. This type of inhibitor is classified into two phases (vapor and liquid phase)<sup>72</sup>.

#### Vapor phase inhibitors

Vapor stage inhibitors which are known as unstable erosion inhibitors are transported compounds in a closed environment to the location of erosion. Shipping holders, unstable strong such as salts of dicyclohexylamine and cyclohexylamine are utilized in near vapor spaces<sup>72</sup>.

#### Liquid phase inhibitors

Liquid phase inhibitors are classified as anodic, cathodic, or mixed inhibitors as shown in the above diagram, but those inhibitors depend on whether they inhibit the anodic, cathodic, or both electrochemical reactions<sup>24</sup>.

- **Anodic inhibitors**

Anodic inhibitors interfere with the anodic process. The anodic inhibitors are known as dangerous inhibitors. They work by shifting the anodic potential to enable passive film which is formed on the surface of the metal by inhibiting the anodic metal. If the anodic inhibitors are not present at a concentration level to block off all anodic sites, localized attacks such as pitting corrosion can become a serious problem<sup>10</sup>.

- **Cathodic inhibitors**

The primary cathodic reaction in cooling systems is the reduction of oxygen. Cathodic inhibitors function by reducing the available area for the cathodic reaction; thus, this is achieved by the precipitation of an insoluble species on the cathodic sites to limit the diffusion of reducing species to the surface<sup>10</sup>. The rates of cathodic reactions can be reduced using cathodic poisons. Cathodic poisons increase the susceptibility of metal during aqueous corrosion or cathodic charging. Cathodic inhibitors are safe because they do not cause localized corrosion<sup>47</sup>.

- **Mixed inhibitors**

Mixed inhibitors involve both anodic and cathodic inhibitors. This type of inhibitor works by reducing both the cathodic and anodic reactions. The most common inhibitors of mixed are silicates and phosphate. This happens because of the danger of anodic inhibitors alone<sup>72</sup>.

## **2.7. Organic compounds used as corrosion inhibitors**

Organic compounds are the foremost well-known inhibitors containing heteroatom (O, N, and S) numerous bonds, heterocyclic compounds, pi electrons, and they ordinarily have hydrophilic parts. Organic corrosion inhibitors comprise oxygen, nitrogen, or sulphur as well as unsaturated bonds, which might serve as adsorption centers utilizing the solitary match on  $\pi$  electrons adsorb on the metallic surface through their dynamic centers<sup>7</sup>.

The adsorbed inhibitor particles secure the metal surface from coordinate assault by implies of destructive particles, and the natural compound is expressed to repress metallic corrosion. The adsorption of atoms that include heteroatoms is more often than not chemisorption, which is regularly gone before by electrostatic intelligence between restraint particles and metal substrate<sup>10,73</sup>. Corrosion restraint properties of most heterocyclic compounds have been portrayed as including both adsorption<sup>7</sup>.



Thiazolidinedione's derivate are employed as corrosion inhibitors in the current investigation.

## 2.8. Thiazolidinediones (TZD)

The thiazolidinediones abbreviated as TZD, also known as glitazones which is vital nucleus in heterocyclic chemistry. TZD is known as important class of drugs that act by increasing the transactivation activity of **PpARS**, as a result of which they reduce hepatic glucose production and increase peripheral utilization of glucose and lipid metabolism<sup>74</sup>. TZD contains a five-membered heterocycle additionally heteroatoms such as oxygen, sulphur, and nitrogen as shown in **figure 2.9**. These are the key useful bunch as they are the most location of adsorption amid the metal and compound.

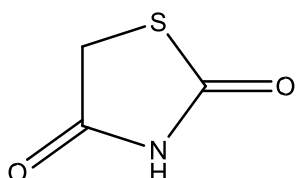


**Figure 2. 8:** Thiazolidinediones

TZD's have existed since **1982s** and they are successful restorative specialists for diabetes. Ciglitazone is the primary compound of TZD which created glycaemic control in creature models of affront resistance was found in Japan<sup>74,75</sup>. TZD shows multi-direction pharmacological exercises such as antioxidant, antihyperglycemic, antibacterial, and anticancer and etc<sup>76</sup>. The **rosiglitazone**, **pioglitazone**, etc. are TZD derivate which acts as sedate candidates<sup>77</sup>.

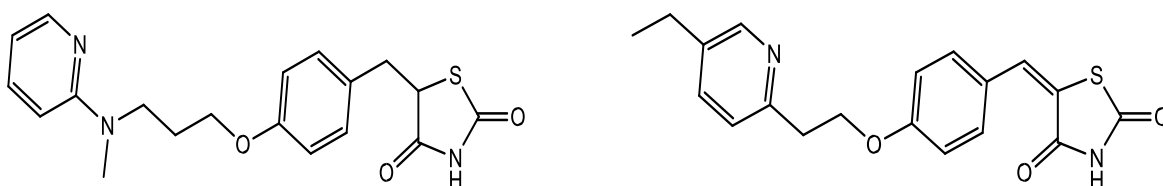


**Figure 2. 9:** Rosiglitazone/Pioglitazone

Due to various pharmacological actions of TZD derivate, the researcher keeps on their full interest in the synthesis of new TZD derivate by using countless synthetic methods and carry out clinical trials for achieving lead target<sup>78</sup>. The synthesis of the ring of TZD has been carried out from  $\alpha$ -harvester or  $\alpha$  halo nitrile by reaction with thiourea or potassium thiocyanate followed by acid hydrolysis. Many derivatives of TZD are prepared by **knoeveruge** condensation between aryl aldehyde and commercial 2,4-thiazolidiones and subsequent olefinic bond reduction<sup>79</sup>.



## CHAPTER 3

### Experimental Procedures:

### 3.1. Introduction

In this study, four TZD derivatives which are ethyl (2,4-dioxo-1,3-thiazolidin-3-yl)acetate, ethyl 2-(5-(benzo[d][1,3] dioxol-5-ylmethylene)-2,4-dioxothiazolidin-3-yl)acetate, ethyl 2-(5-(4-methoxybenzylidene)-2,4-dioxothiazolidin-3-yl)acetate and ethyl (2-(5-(benzo[d][1,3]dioxol-5-ylmethylene)-2,4-dioxothiazolidin-3-yl)acetyl)glycinate were synthesised. These compounds were subjected to different characteristic techniques in order to conform their structures and properties.

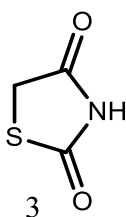
Furthermore, after the synthesis and characterization of organic compounds, corrosion inhibition of zinc and aluminium in 1.5M HCl was carried out using those synthesized compounds as a corrosion inhibitors.

### 3.2. Synthesis procedure of inhibitors

The synthesis of organic inhibitors began with a one-step synthesis of TZD which is the starting material of all target compounds. Spectroscopic Techniques i.e  $^1\text{H}$  NMR (400 MHz) and  $^{13}\text{C}$  NMR (100 MHz) spectra were recorded on a Bruker 400 MHz spectrometer using DMSO- $\text{d}_6$  as NMR solvent. Values for the chemical shifts were expressed in parts per million (ppm). Infrared spectra were run on a Bruker platinum 22 vector Fourier Transform spectrometer (FTIR).

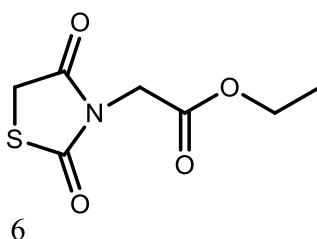
#### 3.2.1. Synthesis of Thiazolidine-2,4-dione

Thiazolidine-2,4-dione was successfully synthesized by reacting 2-Chloroacetic acid (**1**) with thiourea(**2**) in water, the resultant reaction mixture was stirred for 10 minutes at room temperature until the reagents completely reacted to form a white precipitate. Concentrated hydrochloric acid was then added drop-wise to the reaction mixture and stirred for 2 minutes and refluxed for 12 hours. After 12 hours the mixture was allowed to cool down for 30 minutes at room temperature to form a white precipitate. The precipitate was then filtered and washed with a small volume of ice water to give the desired product as a white solid (**3**).



### 3.2.2. Synthesis of ethyl (2,4-dioxo-1,3-thiazolidin-3-yl)acetate

Synthesis of ethyl (2,4-dioxo-1,3-thiazolidin-3-yl) acetate was successfully done by mixing a mixture of the potassium salt (**4**) of thiazolidine-2, 4-dione (4.000 g, 155.22mmol), and ethyl bromoacetate (**5**) (4.30g, 167.01mmol) in 30ml of acetone. The resultant mixture was refluxed for 12 hours after which it was allowed to cool whereby excess solid of KOH was filtered off and the filtrate concentrated using a rotary vapor to provide ethyl (2,4-dioxo-1,3-thiazolidin-3-yl) acetate (**6**) as a colourless oil.

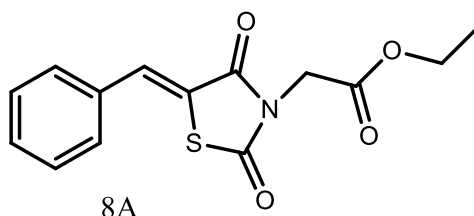


### 3.2.3. General procedure for the synthesis of ethyl 2-(5-(substituted benzylidene)-2,4-dioxothiazolidin-3-yl)acetates using Knoevenagel Condensation reaction.

Appropriate benzaldehyde (**7**) (1mmol) and ethyl (2,4-dioxo-1,3-thiazolidin-3-yl) acetate (1mmol), 3 drops of piperidine as catalyst were reacted in ethanol and refluxed for 12 hours. The resultant mixture was allowed to cool down to room temperature and being poured into ice and formed a precipitate which was then collected by filtration. The solid obtained was washed with water to give the desired products.

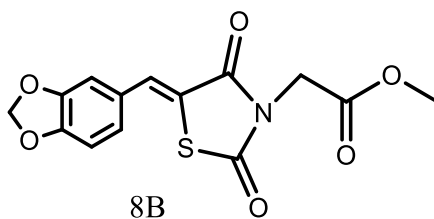
#### 3.2.3.1. Ethyl 2-(5-benzylidene)-2,4-dioxothiazolidin-3-yl)acetate (EBDA).

A reaction bezaldehyde (**7A**) (0.7ml, 6.46mmmol) and (1.3119g, 6.46mmol) ethyl (2,4-dioxo-1,3-thiazolidin- 3-yl) acetate(**6**) gave compound **8A** as pale yellow solid.



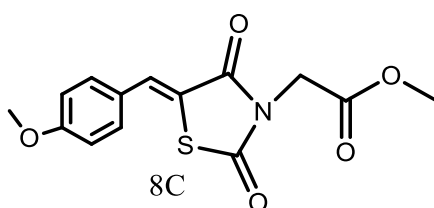
#### 3.2.3.2. Ethyl 2-(5-(benzo[d][1,3] dioxol-5-ylmethylene)-2,4-dioxothiazolidin-3-yl)acetate (EBMDA).

A reaction of piperonal (**7B**) (1.756g, 11.69mmol) and (2.3775g, 11.69mmol) of ethyl (2,4-dioxo-1,3-thiazolidin-3-yl) acetate (**6**) in ethanol gave compound **8B** as a yellow solid.



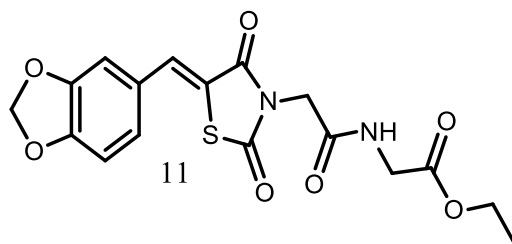
### 3.2.3.3. Ethyl 2-(5-(4-methoxybenzylidene)-2,4-dioxothiazolidin-3-yl)acetate (EMDA).

A reaction of anisaldehyde (**7C**) (0.76g, 4.97mmol) and ethyl (2,4-dioxo-1,3-thiazolidin-3-yl) acetate (**6**) (1.04 g, 4.97 mmol) in ethanol gave compound **8C** as shiny yellow solid.



### 3.2.4. Ethyl (2-(5-(benzo[d][1,3]dioxol-5-ylmethylene)-2,4-dioxothiazolidin-3-yl)acetyl)glycinate (EBDMDG).

A mixture of ethyl 2-(2-(2,4-dioxothiazolidin-3-yl)acetate (**9**) (1.01g, 3.84mmol) and of piperonal (**10**) (0.58g, 3.84mmol) was added into 30ml of ethanol followed by a catalytic amount of piperidine. The resultant mixture was heated under reflux for 12 hours. After being allowed to cool down to room temperature for 5minutes, the mixture was poured into ice water and the resultant precipitate was collected by filtration. The solids obtained were further recrystallized from methanol to afford the desired product **11**.



## 3.3. Preparation of inhibitors

A solution of HCl (1.5M) was prepared by dilution of an analytical grade 32% HCl in a 1000 cm<sup>3</sup> volumetric flask and filled to the mark with distilled water and different concentration were prepared. The synthesized compounds were insoluble in water, to

solve this problem small amounts of dimethyl sulfoxide (DMSO) were added in solution during the preparation of various inhibitor concentrations to ensure the solubility of the compound.

### 3.4. Metal specimen

The specimen used for corrosion test were Zn and Al with a size of 3cm×2cm, containing a small hole of approximately 0.8cm in the middle of the specimen for hanging glass rod. Zinc were executed using zinc specimens of a 99.90 (wt %) purity and approximately 99 (wt %) aluminium sheets were used for all experimental procedures involving aluminum metals.

### 3.5. Gravimetric analysis

The gravimetric analysis requires simple and inexpensive equipment. This is simple and a preferred method in corrosion studies because of its accuracy and reliability. Measurements of weight loss were made by completely immersing each metal in different inhibitor concentrations and left for 6 hours at different temperatures (30, 40, 50 and 60 °C). The metal sheets were first polished and rinsed with distilled water and left for about 3 minutes to dry. For the blank analysis, the metal sheets used were first weighed and their initial mass was noted. After weighing, they were immersed in various concentrations of HCl at different temperatures for 6 hours, then removed, brushed, washed with acetone, dried again for about 3 minutes, and reweighed. For the test experiments the same procedure was repeated using 1.5 M HCl as the blank in the presence of different concentrations of inhibitors. The mass difference of metal sheets before and after with the use of inhibitors was recorded as the weight loss.

From the weight loss experiments, the corrosion rate ( $C_R$ ), % inhibition efficiency (I.E), and the degree of surface coverage ( $\theta$ ) for all metal sheets were calculated by using the following equations<sup>80</sup>.

$$CR = \frac{\Delta W}{st} \quad (15)$$

where:  $W$  = the weight loss of the zinc metal (g)

$S$  = is the surface area of the metal sheet (cm<sup>2</sup>)

$t$  = the exposure time (h)

$$\% IE = \left(1 - \frac{\rho_1}{\rho_2}\right) \times 100\% \quad (16)$$

where: IE = inhibition efficiency

$\rho_1$  = the corrosion rate of metal in the presence of inhibitor

$\rho_2$  = the corrosion rate of metal in the absence of inhibitor

$$\theta = \left(1 - \frac{\rho_1}{\rho_2}\right) \quad (17)$$

where:  $\Theta$  = the degree of surface coverage

$\rho_1$  = the corrosion rate of metal in the presence of inhibitor

$\rho_2$  = the corrosion rate of metal in the absence of inhibitor

### 3.6. Electrochemical studies

Electrochemical studies have been carried out using the Bio-Logic ASA Potentiostat Electrochemical analyzer model of SP-150. The analyzer is prepared with EC-Lab software. Bio-Logic ASA Potentiostat Electrochemical analyzer model of SP-150 is capable of loading many experiments at one time without affecting each other<sup>81</sup>. The analysers were equipped with a three-electrode cell that consist of a saturated calomel with Ag/AgCl as a reference electrode (RE), the platinum counter electrode (CE) and the working electrode (WE). Before running PDP and EIS zinc and aluminium sheets were allowed to corrode freely in an open circuit potential for about 30 minutes to attain steady-state corrosion potential corresponding to that of the working electrode.

#### 3.6.1. Potentiodynamic polarization (PDP)

Potentiodynamic polarization was used to characterize the metals specimen by its current potential relationship. PDP scan rate was  $5\text{mvs}^{-1}$  it started from cathodic to anodic direction, ranging from  $-250\text{mv}$  to  $250\text{mv}$  reference to saturated calomel electrode in OCP. Tafel curves were developed and PDP measurements were obtained<sup>83</sup>. These



measurements were used to determine the corrosion characteristics of metal specimens in aqueous environments.

The percentage inhibition efficiency (% IE) was calculated using the following equation:

$$\%IE = 1 - \frac{I_{corr}}{I^0_{corr}} \times 100 \quad (18)$$

where:  $I_{corr}$  = Corrosion current densities in the presence of the inhibitor

$I^0_{corr}$  = Corrosion current densities in the absence of the inhibitor<sup>83,84</sup>

### 3.6.2. Electrochemical Impedance Spectroscopy (EIS)

EIS was also used to study the corrosion of zinc and aluminium metals in 1.5 M hydrochloric acid. EIS measurements were carried out at OCP in a wide frequency of 100KHz to 0.1Hz to check out the information about corrosion inhibitors. Nyquist and bode plots were analyzed to clarify the behaviour of metals. The electrochemical parameters such as transfer charge resistance, the capacity of double layer, the constant phase element constant, and exponents were obtained and IE% was calculated using the following equation.

$$\%IE_{EIS} = \left(1 - \frac{R^0_{ct}}{R_{ct}}\right) \times 100 \quad (19)$$

where:  $R^0_{ct}$  = the charge transfer resistance in the absence of the inhibitor

$R_{ct}$  = the charge transfer resistance in the presence of the inhibitor<sup>84</sup>

# CHAPTER 4

## RESULTS AND DISCUSSION

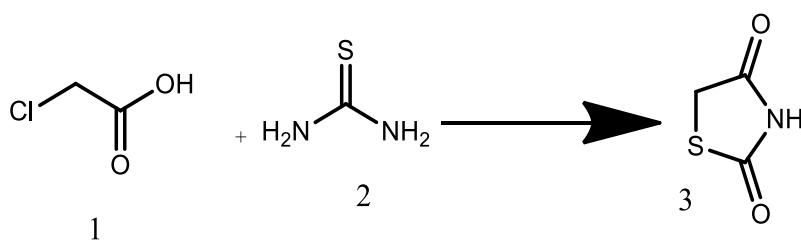
## 4.0. RESULTS AND DISCUSSION

This chapter looks at the detailed results and discussion obtained from different characterization techniques used during the project.

### 4.1. Characterization of synthesized compounds

The target compounds were confirmed by  $^1\text{H}$  NMR,  $^{13}\text{C}$  NMR as well as IR spectroscopy.

#### 4.1.1. Synthesis of glitazone (2,4-thiazolidinediones).



**Scheme 1:** Synthesis of thiazolidine-2,4-dione/glitazone:

**Reagents and conditions:** Water, HCl, reflux 12 hours

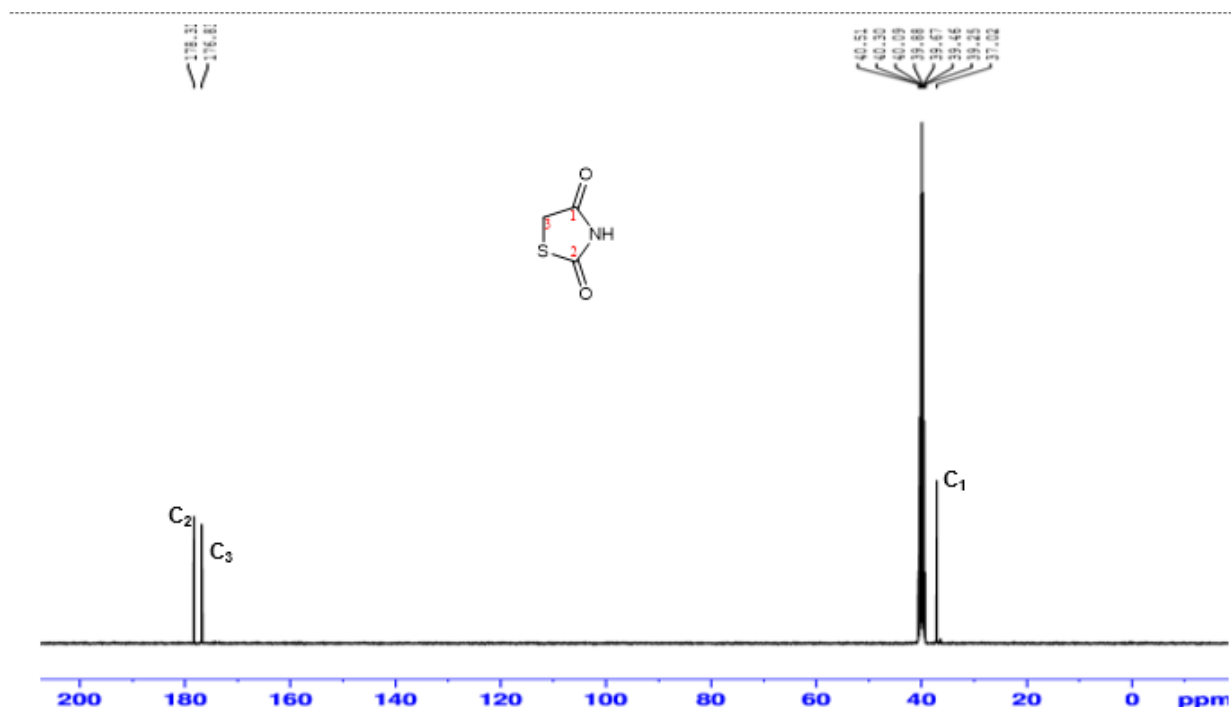


**Figure 4. 1:**  $^{13}\text{C}$  NMR spectra of synthesized Glitazone

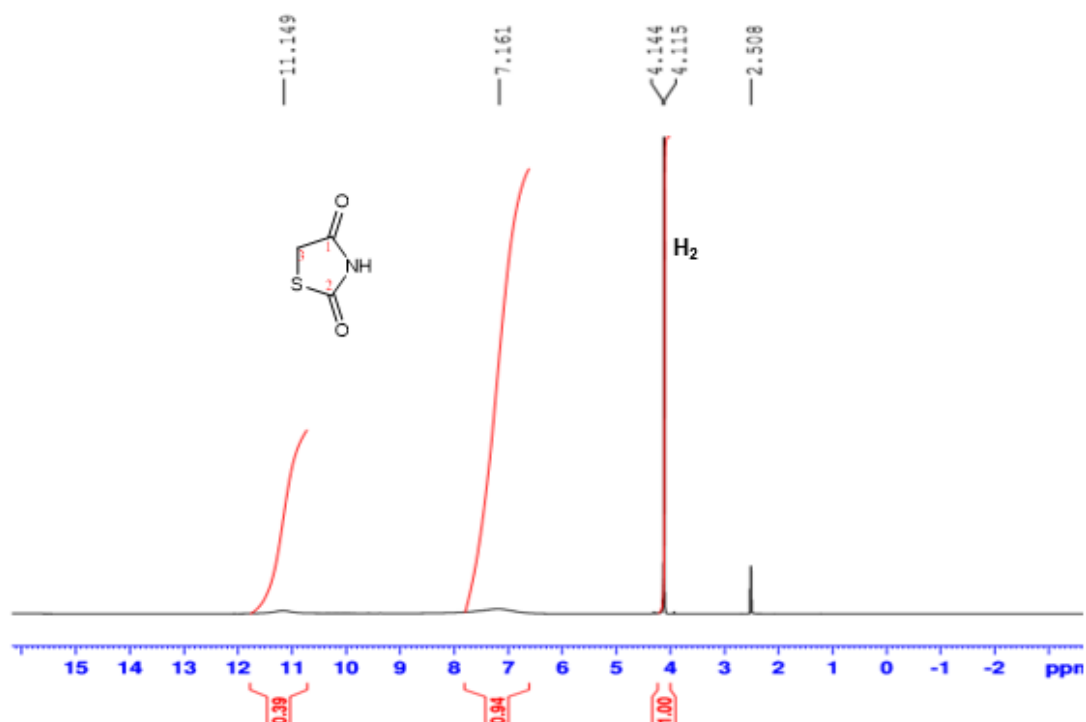
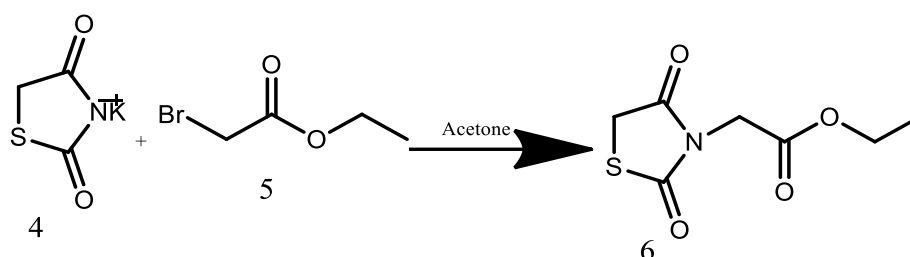


**Figure 4. 2:**  $^1\text{H}$  NMR spectra of synthesized glitazone

As indicated on reaction scheme 1 a solid product was obtained with an 85.25% yield. Mp 123.7-125.2°C (lit Mp= 126-127°C)<sup>84,85</sup>. On  $^1\text{H}$  NMR spectra **figure 4.2** revealed a singlet integrating for 2Hs at 4.115ppm confirming the presence of methylene protons. There was also a broad singlet integrating 1H at 7.161ppm confirming the N-H proton. There were three signals in the  $^{13}\text{C}$  NMR spectra **figure 4.1**, compound **3** was characterized by methylene ( $\text{CH}_2$ ) peaks at 37.02ppm on  $\text{C}_2$  and two carbonyl peaks were observed at 176.89ppm and 178.32ppm for carbon  $\text{C}_1$  and  $\text{C}_3$ .

#### 4.1.2. Synthesis of ethyl (2,4-dioxo-1,3-thiazolidin-3-yl) acetate.



**Scheme 2:** Synthesis of ethyl (2,4-dioxo-1,3-thiazolidin-3-yl) acetate:

**Reagents and conditions:** Acetone, reflux 12 hours.

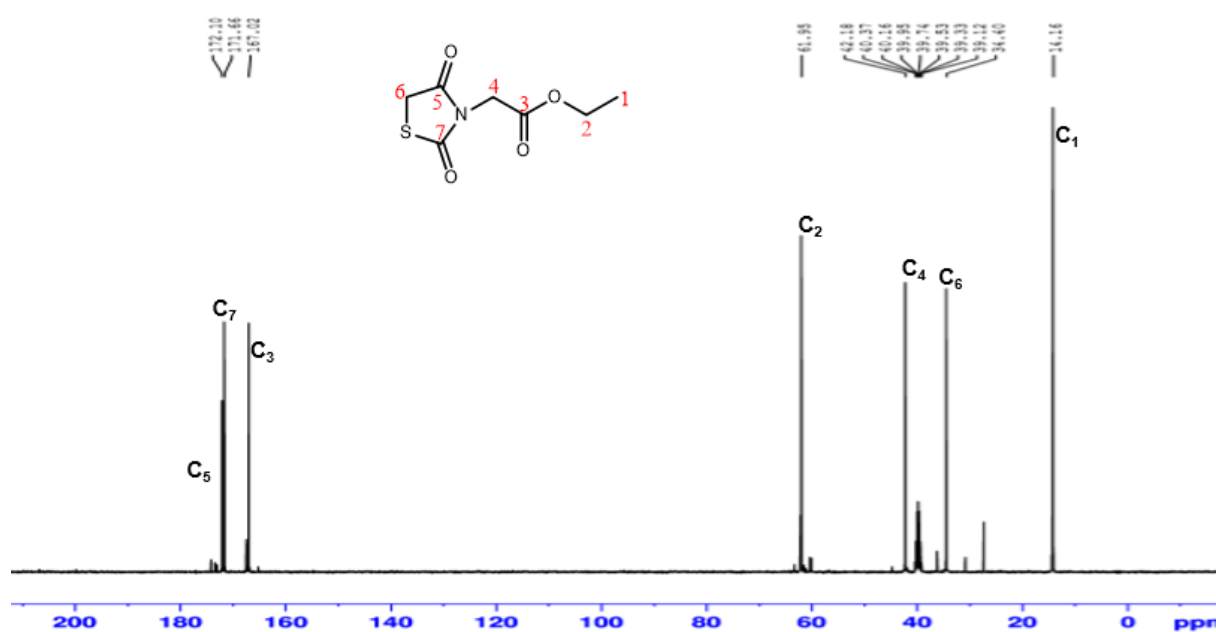


**Figure 4. 3:** <sup>13</sup>C NMR spectra of synthesis of ethyl (2,4-dioxo-1,3-thiazolidin-3-yl) acetate

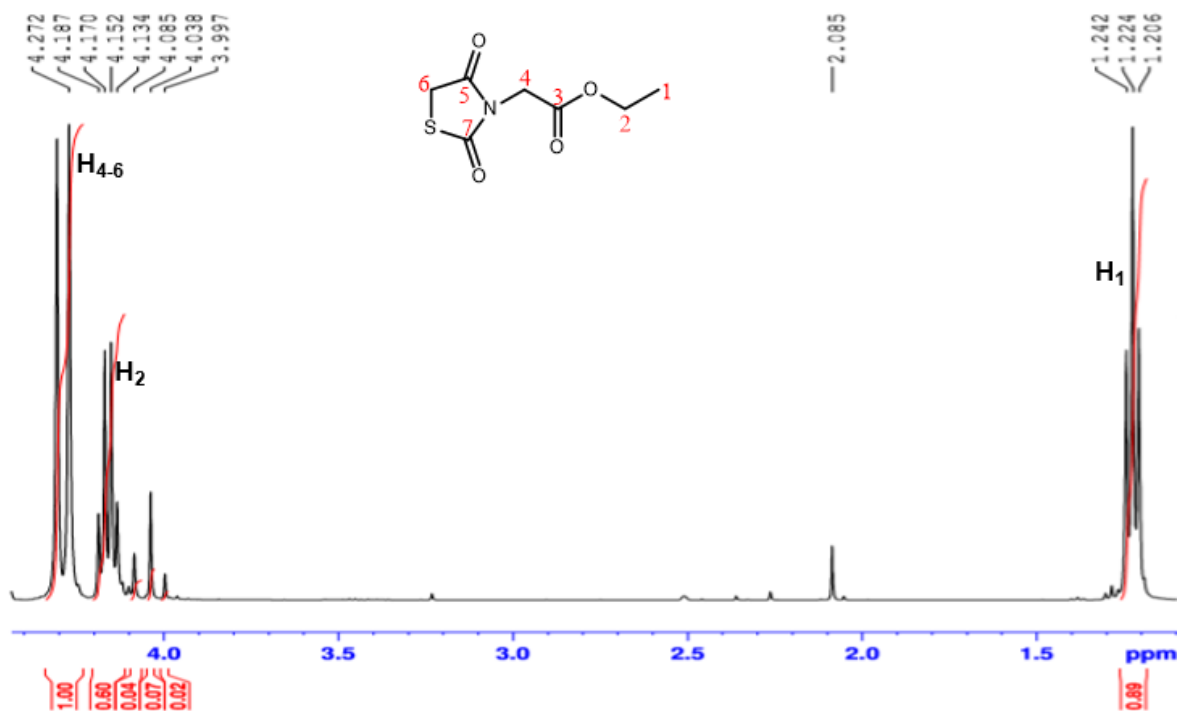
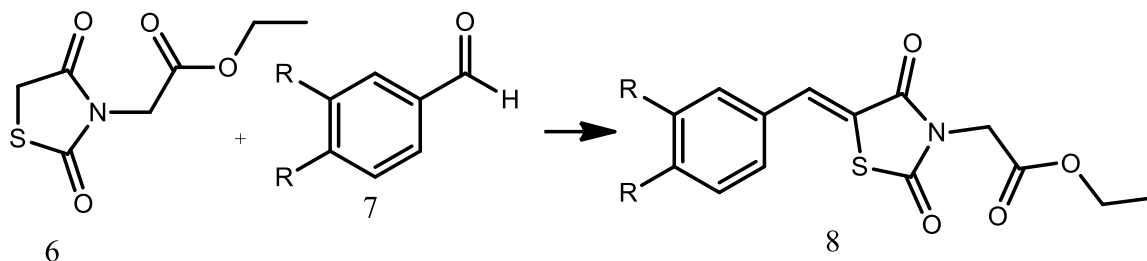


**Figure 4. 4:** <sup>1</sup>H NMR spectra of ethyl (2,4-dioxo-1,3-thiazolidin-3-yl) acetate

As indicated on reaction scheme 2 a colourless oil was formed with 85% yield. <sup>13</sup>C NMR spectrum **figure 4.3** showed 7 peaks, four extra aliphatic signals (C1 at 14.16ppm, C2 at 61.95ppm, C4 at 41.19ppm, and 34.40ppm for C6), and three quaternary carbon (C) signals (C3 at 167.02ppm, C5 at 172.10ppm and C7 at 171.65ppm). The <sup>1</sup>HMR spectrum, (400 MHz, DMSO-d<sub>6</sub>) **figure 4.4** showed the absence of N-H peak at 7.161ppm of a compound. Compound 3 was also characterized by the presence of two extra methylene CH<sub>2</sub> protons where H<sub>2</sub> appears as a quartet due to proton 1 at ~ 4.152ppm(7.2Hz) and H<sub>4</sub> appearing as a singlet at ~ 4.187ppm, all the characterization just confirmed that the product was formed.

#### 4.1.3. Synthesis of ethyl 2-(5-(substituted benzylidene)-2,4- dioxothiazolidin-3-yl) acetates.

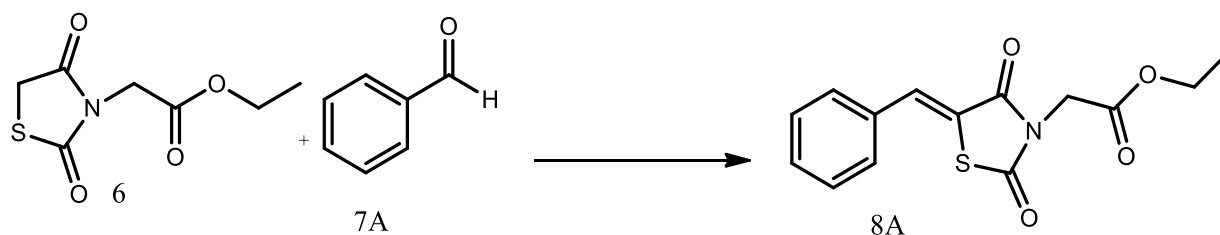


#### Scheme 3: synthesis of acetates.

$^1\text{H}$  NMR spectra of compounds **8A**, **8B**, and **8C** were characterized by the absence of the characteristic aldehydic proton confirming that benzaldehydes were consumed in the reaction. The spectrums were characterized by the absence of singlet methylene protons at **C<sub>7</sub>** from the starting material **3**, confirming that the reaction had taken place.  $^1\text{H}$  NMR spectra of compounds **8A**, **8B**, **8C** also indicated the appearance of a new methine peak on proton at **C<sub>8</sub>** integrating for 1 proton appearing as a singlet at  $\sim 7.90\text{-}8.017$  ppm confirming that the condensation reaction happened. Furthermore, compounds **8A**, **8B**, **8C** showed a characteristic singlet methylene proton integrating for 2H at  $\sim 4$  ppm which represents proton at **C<sub>4</sub>**, a quartet integrating for 2Hs at  $\sim 4.2$  ppm at **C<sub>2</sub>**, and a triplet **C<sub>1</sub>** at  $\sim 1$  ppm integrating for 3Hs.

The  $^{13}\text{C}$  NMR spectra of compounds **8A**, **8B**, and **8C** were characterized by the absence of a signal indicating the characteristic aldehydic carbon peak at  $\sim 190$  ppm. There was an appearance of a new benzylic carbon **C<sub>8</sub>** peak at  $\sim 134$  ppm confirming the target product, the appearance of two carbonyl carbon peaks at  $165\text{-}169$  ppm, and lastly, the formation of the double bond was confirmed by an appearance of a new quaternary carbon peak at **C<sub>7</sub>**  $\sim 120$  ppm also confirming the formation of the double bond. Furthermore,  $^{13}\text{C}$  NMR spectra were characterized by three aliphatic carbon signals which are indicted as C-1, C-2, and C-4.

#### 4.1.3.1. Ethyl 2-(5(substituted benzylidene)-2,4-dioxothiazolidin-3-yl)acetates.



**Scheme 4:** Synthesis of ethyl 2-(5(substituted benzylidene)-2,4-dioxothiazolidin-3-yl)acetates:

**Reagents and conditions:** Ethanol, piperidine, reflux 12 hours

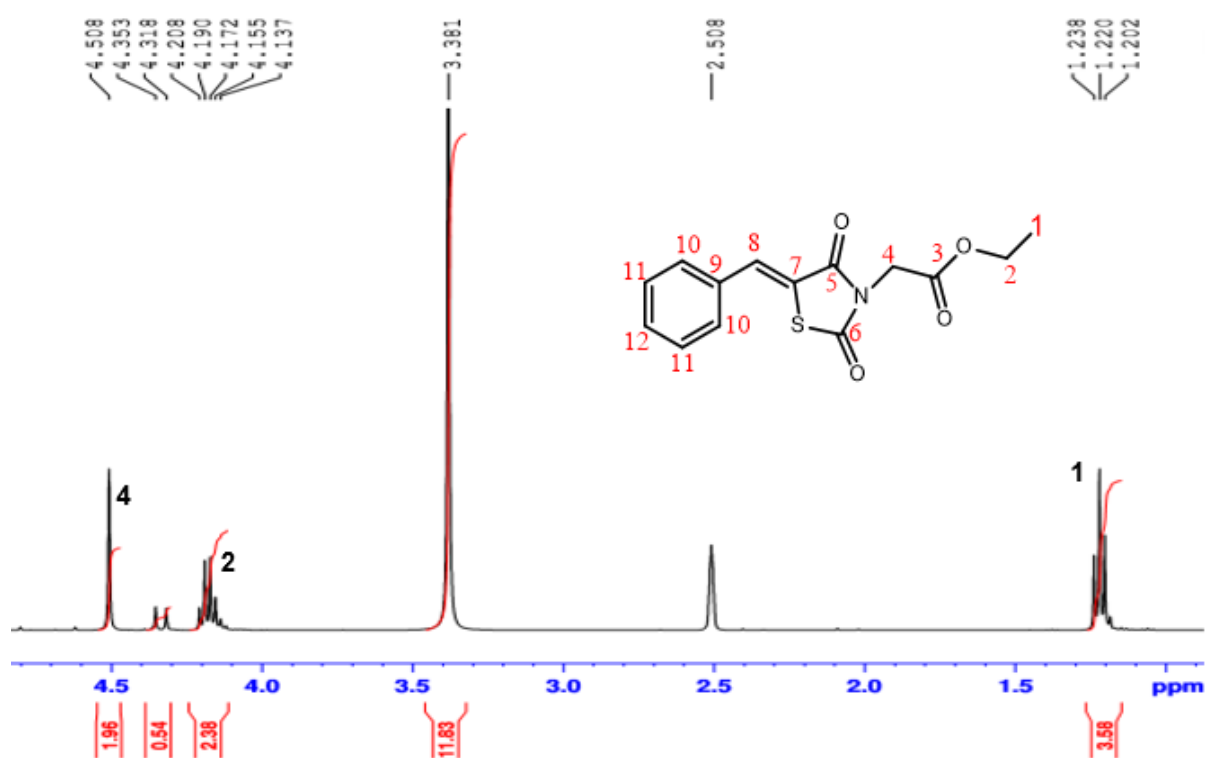


**Figure 4. 5:**  $^1\text{H}$  NMR spectra (aliphatic expansion) of Ethyl 2-(5(substituted benzylidene)-2,4-dioxothiazolidin-3-yl)acetates.



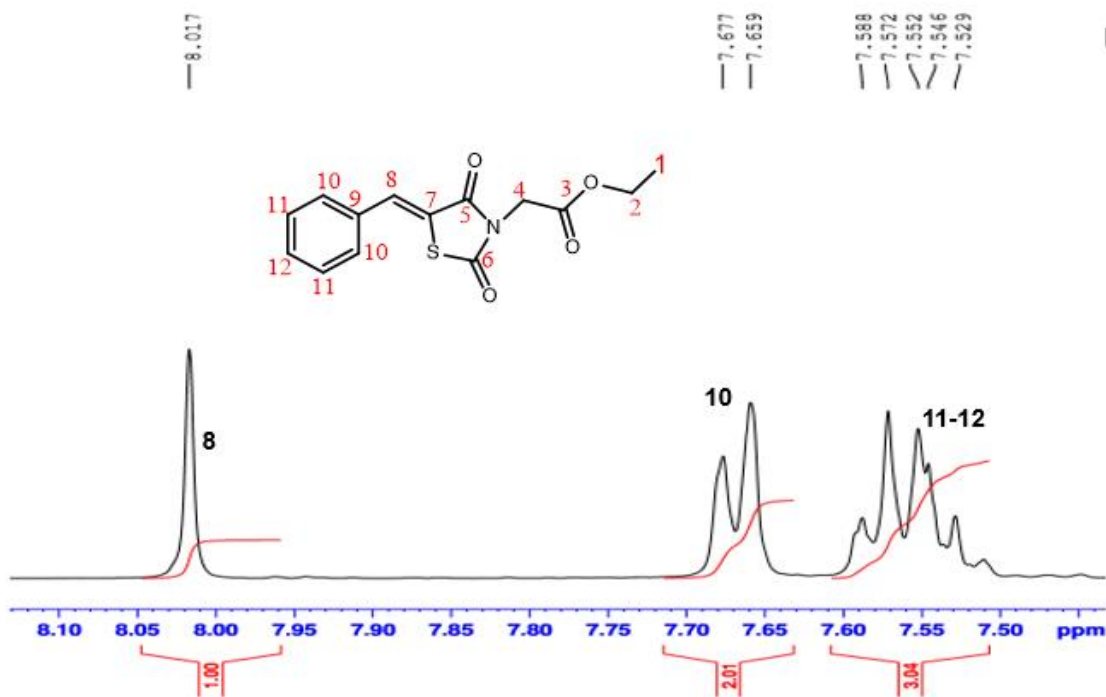


**Figure 4. 6:**  $^1\text{H}$  NMR spectra (aromatic expansion) of Ethyl 2-(5(substituted benzylidene)-2,4-dioxothiazolidin-3-yl)acetates.

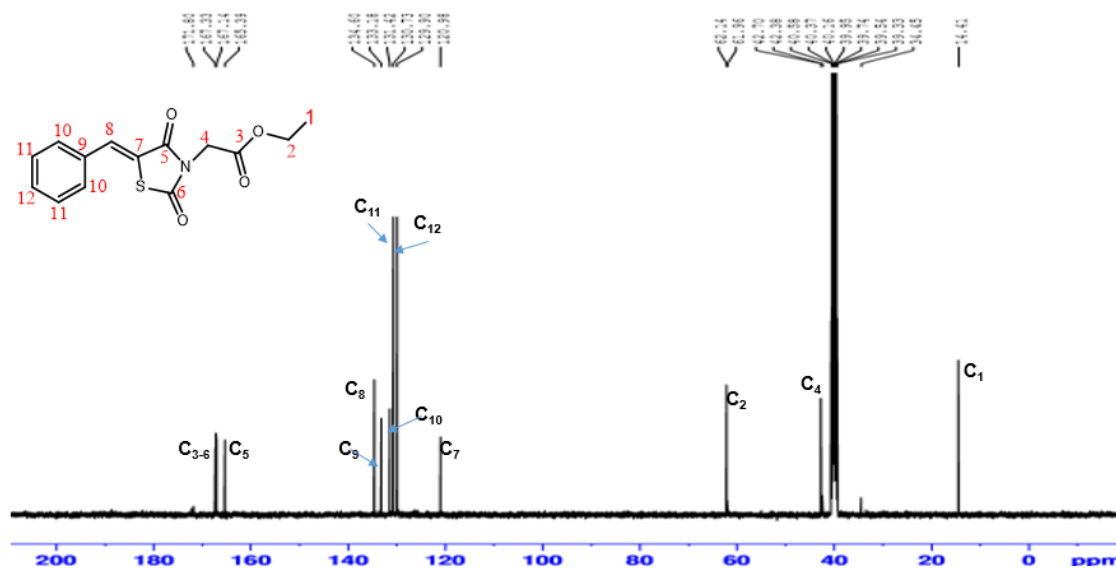
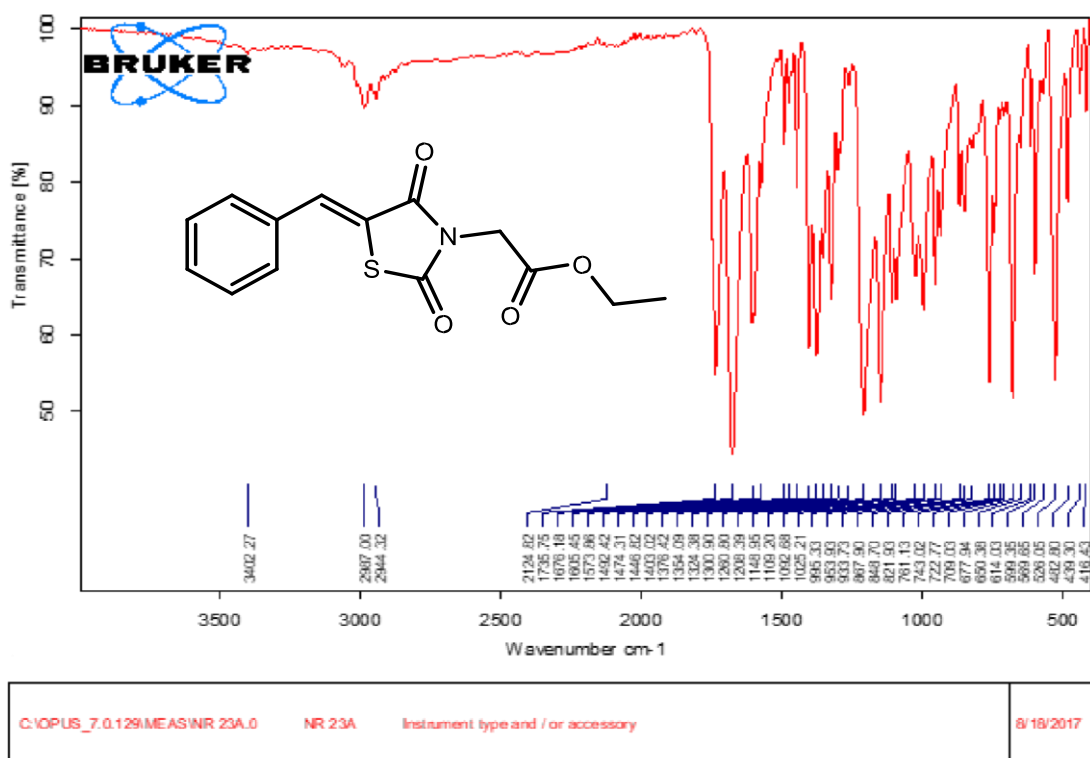


**Figure 4. 7:**  $^{13}\text{C}$  NMR spectra of Ethyl 2-(5(substituted benzylidene)-2,4-dioxothiazolidin-3-yl)acetates.



Page 1/1

**Figure 4. 8:** IR spectrum of ethyl 2-(5(substituted benzylidene)-2,4-dioxothiazolidin-3-yl)acetates.

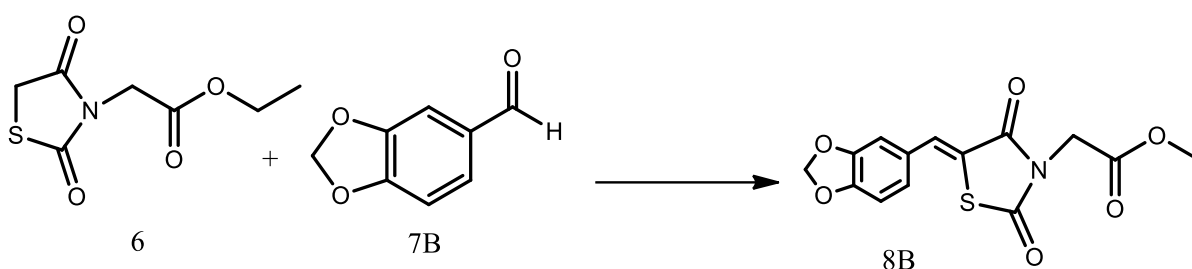
A yellow solid product was obtained as solid with 92.22% as is shown on reaction scheme 4. m.p=84.8-90.0°C (lit m.p= 75-77°C)<sup>86,87</sup>. On <sup>1</sup>H NMR (400 MHz, DMSO-d<sub>6</sub>), the Proton spectrum in **Figures 4.5 and 4.6** indicates six peaks where the integration of 1H is represented by 1.00. δH (ppm). It gives rise to a triplet ranging from 1.202 to 1.238 for 3H with a *J* value of 7.2 Hz due to two neighbouring proton, a quartet of 2H on H<sub>2</sub> ranging from 4.137 to 4.208 with a *J* value of 7.2 Hz it gave rise to quartet due to three neighbouring proton. H<sub>4</sub> gave rise to a singlet of 2H at 4.508 due to none neighbouring proton. On aromatic ring only two peaks were available, doublet peak of 2H at H<sub>10</sub> ranging from 7.659 to 7.677 with *J* value of 7.2 Hz and multiplet at 7.529 on H-11 and H-12. Apart from that broad singlet was available at H<sub>8</sub> with the integration of 1H at 8.017.

<sup>13</sup>C NMR (100 MHz, DMSO-d<sub>6</sub>), Carbon spectrum on **figure 4.7** revealed 12 signals, four on an aromatic ring. δC (ppm) three CH at 131.42 (C-10) which are equivalent to each other and also C-11 at 130, 129.90 (C-12), and one carbonyl carbon at 133.18 (C-9). CH from methane at 134.40 (C-8), two CH<sub>2</sub> from (C-2 and C-4) at 61.96 and 42.70, and CH<sub>3</sub> from C-1 at 14.42. At 167.35 (C-5), 167.16 (C-1), 165.39 (C-3), 134.60 (C-7), 133.14 (C-

9), 131.43 (C-8) 130.72 (C-9), 120.95 (C-6), 62.17 (C-2), 42.67 (C-4), 14.39 (C-1). Apart from carbonyl on the aromatic ring, there is another four carbonyl carbon on (C-3, C-5, C-6, C-7) at ~171.80ppm, ~165.39ppm, ~167.33ppm, and ~120.99ppm.

**IR (KBr cm<sup>-1</sup>)** in **figure 4.8** spectra indicate a stretch at 2987 for C-H on the aromatic ring, three carbonyl carbon (C=O) at (1736, 1676, 1605), and C-O stretch at 1149.

#### 4.1.3.2. Ethyl 2-(5-(Benzo[d][1,3] dioxol-5-ylmethylene)-2,4dioxothiazolidin-3-yl) acetate.



**Scheme 5:** synthesis of Ethyl 2-(5-(Benzo[d][1,3] dioxol-5-ylmethylene)-2,4dioxothiazolidin-3-yl) acetate:

**Reagents and conditions:** Ethanol, piperidine, reflux 12 hours

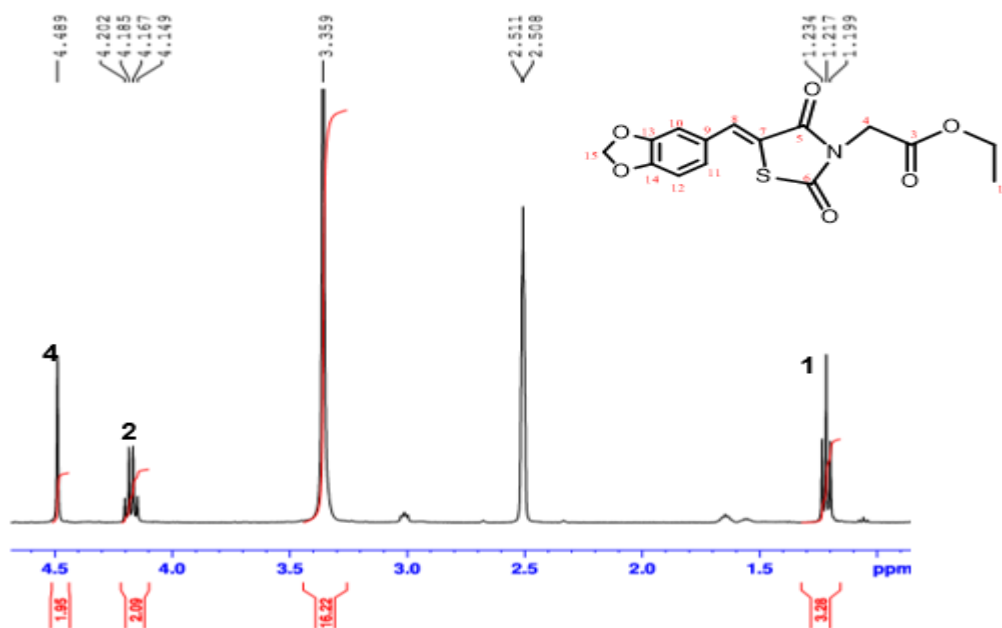


**Figure 4. 9:** <sup>1</sup>H NMR spectra (aliphatic expansion) of Ethyl 2-(5-(Benzo[d][1,3] dioxol-5-ylmethylene)-2,4dioxothiazolidin-3-yl) acetate.

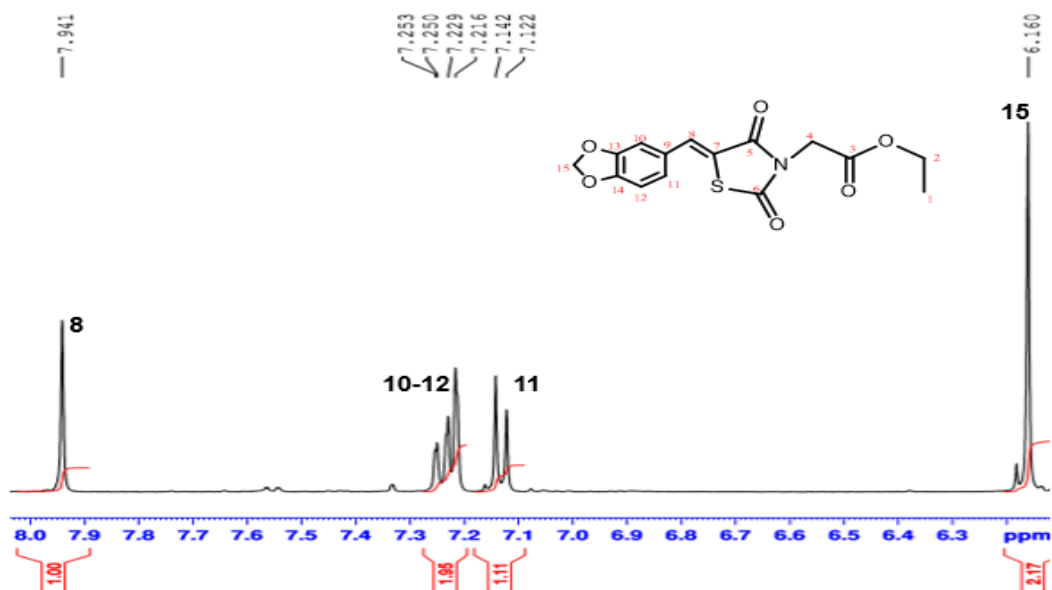


**Figure 4. 10:**  $^1\text{H}$  NMR spectra (aromatic expansion) of Ethyl 2-(5-(Benzo[d][1,3] dioxol-5-ylmethylene)-2,4-dioxothiazolidin-3-yl) acetate.

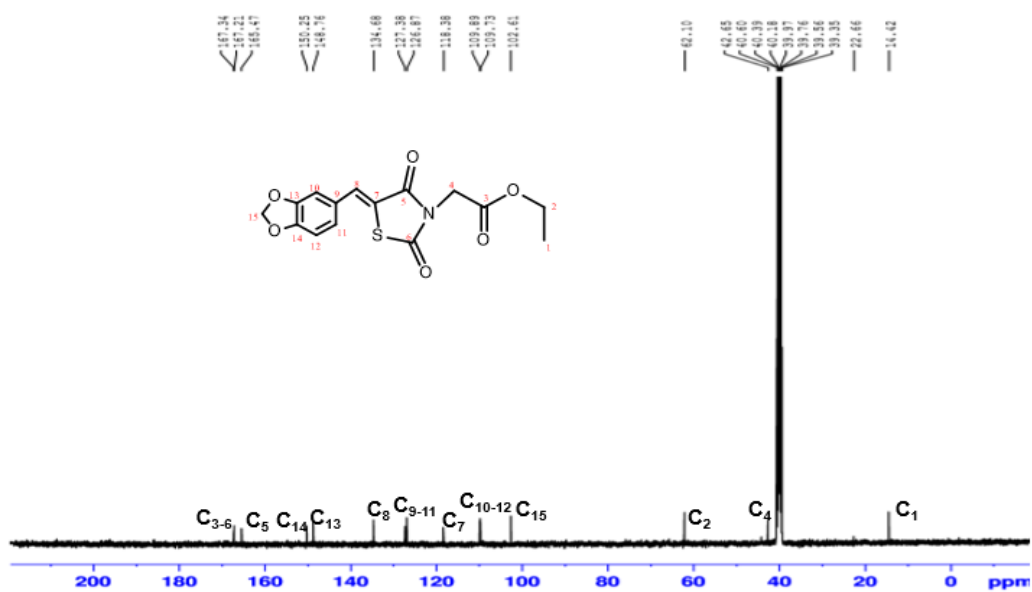
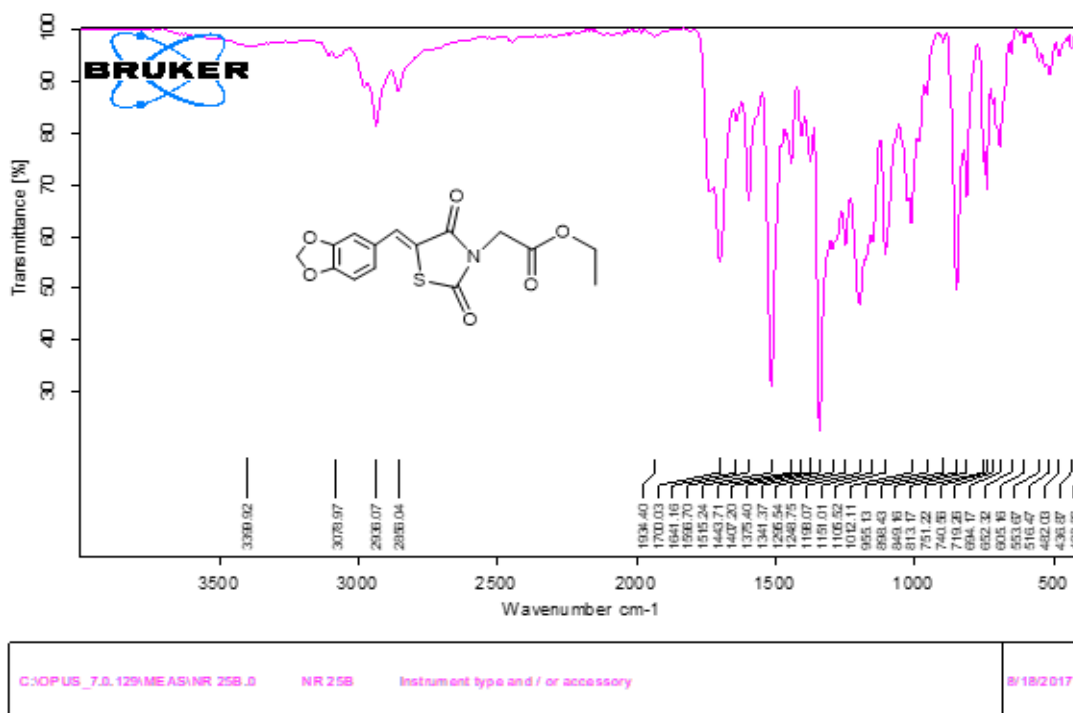


**Figure 4. 11:**  $^{13}\text{C}$  NMR spectra of Ethyl 2-(5-(Benzo[d][1,3] dioxol-5-ylmethylene)-2,4-dioxothiazolidin-3-yl) acetate.



Page 1/1

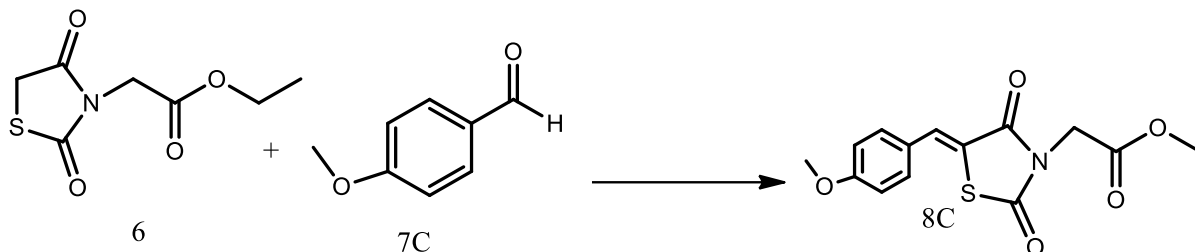
**Figure 4. 12:** IR spectra of Ethyl 2-(5-(Benzo[d][1,3] dioxol-5-ylmethylene)-2,4-dioxothiazolidin-3-yl) acetate.

A yellow solid product was formed with an 84 % yield. Mp= 131.5-133.4°C (lit Mp=130-135)<sup>86,87</sup>. **<sup>1</sup>H NMR (400 MHz, DMSO-d<sub>6</sub>)**, Proton spectrum revealed seven peaks where the integration of 1H is represented by 1.00. δH (ppm). Triplet ranging from 1.199 to 1.234 on H<sub>1</sub> for 3H with *J* value of 6.8 Hz the triplet is due to two neighboring proton, proton (2H) ranging from 4.149 to 4.202 which is quartet peak due to three neighboring proton with a *J* value of 7.2 Hz. Singlet ranging at 4.489 for 2H, another singlet at 7.941 with the integration of 1H on H<sub>8</sub>. On the piperonal ring, there's a doublet peak ranging from 7.122 to 7.142 with a *J* value of 8 Hz on H<sub>11</sub>, proton (2H) ranging from 7.216 to 7.253 which is a doublet of singlet for H<sub>10</sub> and H<sub>12</sub>, last proton peak is a broad peak at 6.160 for H<sub>15</sub>.

**<sup>13</sup>C NMR (100 MHz, DMSO-d<sub>6</sub>)**, Carbon spectrum conform the formation of EBMDA compound with fifteen signal. δC (ppm) seven peaks for carbonyl (C<sub>3</sub>, C<sub>5</sub>, C<sub>6</sub>, C<sub>7</sub>, C<sub>9</sub>, C<sub>13</sub>, and C<sub>14</sub>) at 167.34ppm, 165.47ppm, 167.21ppm, 120.38ppm, 127.36ppm, 148.76ppm and 150.25ppm. Three CH<sub>2</sub> (C<sub>2</sub>, C<sub>4</sub> and C<sub>15</sub>) at 62.10ppm, 42.65ppm and 102.61ppm. Four CH (C<sub>8</sub>, C<sub>10</sub>, C<sub>11</sub> and C<sub>12</sub>) at 134.68ppm, 109.89ppm, 126.87ppm and 109.73ppm, one CH<sub>3</sub> (C<sub>1</sub>) at 14.42ppm.

IR (KBr cm<sup>-1</sup>) indicated stretch at 2994 for C-H on the aromatic ring, 2952 at aromatic-OCH<sub>2</sub>O, three carbonyl carbon (C=O) at 1730, 1688, 1608), and 1150 stretch of C-O.

#### 4.1.3.3. Ethyl 2-(5-(4- methoxybenzylidene)-2,4-dioxothiazolidin-3-yl) acetate



**Scheme 6:** Synthesis of ethyl 2-(5-(4- methoxybenzylidene)-2,4-dioxothiazolidin-3-yl) acetate.

**Reagents and conditions:** Ethanol, piperidine, reflux 12 hours

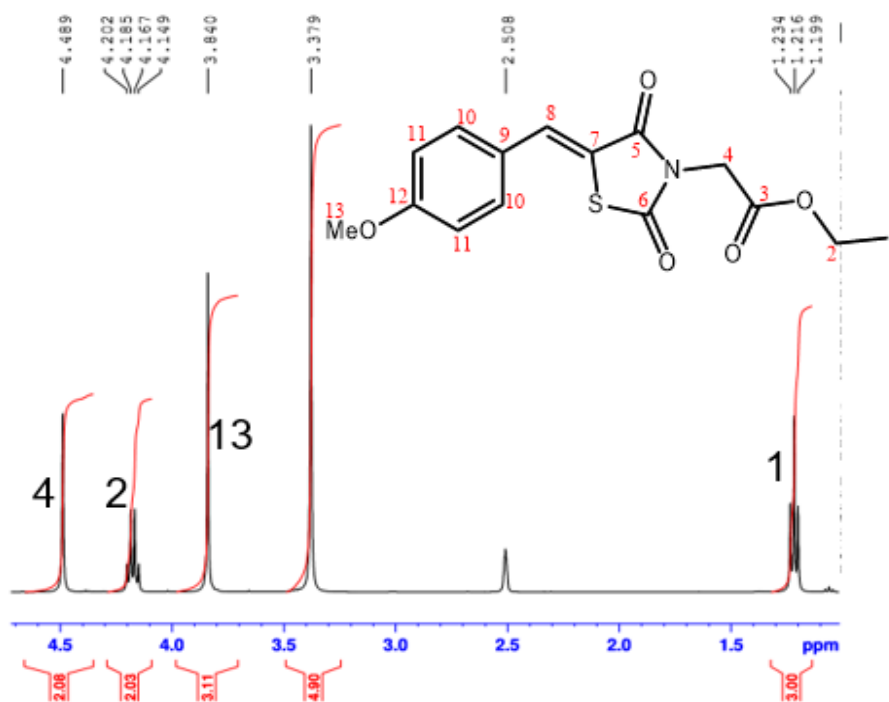


**Figure 4. 13:** <sup>1</sup>H NMR spectra of ethyl 2-(5-(4- methoxybenzylidene)-2,4-dioxothiazolidin-3-yl) acetate.

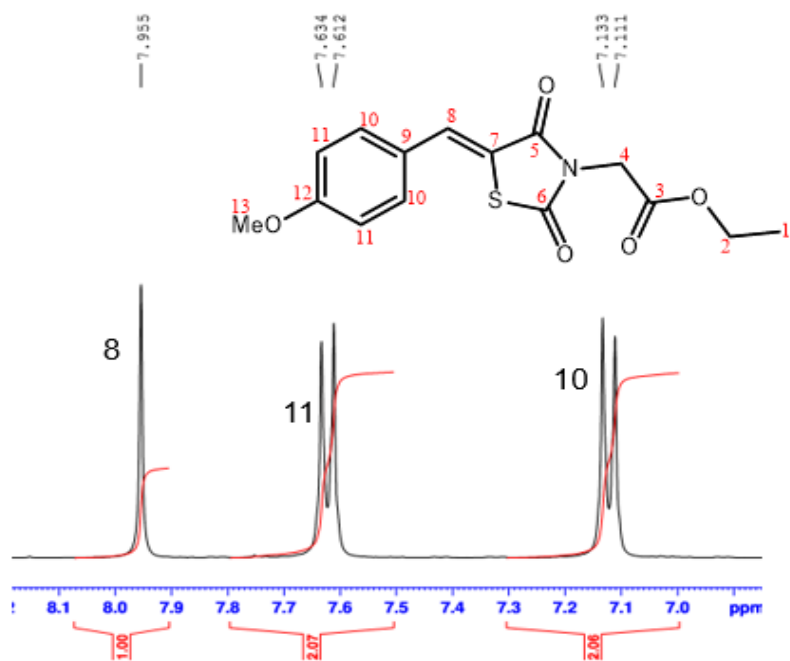


**Figure 4. 14:** <sup>1</sup>H NMR spectra of ethyl 2-(5-(4- methoxybenzylidene)-2,4-dioxothiazolidin-3-yl) acetate.

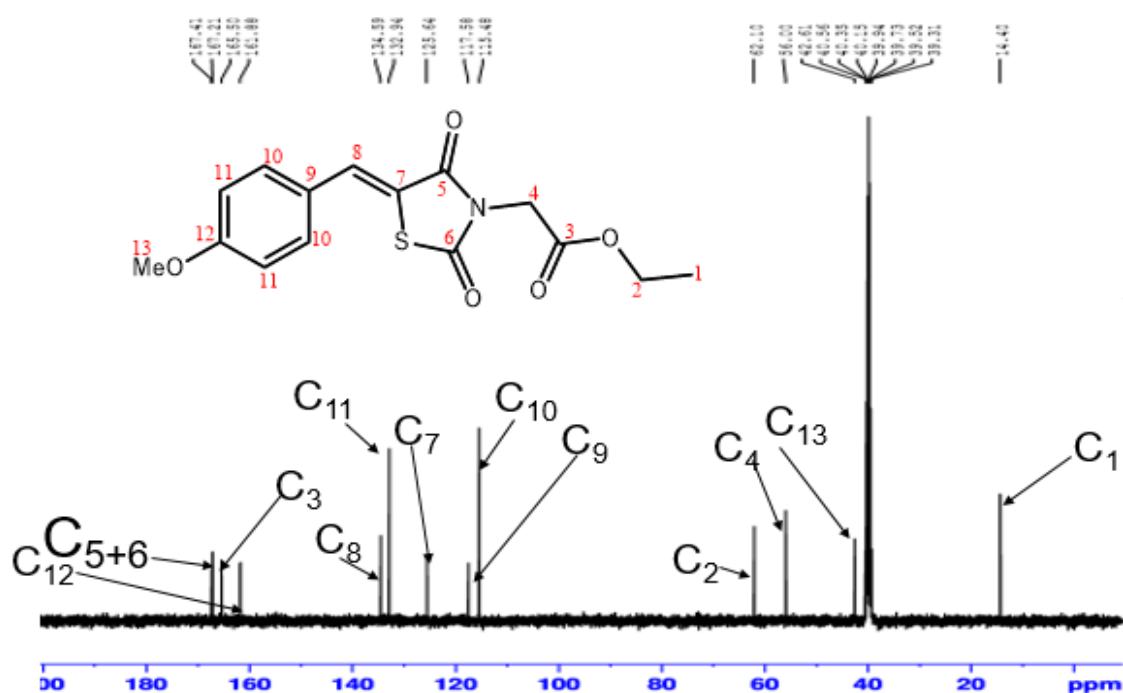
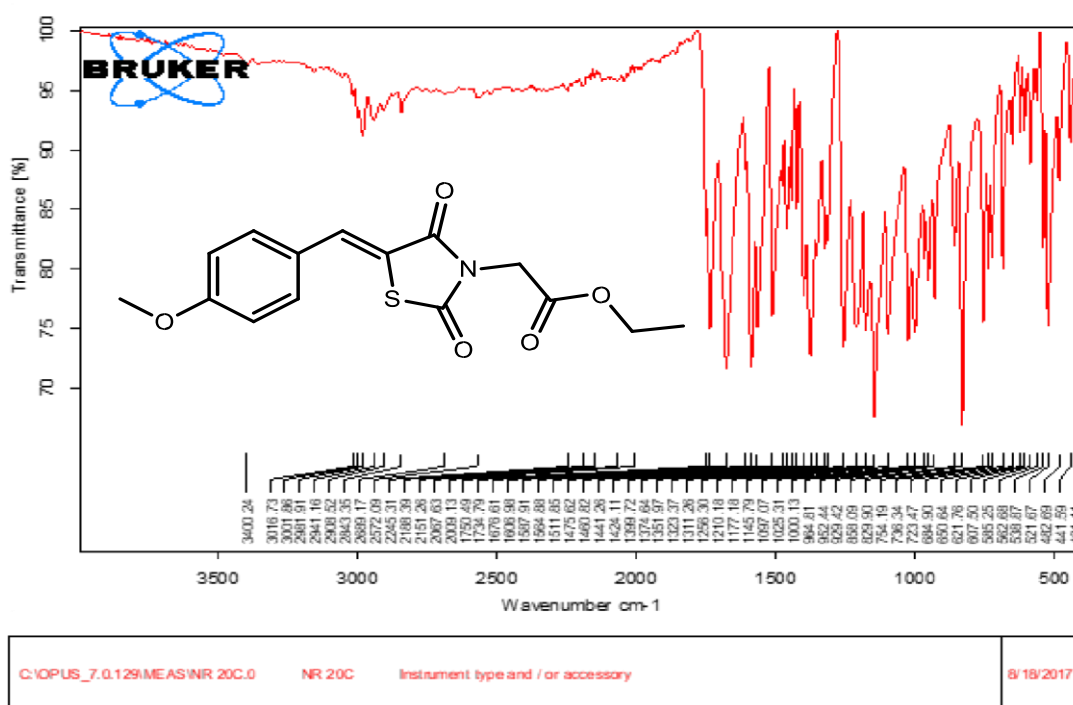


**Figure 4. 15:** <sup>13</sup>C NMR spectra of ethyl 2-(5-(4- methoxybenzylidene)-2,4-dioxothiazolidin-3-yl) acetate.



Page 1/1

**Figure 4. 16:** FT-IR spectra of ethyl 2-(5-(4- methoxybenzylidene)-2,4-dioxothiazolidin-3-yl) acetate.

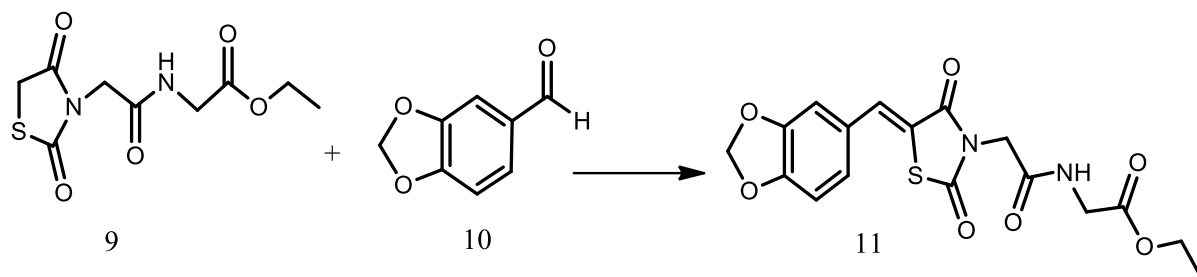
A shiny yellow solid product was formed with a 77 % yield. Mp 134.6-13.7°C (lit Mp= 129-131°C)<sup>88</sup>. **<sup>1</sup>H NMR (400 MHz, DMSO-d<sub>6</sub>)**, proton spectrum with seven peaks  $\delta$ H (ppm). Compound 8C gave rise to four peaks which are the same as compound 8A and 8B, which is a triplet, quartet, and two singlets for H<sub>1</sub>, H<sub>2</sub>, H<sub>4</sub>, and H<sub>8</sub>. Apart from those peaks compound 8C gave rise to a singlet proton (3H) at 3.840 for H<sub>13</sub>, doublet proton peak (2H) which are equivalent to each other ranging from 7.111 to 7.133 with a *J* value of 8.8 Hz and another doublet peak for two equivalent protons ranging from 7.622 to 7.634 with a *J* value of 8.8 Hz.

**<sup>13</sup>C NMR (100 MHz, DMSO-d<sub>6</sub>)**, carbon spectrum gave thirteen peak,  $\delta$ C (ppm) carbonyl carbon at 167.41 (C-6), 167.21 (C-5), 165.50 (C-3), 125.54 (C-7), 117.94 (C-9), 161.88 (C-12). CH at 134.59 (C-8), 115.48 (C-10), 132.94 (C-11), CH<sub>2</sub> at 62.10 (C-2), 54.00(C-4) and CH<sub>3</sub> at 14.40 (C- 1) and 42.61 (C-13).

The **IR (KBr cm<sup>-1</sup>)** spectra of the product show C-H of the aromatic ring at 3016, three carbonyl carbon (C=O) at (2941, 1734, 1677, 1606) and C-O.



#### 4.1.4. Ethyl 2-(2-(5-(Benzo[d][1,3] dioxol-5-ylmethylene)-2,4- dioxothiazolidin-3-yl)acetamido)acetate.



#### Scheme 7: Ethyl 2-(2-(5-(Benzo[d][1,3] dioxol-5-ylmethylene)-2,4- dioxothiazolidin-3-yl)acetamido)glycinate.

Reagents and conditions: Ethanol, piperidine, reflux 12 hours

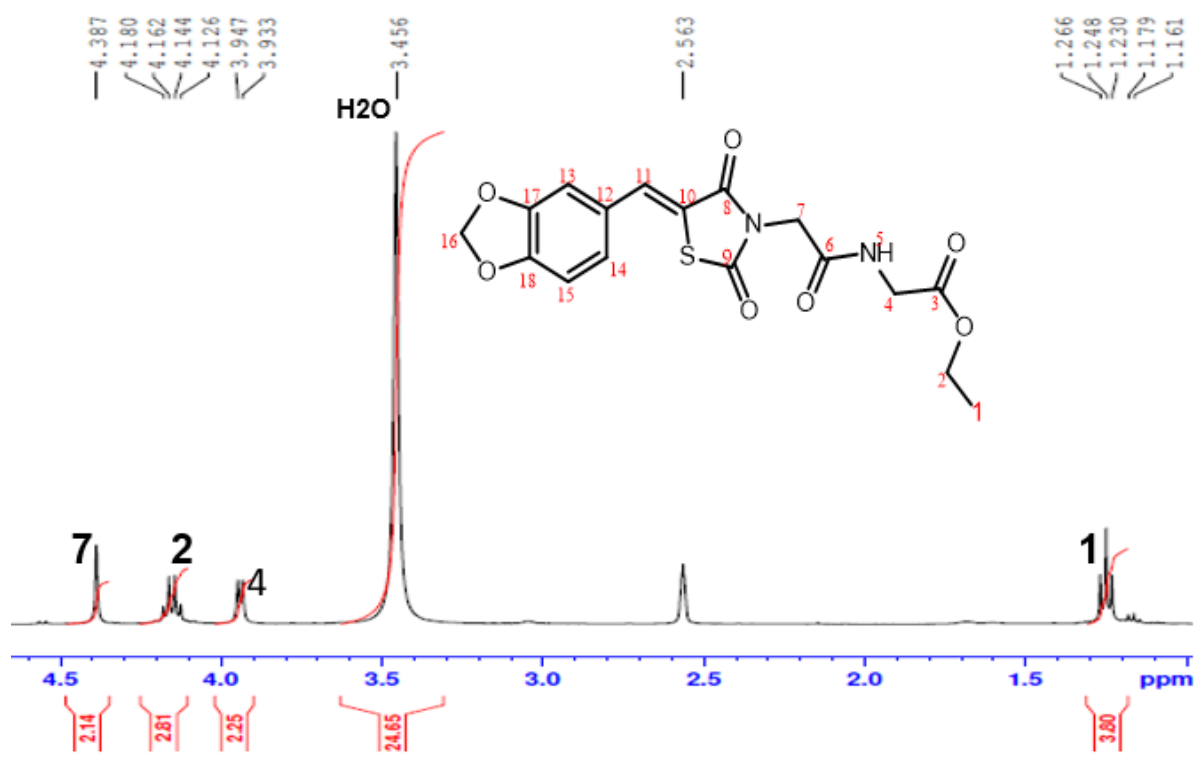
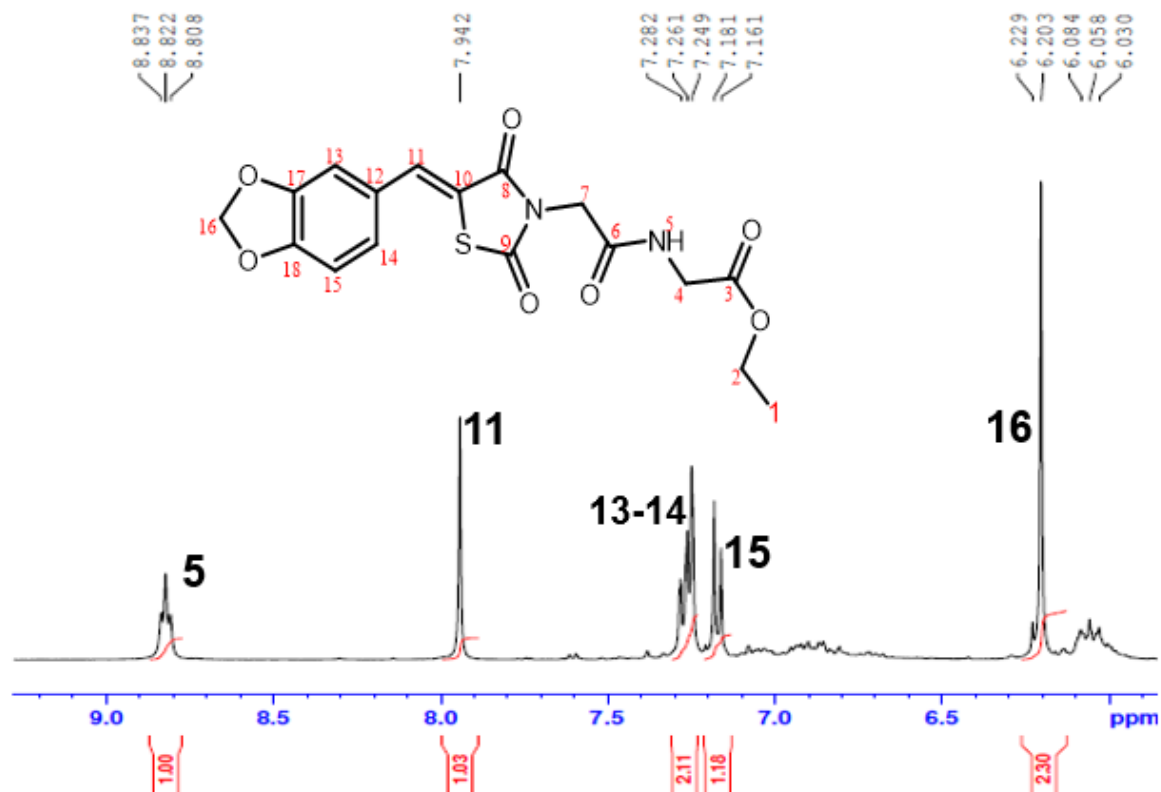
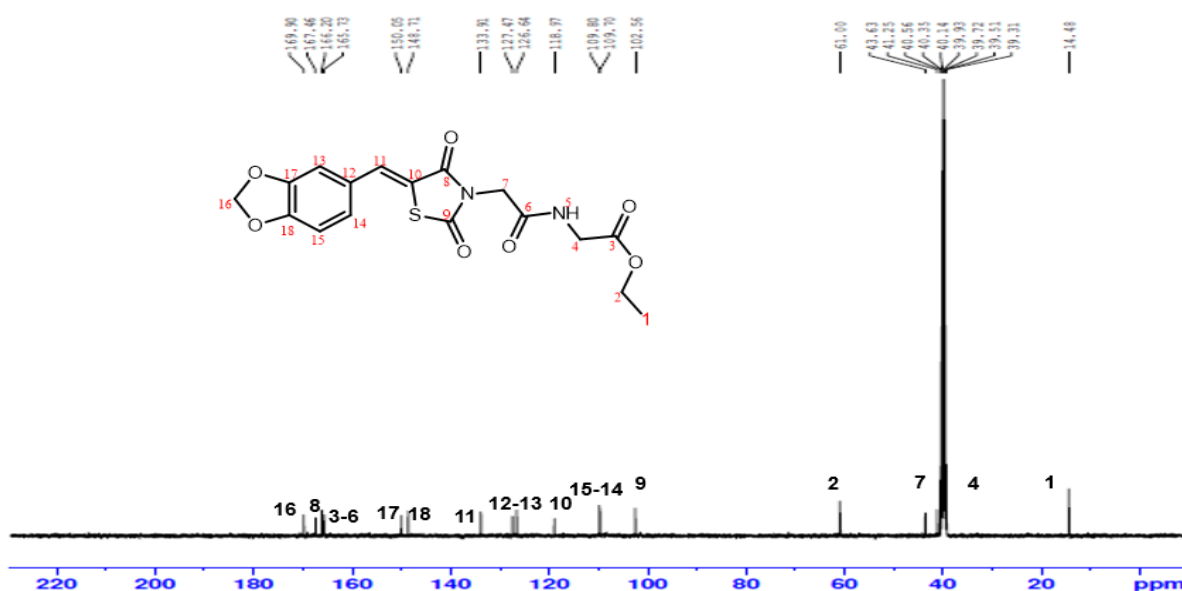


Figure 4. 17: <sup>1</sup>H NMR spectra of Ethyl 2-(2-(5-(Benzo[d][1,3] dioxol-5-ylmethylene)-2,4-dioxothiazolidin-3-yl)acetamido)acetate.



**Figure 4. 18:** <sup>1</sup>H NMR spectra ( aromatic expansion) of Ethyl 2-(2-(5-(Benzo[d][1,3] dioxol-5-ylmethylene)-2,4- dioxothiazolidin-3-yl)acetamido)acetate.



**Figure 4.19:** <sup>13</sup>C NMR spectrum of Ethyl 2-(2-(5-(Benzo[d][1,3] dioxol-5-ylmethylene)-2,4- dioxothiazolidin-3-yl)acetate.ylmethylene)-2,4- dioxothiazolidin-3-yl)acetamido)

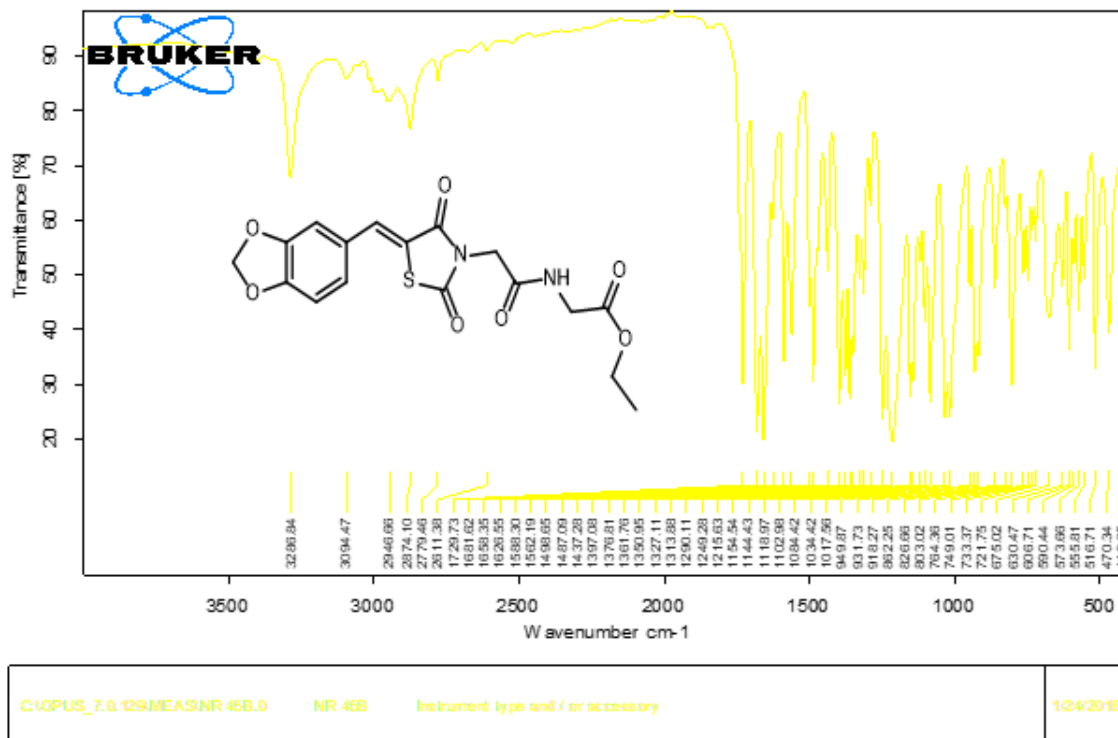


**Figure 4. 20:** FT-IR spectra of Ethyl 2-(2-(5-(Benzo[d][1,3] dioxol-5-ylmethylene)-2,4-dioxothiazolidin-3-yl)acetamido)acetate.

A yellow amorphous solid was formed with a 34% yield. Mp 211.6-212.9°C. <sup>1</sup>H NMR spectra of compounds **11** produce nine peaks. Compound **11** was characterized by the absence of the aldehydic proton peak confirming that benzaldehydes had been consumed. Another characterized was the presence of a downfield N-H proton at ~ 8.8 ppm (**H-5**) with a *J*value of 5.7Hz, appearing as a triplet arising due to coupling to the adjacent methylene protons. Also, <sup>1</sup>H NMR spectra of compound **11** indicated the appearance of a new methine proton as a singlet confirming the formation of a condensation product. Proton spectrum also indicates triplet peak ranging from 1.161 to 1.179ppm (3H) due to two neighboring proton with 7.1Hz, quartet peak (2H) ranging from 4.144 to 4.180ppm for H<sub>2</sub> with 7.1Hz. Proton spectrum shows 3 singlets from H<sub>7</sub>, H<sub>16</sub>, H<sub>11</sub> at 4.39, 6.20, 7.94ppm, and a multiplet peak at H<sub>13-14</sub> ranging from 7.249 to 7.282ppm.

<sup>13</sup>C NMR spectra of compound **11** indicate seventeen peaks. The carbon spectrum was characterized by the absence of the aldehydic carbon peak confirming consumption of benzaldehydes during the reactions according. Spectra were further characterized by the appearance of an extra methine carbon signal in the aromatic region confirming that the condensation reaction had taken place. Spectrum shows seven carbonyl carbon peaks from C-3, C-6, C-8, C-9, C-11, C-13, C-18 at 165.73, 166.20, 167.46, 102.56, 133.91,

126.64, 148.71ppm. CH for C-10, C-12, C-17 and C-16 at 118.97, 127.47, 150.05ppm, CH<sub>2</sub> at 61.00, 41.25, 43.63 and 109.70ppm for C-2, C-4, C-7, C-14 and CH<sub>3</sub> at 14.48ppm for C-1.

The **IR (KBr cm<sup>-1</sup>)** spectra of compound **11** showed the characteristic peaks for N-H stretching at 3287 and C=O stretching in the range of 1685-1730, C-H stretch from an aromatic ring at 3094, and C-O at 1155.

## 4.2. Gravimetric Analysis

The weight loss measurements were performed by weighing zinc and aluminum metal sheets before and after immersion in the absence and presence of various concentrations of the inhibitor at different temperatures. The experiment performed without the inhibitor was taken as the blank. The blank experiments involved immersing the metal sheets in 1.5M of hydrochloric acid at different temperatures. The inhibited experiments were performed in the presence of the inhibitor at the same temperature with the concentration of the HCl fixed to 1.5M for zinc metal was for 6 hours and aluminium metal was for 3 hours.

**Table 4. 1:** Weight loss measurements on zinc metal in the presence of EMDA and EBMDA as the corrosion inhibitor.

Temperature (°C)	Concentration (M)	EMDA	EBMDA
		Weight loss (g)	Weight loss (g)
30	Blank	0.232	0.232
	$1 \times 10^{-4}$	0.080	0.137
	$2 \times 10^{-4}$	0.074	0.136
	$3 \times 10^{-4}$	0.071	0.125
	$4 \times 10^{-4}$	0.057	0.111
	$5 \times 10^{-4}$	0.049	0.106
40	Blank	0.314	0.314
	$1 \times 10^{-4}$	0.123	0.139
	$2 \times 10^{-4}$	0.115	0.134
	$3 \times 10^{-4}$	0.086	0.130
	$4 \times 10^{-4}$	0.079	0.126
	$5 \times 10^{-4}$	0.069	0.115
50	Blank	0.541	0.541
	$1 \times 10^{-4}$	0.265	0.242
	$2 \times 10^{-4}$	0.247	0.222
	$3 \times 10^{-4}$	0.225	0.219
	$4 \times 10^{-4}$	0.197	0.204
	$5 \times 10^{-4}$	0.156	0.173
60	Blank	0.942	0.942
	$1 \times 10^{-4}$	0.492	0.271
	$2 \times 10^{-4}$	0.454	0.258
	$3 \times 10^{-4}$	0.411	0.245
	$4 \times 10^{-4}$	0.400	0.229
	$5 \times 10^{-4}$	0.377	0.208

**Table 4. 2:** Weight loss measurements on zinc metal in the presence of EBDA and EBDMDG as the corrosion inhibitor.

Temperature (°C)	Concentration (M)	EBDA	EBDMG
		Weight loss (g)	Weight loss (g)
30	Blank	0.232	0.232
	$1 \times 10^{-3}$	0.129	0.117
	$2 \times 10^{-3}$	0.121	0.114
	$3 \times 10^{-3}$	0.118	0.110
	$4 \times 10^{-3}$	0.117	0.109
	$5 \times 10^{-3}$	0.116	0.106
40	Blank	0.314	0.314
	$1 \times 10^{-3}$	0.147	0.159
	$2 \times 10^{-3}$	0.146	0.150
	$3 \times 10^{-3}$	0.145	0.138
	$4 \times 10^{-3}$	0.143	0.121
	$5 \times 10^{-3}$	0.139	0.118
50	Blank	0.541	0.541
	$1 \times 10^{-3}$	0.241	0.197
	$2 \times 10^{-3}$	0.233	0.156
	$3 \times 10^{-3}$	0.227	0.130
	$4 \times 10^{-3}$	0.218	0.091
	$5 \times 10^{-3}$	0.211	0.075
60	Blank	0.942	0.942
	$1 \times 10^{-3}$	0.360	0.492
	$2 \times 10^{-3}$	0.339	0.454
	$3 \times 10^{-3}$	0.294	0.411
	$4 \times 10^{-3}$	0.280	0.400
	$5 \times 10^{-3}$	0.209	0.377

**Table 4. 3:** Weight loss measurements on aluminium metal in the presence of EMDA and EBMDA as the corrosion inhibitor.

Temperature (°C)	Concentration (M)	EMDA	EBMDA
		Weight loss (g)	Weight loss (g)
30	Blank	0.6835	0.6835
	$1 \times 10^{-4}$	0.1049	0.0625
	$2 \times 10^{-4}$	0.0624	0.0616
	$3 \times 10^{-4}$	0.0623	0.0551
	$4 \times 10^{-4}$	0.0572	0.0537
	$5 \times 10^{-4}$	0.0478	0.0516
40	Blank	0.7351	0.7351
	$1 \times 10^{-4}$	0.0526	0.0898
	$2 \times 10^{-4}$	0.0474	0.797
	$3 \times 10^{-4}$	0.0472	0.0724
	$4 \times 10^{-4}$	0.0369	0.0610
	$5 \times 10^{-4}$	0.0312	0.0618
50	Blank	0.8051	0.8051
	$1 \times 10^{-4}$	0.0456	0.1207
	$2 \times 10^{-4}$	0.0413	0.1002
	$3 \times 10^{-4}$	0.0345	0.0956
	$4 \times 10^{-4}$	0.0329	0.0865
	$5 \times 10^{-4}$	0.0312	0.0686
60	Blank	0.8875	0.8875
	$1 \times 10^{-4}$	0.0476	0.3421
	$2 \times 10^{-4}$	0.0396	0.2814
	$3 \times 10^{-4}$	0.0290	0.2510
	$4 \times 10^{-4}$	0.0203	0.2459
	$5 \times 10^{-4}$	0.0082	0.1941

**Table 4. 4:** Weight loss measurements on aluminium metal in the presence of EBDA and EBDMDG as the corrosion inhibitor.

Temperature (°C)	Concentration (M)	EBDA	EBDMDG
		Weight loss (g)	Weight loss (g)
30	Blank	0.6835	0.6835
	$1 \times 10^{-4}$	0.1005	0.0365
	$2 \times 10^{-4}$	0.0915	0.0239
	$3 \times 10^{-4}$	0.0738	0.0173
	$4 \times 10^{-4}$	0.0690	0.0163
	$5 \times 10^{-4}$	0.0522	0.0135
40	Blank	0.7351	0.7351
	$1 \times 10^{-4}$	0.1016	0.0724
	$2 \times 10^{-4}$	0.0937	0.0688
	$3 \times 10^{-4}$	0.0747	0.0600
	$4 \times 10^{-4}$	0.0698	0.0471
	$5 \times 10^{-4}$	0.0603	0.0335
50	Blank	0.8051	0.8051
	$1 \times 10^{-4}$	0.1553	0.3135
	$2 \times 10^{-4}$	0.1061	0.1407
	$3 \times 10^{-4}$	0.0977	0.1297
	$4 \times 10^{-4}$	0.0831	0.1091
	$5 \times 10^{-4}$	0.0801	0.1044
60	Blank	0.8875	0.8875
	$1 \times 10^{-4}$	0.2227	0.3483
	$2 \times 10^{-4}$	0.1686	0.2168
	$3 \times 10^{-4}$	0.1142	0.1891
	$4 \times 10^{-4}$	0.1045	0.1008
	$5 \times 10^{-4}$	0.1000	0.0890

Tables 4.1-4.4 show the different concentrations of various inhibitors and the weight loss of zinc and aluminium metals at different temperatures (30, 40, 50, 60°C). There is a rapid decrease in the weight loss observed at different temperatures, for example, the weight loss at 30°C on blank was high but when the inhibitor is introduced the weight loss decreases, and when the concentration of inhibitor increases the weight loss of the metal decrease. When the temperature increases the weight loss of all inhibitors increased.

Inhibitor of EMDA at Table 4.1 for zinc metal; the weight loss decrease with an increase in concentration as it can be seen on results that the weight loss at 30°C without the inhibitor was 0.232g and decrease to 0.080g at  $1 \times 10^{-4}$ M; at  $2 \times 10^{-4}$ M was 0.074g, decrease to 0.071g at  $3 \times 10^{-4}$ M, at  $4 \times 10^{-4}$ M it decreased to 0.057g and when the concentration of the inhibitor increase to  $5 \times 10^{-4}$  the weight loss decrease to 0.049g. The same trend was observed on all inhibitors even on an inhibitor that has the concentration



of  $\times 10^{-3}$  for example in Table 4.2 EBDA inhibitor at  $30^{\circ}\text{C}$  with a concentration of  $1 \times 10^{-3}\text{M}$  weight loss was 0.1005g and decrease to 0.116g with an increase in the concentration of  $5 \times 10^{-3}\text{M}$ .

For aluminium metal in Table 4.3, EMDA it was 0.6835g without inhibitor immediately when the inhibitor is introduced it decrease to 0.1049 with a concentration of  $1 \times 10^{-4}$  at  $30^{\circ}\text{C}$ ; at  $2 \times 10^{-4}\text{M}$  it decreases to 0.1049, at  $3 \times 10^{-4}\text{M}$  was 0.0623g and decrease to 0.0478g when the concentration increases to  $5 \times 10^{-4}\text{M}$ . The same trend was observed using EBDA inhibitor at Table 4.4 weight loss decrease from 0.6835g using inhibitor concentration of  $1 \times 10^{-3}\text{M}$  to 0.1005g and even when the inhibitor increase to  $5 \times 10^{-3}\text{M}$  the weight loss of aluminium metal decrease to 0.0522g. This observation is due to the inhibitor adsorbing onto the metal surface forming a protective film and surface coverage of the inhibitor as its concentration increases<sup>89</sup>.

The increase in temperature however still resulted in an increase in the weight loss of the metal even in the presence of the inhibitors. From weight loss results corrosion rate, percentage inhibition efficiency, and surface coverage were calculated and summaries in Tables 4.5 and 4.8.

#### **4.2.1. Effect of temperature**

Weight loss analyses were also used to study the effect of temperature on corrosive metal with the presence of organic corrosion inhibitor. The effect of temperatures is to speed up a chemical reaction and to reduce oxygen solubility, which allows the cathodic reaction to occur<sup>90,91</sup>. Higher temperature also leads to an increase of diffusion, which allows an increase in transport of reactants and product on the metal surface<sup>90,92</sup>. From the results shown in Tables 4.5-4.8, it can be seen that the effect of temperature on the corrosion rate of blank decreases with of inhibitors, this is due to the inhibitors that isolated the metal from the solution. The inhibitor corrosion rate increase with an increase in temperature. The results below temperature indicate a negative and positive effect on inhibition efficiency.

#### 4.2.1.1. Zinc metal

**Table 4. 5:** Corrosion parameters for zinc in an aqueous solution of 1.5M HCl in the absence and presence of different concentrations of EMDA and EBMDA from weight loss of different temperature:

Inhibitor	Temperature (°C)	Inhibitor concentration (M)	Corrosion rate (g.cm <sup>-2</sup> .h <sup>-1</sup> )	Inhibition Efficiency (%)	Surface coverage (θ)
EMDA	30	Blank	0.00644	-	-
		1×10 <sup>-4</sup>	0.00222	65.53	0.6553
		2×10 <sup>-4</sup>	0.00206	68.01	0.6801
		3×10 <sup>-4</sup>	0.00197	69.41	0.6941
		4×10 <sup>-4</sup>	0.00158	75.47	0.7547
		5×10 <sup>-4</sup>	0.00136	78.88	0.7888
	40	Blank	0.00872	-	-
		1×10 <sup>-4</sup>	0.00342	60.82	0.6082
		2×10 <sup>-4</sup>	0.00319	63.38	0.6338
		3×10 <sup>-4</sup>	0.00239	72.61	0.7261
		4×10 <sup>-4</sup>	0.00219	74.85	0.7485
		5×10 <sup>-4</sup>	0.00192	78.02	0.7802
	50	Blank	0.015	-	-
		1×10 <sup>-4</sup>	0.00736	50.93	0.5093
		2×10 <sup>-4</sup>	0.00686	54.26	0.5426
		3×10 <sup>-4</sup>	0.00625	58.33	0.5833
		4×10 <sup>-4</sup>	0.00547	63.52	0.6352
		5×10 <sup>-4</sup>	0.00433	71.11	0.7111
	60	Blank	0.026	-	-
		1×10 <sup>-4</sup>	0.014	46.15	0.4615
		2×10 <sup>-4</sup>	0.013	50	0.50
3×10 <sup>-4</sup>		0.0114	56.15	0.5615	
4×10 <sup>-4</sup>		0.011	57.69	0.5769	
5×10 <sup>-4</sup>		0.010	61.54	0.6154	
EBMDA	30	Blank	0.00644	-	-
		1×10 <sup>-4</sup>	0.00381	40.94	0.4094
		2×10 <sup>-4</sup>	0.00378	41.34	0.4134
		3×10 <sup>-4</sup>	0.00347	46.12	0.4612
		4×10 <sup>-4</sup>	0.00308	52.16	0.5216
		5×10 <sup>-4</sup>	0.00294	54.31	0.5431
40	Blank	0.00872	-	-	
	1×10 <sup>-4</sup>	0.00386	55.73	0.5573	
	2×10 <sup>-4</sup>	0.00372	57.33	0.5733	
	3×10 <sup>-4</sup>	0.00361	58.60	0.5860	
		4×10 <sup>-4</sup>	0.0035	59.87	0.5987

EBMDA		$5 \times 10^{-4}$	0.00319	63.38	0.6338	
	50	Blank		0.015	-	-
		$1 \times 10^{-4}$		0.00672	55.19	0.5519
		$2 \times 10^{-4}$		0.00617	58.89	0.5889
		$3 \times 10^{-4}$		0.00608	59.45	0.5945
		$4 \times 10^{-4}$		0.00567	62.22	0.6222
		$5 \times 10^{-4}$		0.00481	67.96	0.6796
	60	Blank		0.026	-	-
		$1 \times 10^{-4}$		0.00753	71.05	0.7105
		$2 \times 10^{-4}$		0.00717	72.43	0.7243
		$3 \times 10^{-4}$		0.00681	73.82	0.7362
$4 \times 10^{-4}$			0.00636	75.53	0.7553	
$5 \times 10^{-4}$			0.00578	77.78	0.7778	

**Table 4.6:** The corrosion parameters for zinc in an aqueous solution of .5M HCl in the absence and presence of different concentrations of EBDA and EBDMDG from weight loss at different temperatures.

Inhibitor	Temperature (°C)	Inhibitor concentration (M)	Corrosion rate ( $\text{g.cm}^{-2}\text{h}^{-1}$ )	Inhibition Efficiency (%)	Surface coverage ( $\theta$ )	
EMDA	30	Blank	0.00644	-	-	
		$1 \times 10^{-3}$	0.00358	44.40	0.4440	
		$2 \times 10^{-3}$	0.00336	47.84	0.4784	
		$3 \times 10^{-3}$	0.00328	49.13	0.4913	
		$4 \times 10^{-3}$	0.00325	49.57	0.4957	
		$5 \times 10^{-3}$	0.00322	50.00	0.5000	
	40	Blank	0.00872	-	-	
		$1 \times 10^{-3}$	0.00408	53.19	$1 \times 10^{-3}$	
		$2 \times 10^{-3}$	0.00406	53.50	$2 \times 10^{-3}$	
		$3 \times 10^{-3}$	0.00403	53.82	$3 \times 10^{-3}$	
		$4 \times 10^{-3}$	0.00397	54.46	$4 \times 10^{-3}$	
		$5 \times 10^{-3}$	0.00386	55.73	$5 \times 10^{-3}$	
	50	Blank	0.015	-	-	
		$1 \times 10^{-3}$	0.00669	55.4	0.5540	
		$2 \times 10^{-3}$	0.00647	56.87	0.5687	
		$3 \times 10^{-3}$	0.00631	57.93	0.5793	
		$4 \times 10^{-3}$	0.00606	59.60	0.5960	
		$5 \times 10^{-3}$	0.00586	60.93	0.6093	
60	Blank	0.026	-	-		
	$1 \times 10^{-3}$	0.0100	61.54	0.6154		
	$2 \times 10^{-3}$	0.0094	63.85	0.6385		
	$3 \times 10^{-3}$	0.0082	68.46	0.6846		

		$4 \times 10^{-3}$	0.0077	70.38	0.7038
		$5 \times 10^{-3}$	0.0058	77.69	0.7769
EBDMDG	30	Blank	0.00644	-	-
		$1 \times 10^{-3}$	0.00331	48.76	0.4876
		$2 \times 10^{-3}$	0.0032	50.31	0.5031
		$3 \times 10^{-3}$	0.0031	51.86	0.5186
		$4 \times 10^{-3}$	0.0030	53.43	0.5343
		$5 \times 10^{-3}$	0.0029	54.97	0.5497
	40	Blank	0.00872	-	-
		$1 \times 10^{-3}$	0.0044	49.55	0.4955
		$2 \times 10^{-3}$	0.0042	51.85	0.5185
		$3 \times 10^{-3}$	0.0038	56.43	0.5643
		$4 \times 10^{-3}$	0.0034	61.02	0.6102
		$5 \times 10^{-3}$	0.0033	62.16	0.6216
	50	Blank	0.015	-	-
		$1 \times 10^{-3}$	0.0055	63.33	0.6333
		$2 \times 10^{-3}$	0.0044	70.67	0.7067
		$3 \times 10^{-3}$	0.0036	76.00	0.7600
		$4 \times 10^{-3}$	0.0025	83.33	0.8333
		$5 \times 10^{-3}$	0.0021	86.00	0.8600
	60	Blank	0.026	-	-
		$1 \times 10^{-3}$	0.0075	71.15	0.7115
		$2 \times 10^{-3}$	0.0068	73.85	0.7385
$3 \times 10^{-3}$		0.0058	77.69	0.7769	
$4 \times 10^{-3}$		0.0057	78.08	0.7808	
$5 \times 10^{-3}$		0.0053	79.62	0.7962	

The results in Table 4.5 indicates that EMDA inhibitor shows a different trend from the other three inhibitors EBMDA, EBDA, and EBDMDG. With EMDA, temperature has a negative effect on %IE, an increase in temperature leads to an increase of the dynamic energy for the inhibitor molecules which gives rise to the rate of collision with each other. The maximum %IE for EMDA, EBDA, EBDMDG, and EBMDA inhibitors for all metals was obtained at the highest concentration. The highest %IE for EMDA was at 30°C for 6 hours, the %IE decrease from 78.88% to 61.54% at 60°C. The decrease in the %IE of inhibitor indicates that the formation of protective film of the inhibitor to the metal surface is slow and delaying, the adsorption of this reaction is an exothermic reaction<sup>92</sup>.

A different trend was observed on EBMDA, EBDA, and EBDMDG inhibitor the %IE increases as the temperature increases, this means that the inhibitors are trying, by all

means, to form the protective films on the metals fast and facilitate. At 30°C the %IE for EBDA, EBMDA and EBDMDG was 54.31%, 50% and 54.97% increase to 77.78%, 77.69% and 79.62% at 60°C. The adsorption reaction that is occurring is endothermic. EBMDA, EBDA, and EBDMDG are the best inhibitor of zinc metal.

#### 4.2.1.2. Aluminium metal

**Table 4. 7:** Corrosion parameters for aluminium in an aqueous solution of 1.5M HCl in the absence and presence of different concentrations of EMDA and EBMDA from weight loss of different temperature

Inhibitor	Temperature (°C)	Inhibitor concentration (M)	Corrosion rate (g.cm <sup>-2</sup> .h <sup>-1</sup> )	Inhibition Efficiency (%)	Surface coverage (θ)
EMDA	30	Blank	0.0380	-	-
		1×10 <sup>-4</sup>	0.0058	84.74	0.8474
		2×10 <sup>-4</sup>	0.0035	90.79	0.9079
		3×10 <sup>-4</sup>	0.00346	90.89	0.9089
		4×10 <sup>-4</sup>	0.0032	91.58	0.9158
		5×10 <sup>-4</sup>	0.0027	92.89	0.9289
	40	Blank	0.0408	-	-
		1×10 <sup>-4</sup>	0.0029	92.89	0.9289
		2×10 <sup>-4</sup>	0.00263	93.55	0.9355
		3×10 <sup>-4</sup>	0.00262	93.57	0.9357
		4×10 <sup>-4</sup>	0.0020	94.97	0.9497
		5×10 <sup>-4</sup>	0.0017	95.82	0.9582
	50	Blank	0.0447	-	-
		1×10 <sup>-4</sup>	0.0025	94.41	0.9441
		2×10 <sup>-4</sup>	0.0023	94.85	0.9485
		3×10 <sup>-4</sup>	0.0019	95.75	0.9575
		4×10 <sup>-4</sup>	0.0018	95.97	0.9597
		5×10 <sup>-4</sup>	0.0017	96.20	0.9620
	60	Blank	0.0493	-	-
		1×10 <sup>-4</sup>	0.0022	94.72	0.9472
		2×10 <sup>-4</sup>	0.0026	95.54	0.9554
3×10 <sup>-4</sup>		0.0016	96.75	0.9675	
4×10 <sup>-4</sup>		0.0011	97.77	0.9777	
5×10 <sup>-4</sup>		0.0005	98.99	0.9899	
	30	Blank	0.0380	-	-
		1×10 <sup>-4</sup>	0.0035	90.79	0.9079
		2×10 <sup>-4</sup>	0.0034	91.05	0.9105
		3×10 <sup>-4</sup>	0.0031	91.84	0.9184
		4×10 <sup>-4</sup>	0.0030	92.11	0.9211

EBMDA		$5 \times 10^{-4}$	0.0029	92.37	0.9237	
	40	Blank		0.0408	-	-
		$1 \times 10^{-4}$		0.0050	87.75	0.8775
		$2 \times 10^{-4}$		0.0044	89.21	0.8921
		$3 \times 10^{-4}$		0.0040	90.20	0.9020
		$4 \times 10^{-4}$		0.0033	91.91	0.9191
		$5 \times 10^{-4}$		0.0034	91.67	0.9167
	50	Blank		0.0493	-	-
		$1 \times 10^{-4}$		0.0067	85.01	0.8501
		$2 \times 10^{-4}$		0.0056	87.47	0.8747
		$3 \times 10^{-4}$		0.0053	88.14	0.8814
		$4 \times 10^{-4}$		0.0048	89.26	0.8926
		$5 \times 10^{-4}$		0.0038	91.50	0.9150
	60	Blank		0.0493	-	-
		$1 \times 10^{-4}$		0.0190	61.46	0.6146
		$2 \times 10^{-4}$		0.0156	68.36	0.6836
		$3 \times 10^{-4}$		0.0139	71.80	0.7180
		$4 \times 10^{-4}$		0.0137	72.21	0.7221
$5 \times 10^{-4}$			0.0108	78.09	0.7809	

**Table 4. 8:** Corrosion parameters for aluminium in an aqueous solution of 1.5M HCl in the absence and presence of different concentrations of EBDA and EBDMDG from weight loss of different temperature

Inhibitor	Temperature (°C)	Inhibitor concentration (M)	Corrosion rate ( $\text{g.cm}^{-2}\text{.h}^{-1}$ )	Inhibition Efficiency (%)	Surface coverage ( $\theta$ )	
EBDA	30	Blank	0.0380	-	-	
		$1 \times 10^{-3}$	0.0056	85.26	0.8526	
		$2 \times 10^{-3}$	0.0051	86.57	0.8657	
		$3 \times 10^{-3}$	0.0041	89.11	0.8911	
		$4 \times 10^{-3}$	0.0038	90.00	0.9000	
		$5 \times 10^{-3}$	0.0029	92.37	0.9237	
	40	Blank	0.0408	-	-	
		$1 \times 10^{-3}$	0.0056	86.27	0.8627	
		$2 \times 10^{-3}$	0.0052	87.25	0.8725	
		$3 \times 10^{-3}$	0.0041	89.71	0.8971	
		$4 \times 10^{-3}$	0.0039	90.44	0.9044	
		$5 \times 10^{-3}$	0.0034	91.67	0.9167	
	50	Blank	0.0447	-	-	
		$1 \times 10^{-3}$	0.0064	80.76	0.8076	
		$2 \times 10^{-3}$	0.0059	86.80	0.8680	
		$3 \times 10^{-3}$	0.0054	87.92	0.8792	

EBDMDG		$4 \times 10^{-3}$	0.0046	89.71	0.8971
		$5 \times 10^{-3}$	0.0045	89.93	0.8993
	60	Blank	0.0493	-	-
		$1 \times 10^{-3}$	0.0124	74.85	0.7485
		$2 \times 10^{-3}$	0.0094	80.93	0.8093
		$3 \times 10^{-3}$	0.0071	85.60	0.8560
		$4 \times 10^{-3}$	0.0058	88.24	0.8824
		$5 \times 10^{-3}$	0.0056	88.64	0.8864
		30	Blank	0.0380	-
	$1 \times 10^{-3}$		0.0020	94.74	0.9474
	$2 \times 10^{-3}$		0.0013	96.58	0.9658
	$3 \times 10^{-3}$		0.0010	97.37	0.9737
	$4 \times 10^{-3}$		0.0009	97.63	0.9763
$5 \times 10^{-3}$	0.0007		97.89	0.9789	
40	Blank	0.0408	-	-	
	$1 \times 10^{-3}$	0.0040	90.20	0.9020	
	$2 \times 10^{-3}$	0.0038	90.69	0.9069	
	$3 \times 10^{-3}$	0.0035	91.11	0.9111	
	$4 \times 10^{-3}$	0.0026	93.63	0.9363	
	$5 \times 10^{-3}$	0.0019	95.34	0.9534	
50	Blank	0.0493	-	-	
	$1 \times 10^{-3}$	0.0174	61.07	0.6107	
	$2 \times 10^{-3}$	0.0078	82.55	0.8255	
	$3 \times 10^{-3}$	0.0072	83.89	0.8389	
	$4 \times 10^{-3}$	0.0061	86.35	0.8635	
	$5 \times 10^{-3}$	0.0053	87.02	0.8702	
60	Blank	0.0493	-	-	
	$1 \times 10^{-3}$	0.0194	60.65	0.6065	
	$2 \times 10^{-3}$	0.0120	75.66	0.7566	
	$3 \times 10^{-3}$	0.0105	78.70	0.7870	
	$4 \times 10^{-3}$	0.0056	88.64	0.8864	
	$5 \times 10^{-3}$	0.0049	90.06	0.9006	

Tables 4.7-4.8 show the result of %IE for aluminium metal where the EMDA inhibitor increase with an increase in temperature. From Table 4.7 at 30°C the highest %IE was 92.89 increase to 98.99% at 60°C. The different trend on %IE for EBDA, EBDMDG, and EBMDA decreases with an increase in temperature. For example in table 4.8 at 30°C the highest %IE of EBDA was 92.37% and decrease to 88.64%. From the result, EMDA is the best inhibitor because it contains the highest %IE at the highest temperature of the study.

## 4.2.2. Effect of inhibitor concentration

Higher concentration there is greater availability of inhibitor molecules than at a lower concentration. The presence of more inhibitor molecules leads to a greater tendency of adsorption of inhibitor molecules on the surface of the metal and providing large surface coverage<sup>93</sup>. The fact that the weight loss is decreased with the increase in the inhibitor concentration indicates that the corrosion rate is reduced. From the corrosion rate %IE was calculated and plotted against inhibitor concentrations to explain the effect of inhibitor concentration on %IE.

### 4.2.2.1. Zinc metal

Below is the graph of concentration against %IE of zinc metal which was used to explain the effect of concentration on the metal.

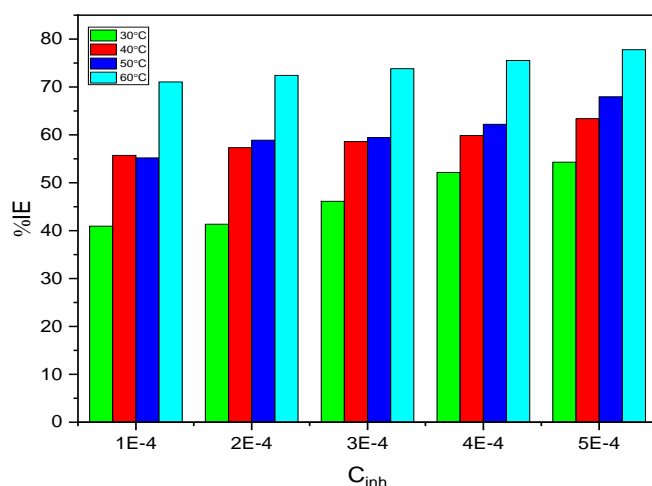


**Figure 4.21:** The graph of inhibition efficiency using EMDA at different temperature



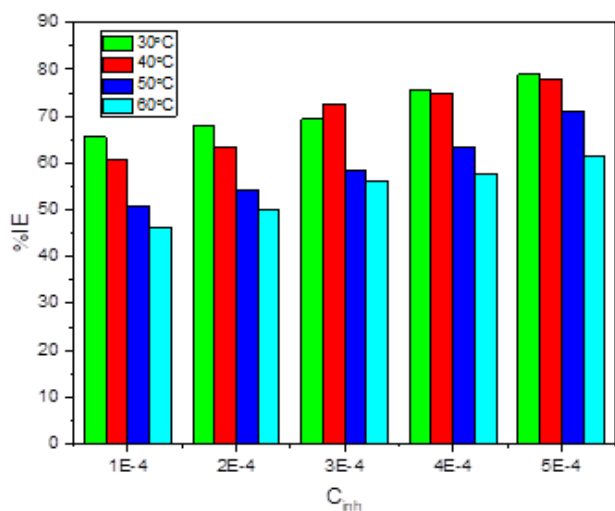


**Figure 4.22:** The graph of inhibition efficiency using EBMDA at different temperature

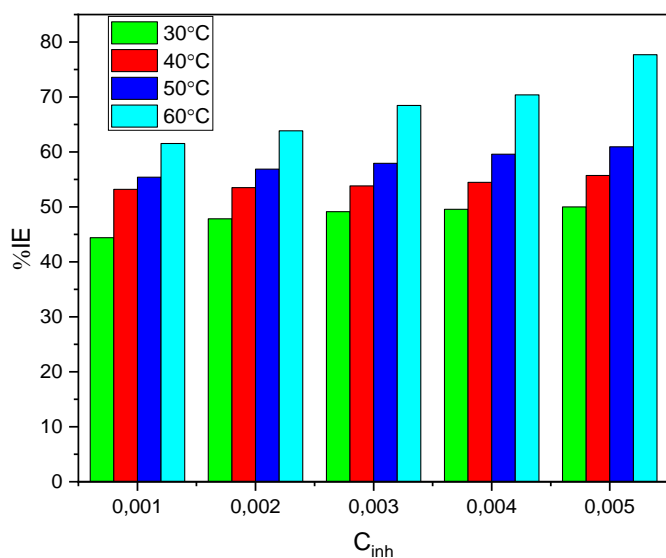


**Figure 4.23:** Graph of inhibition efficiency using EBDA at different temperature

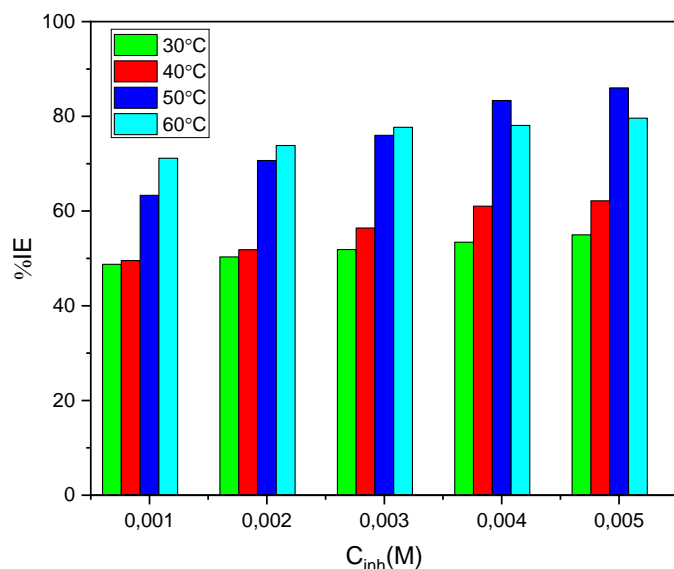


**Figure 4.24:** Graph of inhibition efficiency using EBDMDG at different temperature

The corrosion rate for zinc in 1.5M without the concentration of the inhibitor was higher 0.00644, 0.00872, 0.0150, and 0.0260  $\text{g.cm}^{-2}.\text{h}^{-1}$  at 30°C, 40°C, 50°C and 60°C. However, when the concentration of inhibitors was introduced, the corrosion rate was also reduced. The corrosion rate of zinc metal in the presence of EMDA, EBMDA it was 0.010 and 0.0057  $\text{g.cm}^{-2}.\text{h}^{-1}$  at 60°C with the highest concentration of  $5 \times 10^{-4}\text{M}$ . 0.00586 and 0.0021  $\text{g.cm}^{-2}.\text{h}^{-1}$  at 50°C with  $5 \times 10^{-3}\text{M}$  in the presence of EBDA and EBDMDG. When the corrosion rate decrease the percentage inhibition efficiency increases with an increase in the concentration of inhibitor.

The inhibiting effect increased with the increase of EMDA, EBDA, EBMDA, EBDMDG concentration as shown in figures 4.21-4.24. It was obvious that there was an ascending order in the %IE with an increasing concentration for all inhibitors. Inhibition efficiency for EBDMDG inhibitor in figure 4.24 as an example at 30°C with a concentration of  $1 \times 10^{-3}\text{M}$  was 48.70%; at  $3 \times 10^{-3}\text{M}$  was 51.86% and  $4 \times 10^{-3}\text{M}$  was 54.97%, and increase to 79.62% at  $5 \times 10^{-3}\text{M}$  concentration. At 60°C with the lowest inhibitor concentration, it was 46.15% and 40.94% increase to 61.54% and 77.78% at the highest concentration of  $5 \times 10^{-4}\text{M}$  in the presence of EMDA and EBMDA inhibitor.

#### 4.2.2.2 Aluminium metal

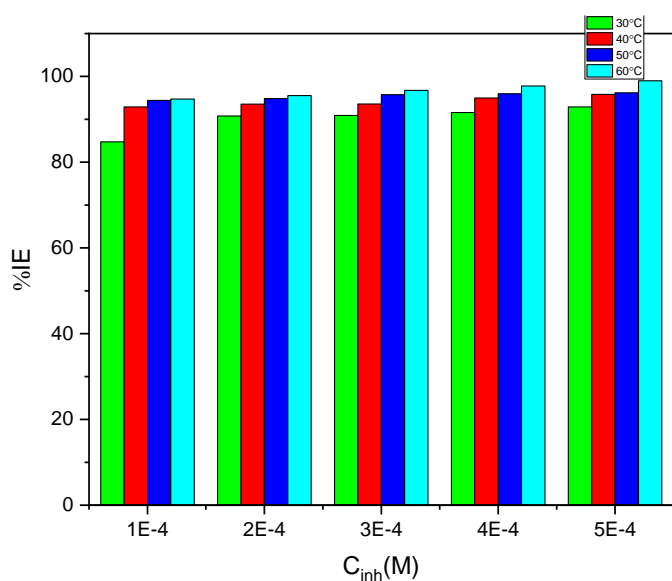


**Figure 4.25:** The graph of inhibition efficiency on aluminium using EMDA at different temperatures.

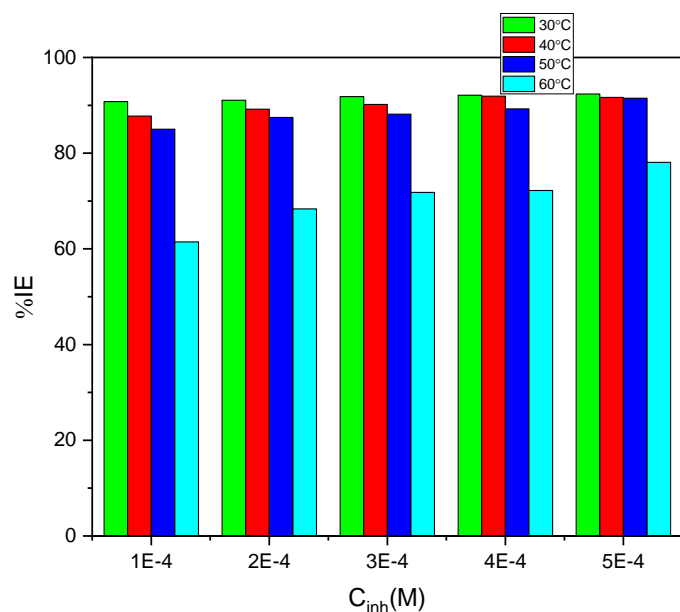


**Figure 4.26:** The graph of inhibition efficiency on aluminium using EBMDA at different temperatures.

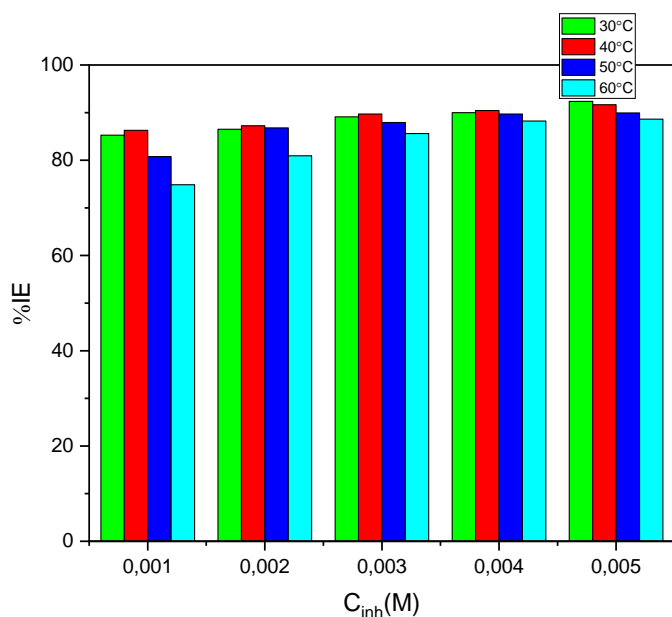


**Figure 4.27:** The graph of inhibition efficiency on aluminium using EBDA at different temperatures.

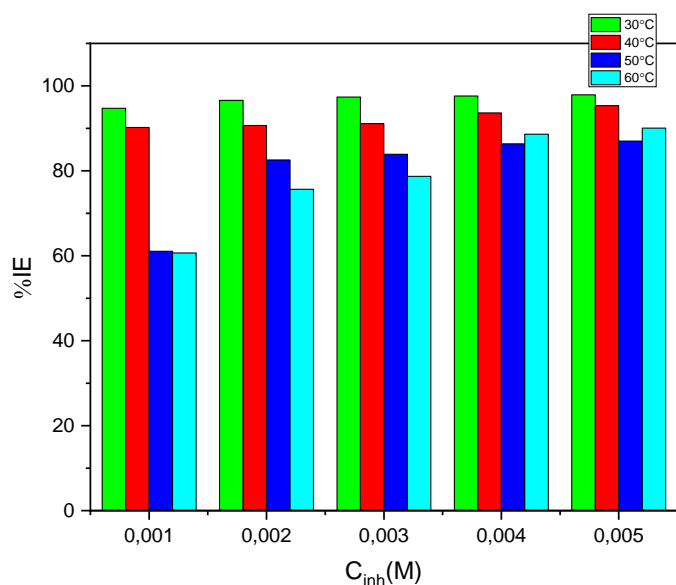


**Figure 4.28:** The graph of inhibition efficiency on aluminium using EBDA at different temperatures.

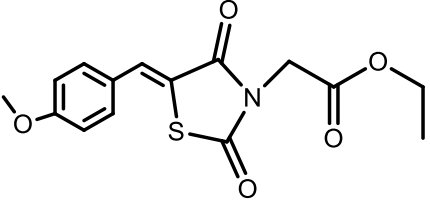
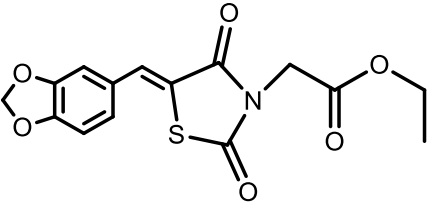
The corrosion rate for the aluminium metal in 1.5M was 0.0380, 0.0408, 0.0447, and 0.0493 g.cm<sup>-2</sup>. h<sup>-1</sup> with respectively to 30°C, 40°C, 50°C and 60°C without concentration inhibitors. However when the EBDA and EBDMDG inhibitor concentration is added the corrosion rate decrease to 0.00075 and 0.0029 g.cm<sup>-2</sup>. h<sup>-1</sup> at 30°C with the highest concentration of 5×10<sup>-3</sup>M. In the presence of EMDA and EBMDA at 40°C with 5×10<sup>-4</sup>M was 0.0017 and 0.0034 g.cm<sup>-2</sup>. h<sup>-1</sup>.

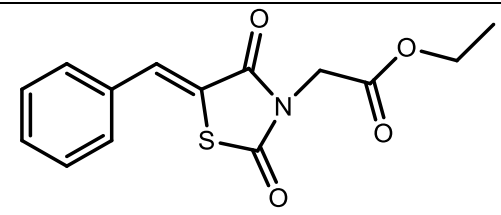
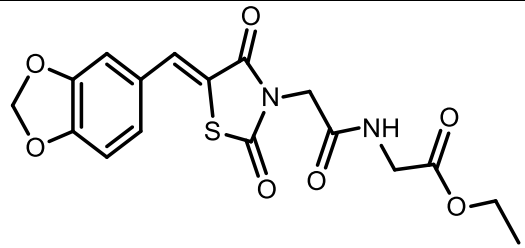
Figure 4.25-4.26 shows the %IE for EMDA and EBMDA against inhibitor concentration. When the inhibitor concentration increases the %IE also increases. The %IE for EMDA was 84.74, 90.79, 90.89, 91.58, and 92.89% at 30°C with a concentration of  $1 \times 10^{-4}$ M,  $2 \times 10^{-4}$ M,  $3 \times 10^{-4}$ M,  $4 \times 10^{-4}$ M,  $5 \times 10^{-4}$ M. In the presence of EBMDA the %IE was 90.79%, 91.05%, 91.84%, 92.11, 92.37%. EBDA and EBDMDG inhibitor concentration show the same trend at 30°C the %IE increase with inhibitor concentration, at the lowest concentration ( $1 \times 10^{-3}$ M) for EBDA and EBDMDA it was 85.26%, 94.74% and increase to 92.37%, 97.89% at the highest temperature of  $5 \times 10^{-3}$ M.

#### 4.2.3. Effects of molecular structures

The mechanism action of organic corrosion inhibitors is based on the adsorption surface to form a protective film that displaces water from the metal surface and protects it against decomposition<sup>65</sup>. The inhibition efficiency is influenced by several adsorption sites, their charge density, and molecular size, the heat of hydrogenation, and mode of interaction with the metal surface. Inhibition of the corrosion process takes place through two effects including blocking and hydrophobic effects<sup>93, 94</sup>. The process occurs when the inhibitor molecule is adsorbed on the metal surface.

**Table 4. 9:** The abbreviations and molecular structures of the acetate and glycinate compounds.

Abbreviation	Molecular structure
EMDA	
EBMDA	

EBDA	
EBDMDG	

In the study (EMDA, EBMDA, EBDA, EBDMDG) inhibitors there were more O-atom, one or more N-atom, and only S-atom which act as adsorption centers. Those inhibitors were hydrophobic the interface by the hydrophobic group. When (EMDA, EBMDA, EBDA, and EBDMDG) were dissolved in water they form the hydrophobic group in the solvent that increase the free energy of the system.

According to the molecular structures of the inhibitors, there were  $\pi$ -electrons in the aromatic ring and active adsorption centers. All the inhibitors play a part in strong adsorption on the metal surface. EMDA consists of 5 O-atom, only one N-atom, and S-atom, while EBMDA has 6 O-atom, one N-atom, and only S-atom in which they will be adsorbed on the metal surface.

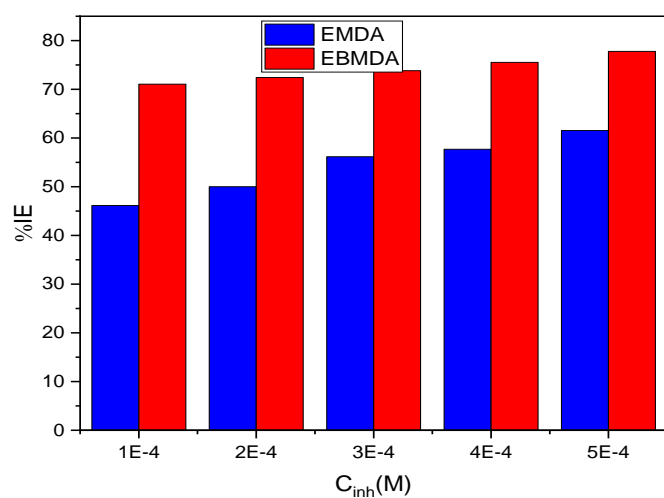


**Figure 4. 29:** Graph of inhibition efficiency using EMDA and EBMDA as a corrosion inhibitor at 60°C.

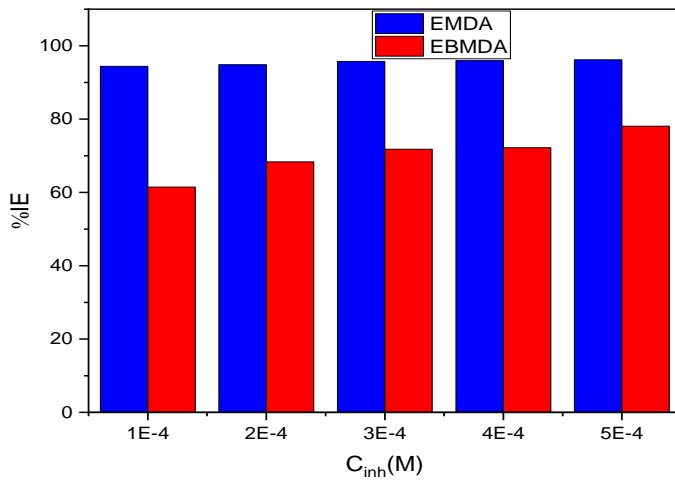


**Figure 4. 30:** Graph of inhibition efficiency on aluminium metal using EMDA and EBMDA inhibitor at 60°C

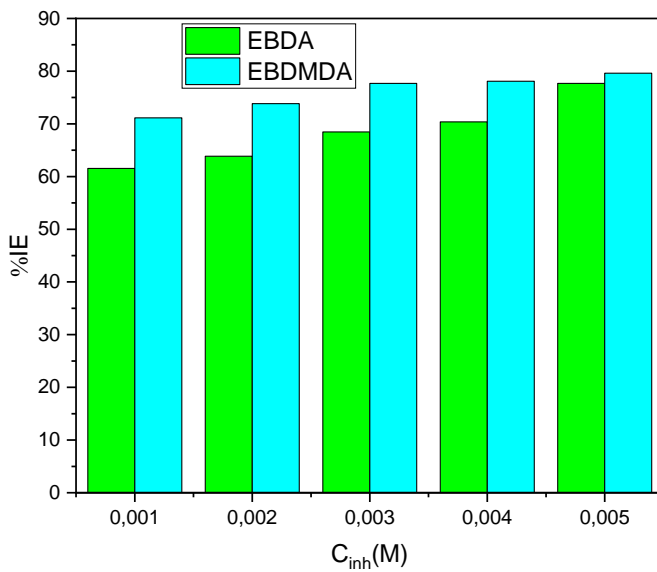


**Figure 4.31:** Graph of inhibition efficiency on zinc metal using EBDA and EBDMDG inhibitor at 60°C.

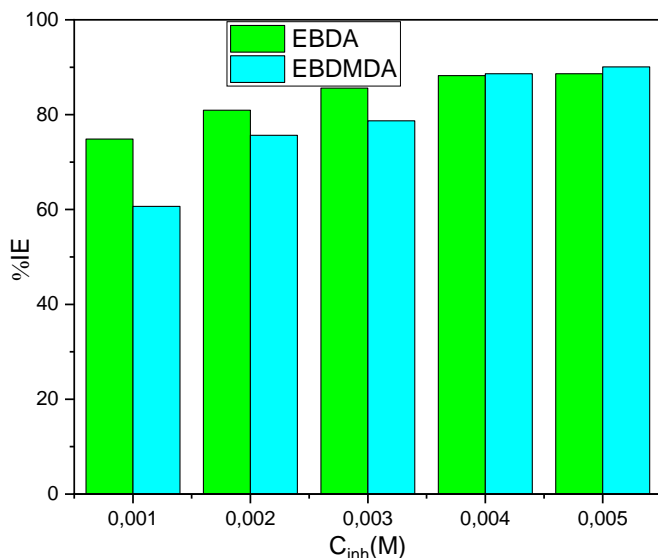


**Figure 4.32:** Graph of inhibition efficiency on aluminium metal EBDA and EBDMDG inhibitor at 60°C.

It can be noted in figure 4.29 between the %IE of EMDA and EBMDA which used the same concentration that, EBMDA has a good inhibition efficiency because when the temperature increases its also increase with %IE, not like EMDA on zinc metal. EBMDA at 30°C the highest %IE was 54.31% and 77.78% at 60°C, while EMDA at 30°C it was 78.88% and decrease to 61.54% at 60°C. Figure 4.30 for aluminium metal EMDA and EBMDA gave different trend EMDA was having the highest %IE than EBMDA this is because EMDA contains electron releasing which is methoxy (-OCH<sub>3</sub>).

Figure 4.31 It can be noted that the %IE of EBDA(77.69%) and EBDMDG (86.00%) on zinc metal at the highest inhibitor concentration ( $5 \times 10^{-3}M$ ) at 60°C increase with the increasing number of functional groups(oxygen, nitrogen, and sulphur) which cause the adsorption on the metal surface<sup>95-97</sup>. EBDMDG consists of amino that increases the electron density at the active site that favours inhibitor and metal interaction. This was the reason why EBDMDG has a higher %IE. The same trend was observed on aluminum metal in figure 4.32, EBDA (88.64%) and EBDMDG (90.06%).

#### 4.3. Adsorption Isotherm and Thermodynamic Parameters for zinc and aluminium

The adsorption isotherm is the primary step for the interaction of organic inhibitor with the metal surface and it depends on the type of metal, the chemical structure of the inhibitor, and the type of electrolyte. The degree of surface coverage obtained from weight loss at different concentration of inhibitors and different temperature were used to determine the



type of adsorption isotherm. The best relationship between the results and isotherm functions was obtained by Langmuir adsorption<sup>95</sup>. The Langmuir produced the best linear relationships, Langmuir adsorption equation relating the concentration of inhibitors to their surface coverage is indicated in the equation below.

$$\frac{C_{inh}}{\theta} = \frac{1}{K_{ads}} + C_{inh} \quad (20)$$

where:  $C_{inh}$  = concentration of the inhibitor

$\theta$  = degree of the surface coverage

$K_{ads}$  = adsorption equilibrium constant which can be obtained from the intercept of the straight line.  $K_{ads}$  is associated with the standard free energy of adsorption ( $\Delta G_{ads}$ ) and given by the equation shown below.

$$K_{ads} = \frac{1}{55.55} \exp\left(-\frac{\Delta G}{RT}\right) \quad (21)$$

where: R = Universal gas constant

T = Absolute temperature

55.5 = Molar concentration of water<sup>66</sup>

The values of ( $\Delta G_{ads}$ ) are recorded in the tables below.

#### 4.3.1. Zinc metal

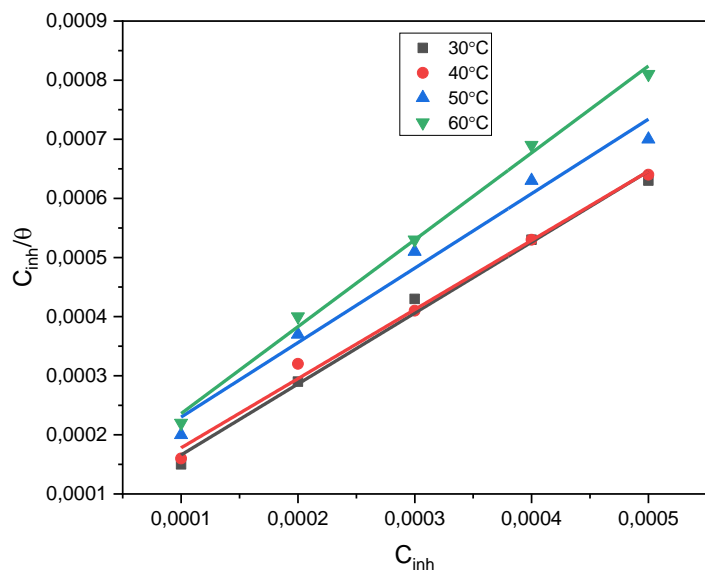


**Figure 4. 33:** Langmuir adsorption isotherm for the adsorption of EMDA on zinc metal.

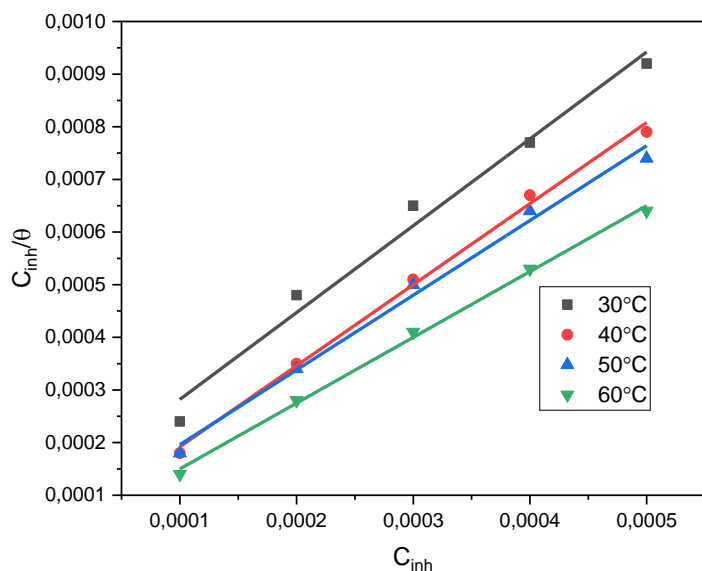


**Figure 4. 34:** Langmuir adsorption isotherm for the adsorption of EBMDA on zinc metal.

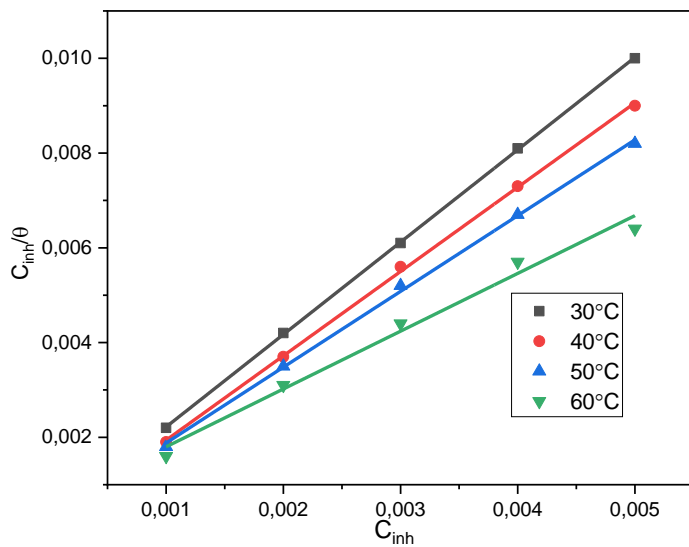


**Figure 4. 35:** Langmuir adsorption isotherm for the adsorption of EBDA on zinc metal.

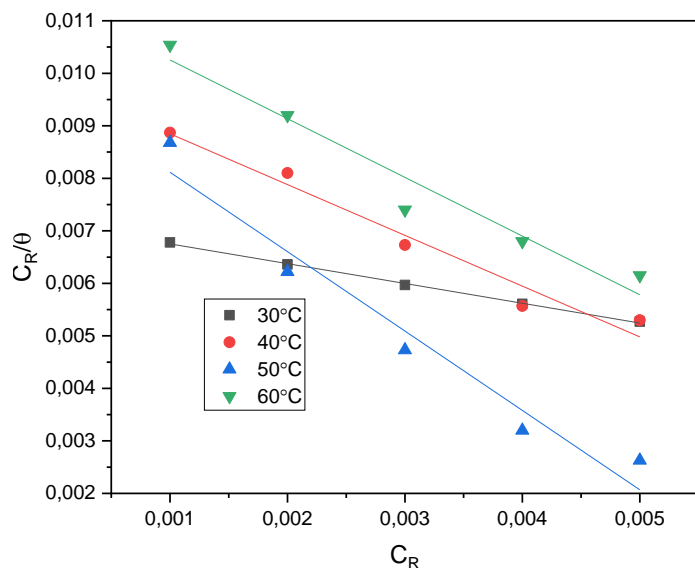


**Figure 4. 36:** Langmuir adsorption isotherm for the adsorption of EBDMDG on zinc metal.

**Table 4. 10:** Adsorption parameters from Langmuir Adsorption Isotherm plots for EMDA, EBMDA, EBDA, and EBDMDG on Zinc metal.

Inhibitor	Temperature(°C)	$K_{ads}(L/mol)$	$-\Delta G^{\circ}_{ads}(kJ.mol^{-1})$
EMDA	30°C	21.74	17.88
	40°C	16.39	17.73
	50°C	9.62	16.87
	60°C	11.24	17.82
EBMDA	30°C	8.55	15.52
	40°C	26.32	18.97
	50°C	18.52	18.63
	60°C	40	21.34
EBDA	30°C	3.70	13.42
	40°C	6.25	15.22
	50°C	5.7	15.46
	60°C	1.72	12.62
EBDMDG	30°C	0.140	5.17
	40°C	0.102	4.51
	50°C	0.104	4.71
	60°C	0.088	4.39

The values of change in Gibbs energy of adsorption of all inhibitors on zinc obtained are negative which indicates the spontaneous process and the strong interaction that occurred between the molecules of the inhibitors and Zinc surface. The values of  $\Delta G_{ads}$  that are around -20 kJ/mol are generally consistent with physical adsorption (physisorption process) which is a process that possesses weak Van Der Waals interaction rather than chemical bonding and those that are around -40 kJ/mol or even higher are consistent with the chemical adsorption (chemisorption process) that occurs with the sharing or transfer of an electron from the organic molecules with the surface of the metal<sup>67</sup>. In Table 4.9, the  $\Delta G_{ads}$  for the inhibitors were closer to -20 kJ/mol which indicates the physisorption process on zinc.

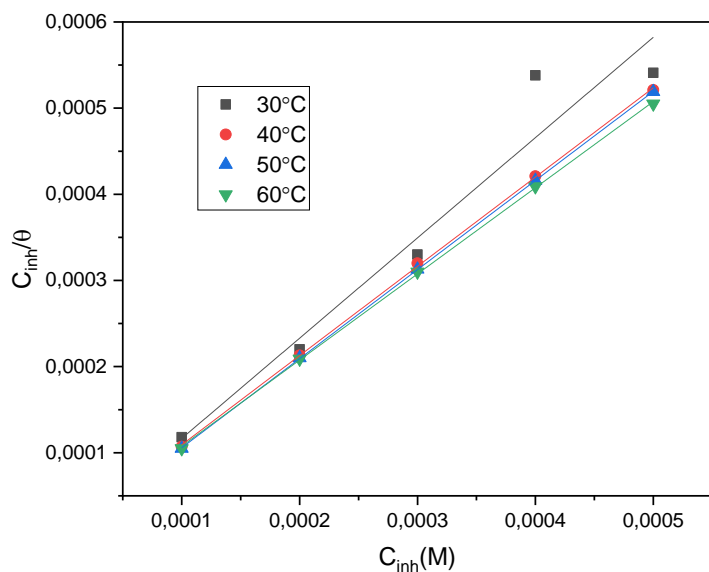


**Figure 4. 37:** Langmuir adsorption isotherm for the adsorption of EMDA on aluminium metal.

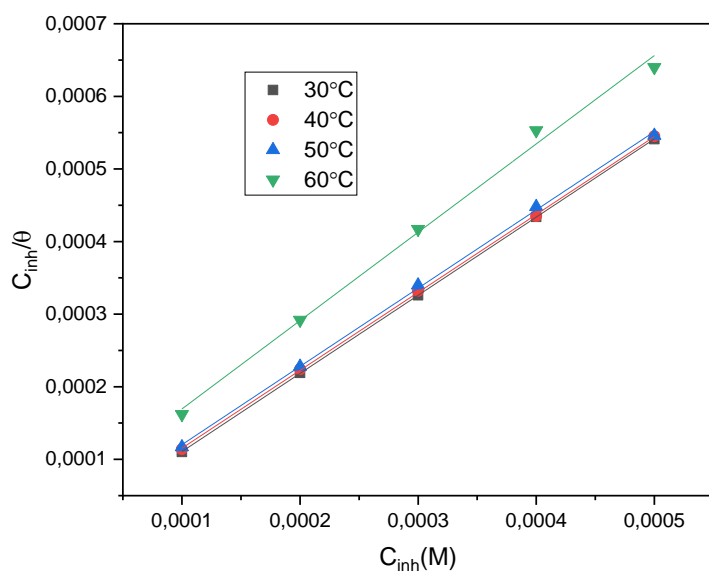


**Figure 4. 38:** Langmuir adsorption isotherm for the adsorption of EBMDA on aluminium metal.

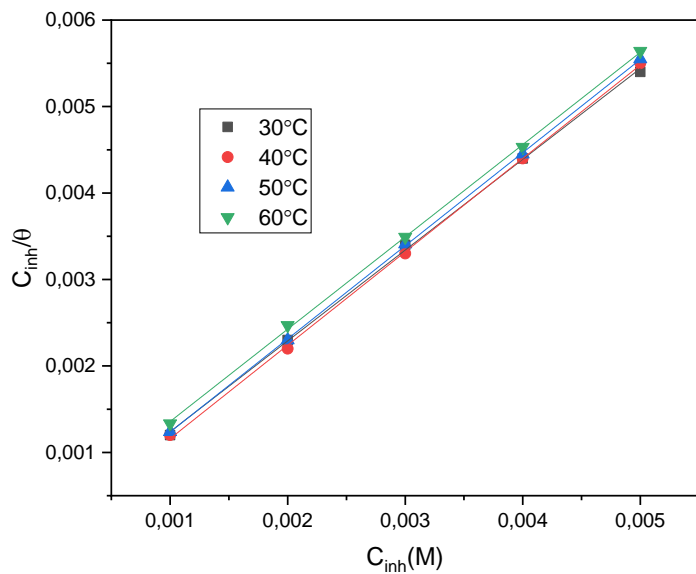


**Figure 4. 39:** Langmuir adsorption isotherm for the adsorption of EBDA on aluminium metal.

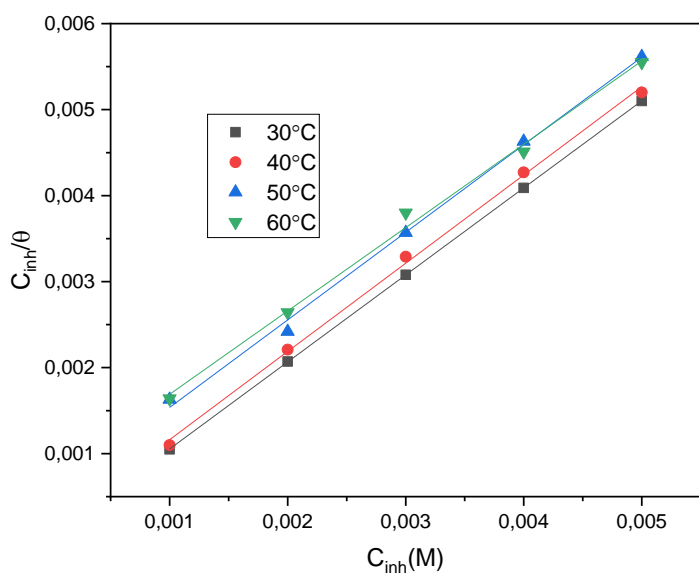


**Figure 4. 40:** Langmuir adsorption isotherm for the adsorption of EBDMDG on aluminium metal.

**Table 4. 11:** Adsorption parameters from Langmuir Adsorption Isotherm plots for EMDA, EBMDA, EBDA, and EBDMDG on Aluminium metal.

Inhibitor	Temperature(°C)	$K_{ads}(L/mol)$	$-\Delta G^{\circ}_{ads}(kJ.mol^{-1})$
EMDA	30°C	5000	31.58
	40°C	178.57	23.95
	50°C	416.67	26.99
	60°C	131.58	24.63
EBMDA	30°C	335.57	24.77
	40°C	124.69	23.01
	50°C	80.65	22.58
	60°C	20.96	19.55
EBDA	30°C	5.26	14.30
	40°C	12.50	17.03
	50°C	6.29	15.73
	60°C	3.44	14.54
EBDMDG	30°C	23.81	18.11
	40°C	7.35	15.65
	50°C	1.93	12.55
	60°C	1.39	12.03

The values of  $\Delta G_{ads}$  for EMDA inhibitor were close to -20kJ/mol and -40kJ/mol, therefore the mixed type of adsorption occurred. The process adsorption of EBMDA, EBDA, and EBDMDG inhibitor possess weak Van Der Waals interaction rather than chemical bonding this was because of their  $\Delta G_{ads}$  values which were closer to -20kJ/mol. The  $\Delta G_{ads}$  value was decreasing with temperature which employs endothermic adsorption.

#### 4.4. Thermodynamic and a Kinetic models

The adsorption process was well explained by using thermodynamic and kinetic models which are other useful tools to explain the mechanism of corrosion inhibition for the inhibitor<sup>98</sup>. The logarithm of the corrosion rate could be represented as a straight-line function of  $1/T$  of zinc and aluminium in an acid medium.

$$\log C_R = \log A - \frac{E_A}{2.303RT} \quad (22)$$

where:  $C_R$  = Corrosion rate ( $\text{g}\cdot\text{cm}^{-2}\cdot\text{h}^{-1}$ )

$A$  = Arrhenius pre-exponential factor (frequency factor)

$E_a$  = Corrosion activation energy

$R$  = Gas constant ( $8.3145 \text{ JK}^{-1}\text{mol}^{-1}$ ) and

$T$  = Absolute temperature

The values of the standard enthalpy ( $\Delta H^*$ ) and entropy of activation ( $\Delta S^*$ ) were calculated from the transition state equation

$$\log\left(\frac{C_R}{T}\right) = \left[ \log\left(\frac{R}{Nh}\right) + \left(\frac{\Delta S^*}{2.303R}\right) \right] + \left(\frac{-\Delta H^*}{2.303R}\right)\left(\frac{1}{T}\right) \quad (23)$$

where:  $h$  = Planck's constant and

$N$  = Avogadro number<sup>98</sup>.

#### 4.4.1. Zinc metal

The Arrhenius plots ( $\log C_R$  vs.  $1/T$ ) and the transition state plots ( $\log (C_R/T)$  vs.  $1/T$ ) for zinc corrosion in 1.5 M HCl without and with various concentrations of the inhibitors are shown in figures 4.41-46.

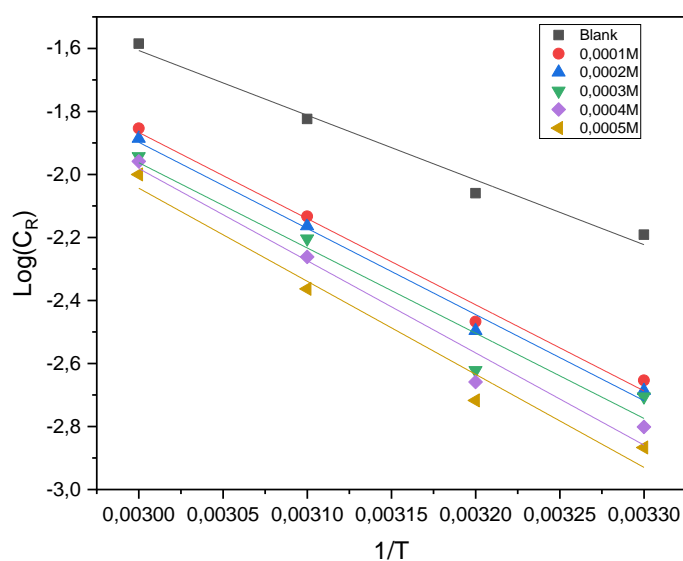




**Figure 4. 41:** Arrhenius plots for zinc metal corrosion in 1.5 M HCl solution in the absence and presence of a different concentration of EMDA as an inhibitor

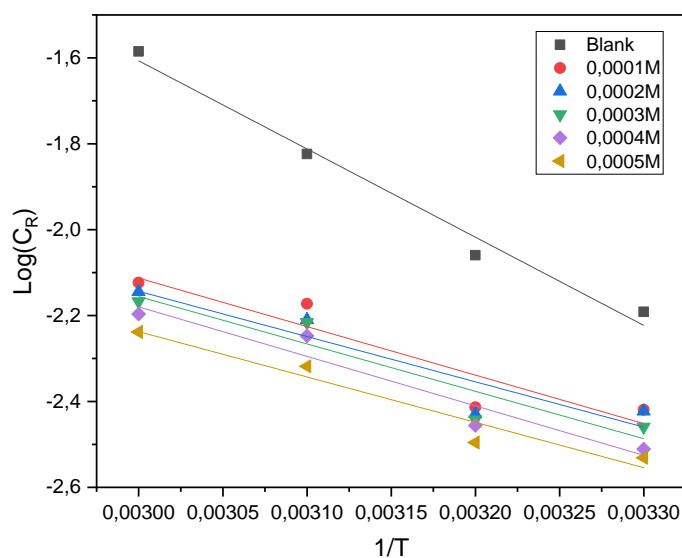


**Figure 4. 42:** Arrhenius plots for zinc metal corrosion in 1.5 M HCl solution in the absence and presence of a different concentration of EBMDA as an inhibitor

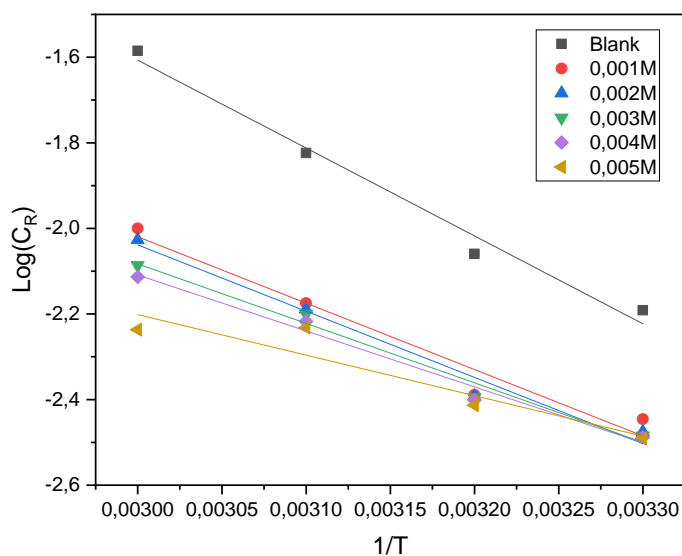


**Figure 4. 43:** Arrhenius plots for zinc metal corrosion in 1.5 M HCl solution in the absence and presence of a different concentration of EBDA as an inhibitor

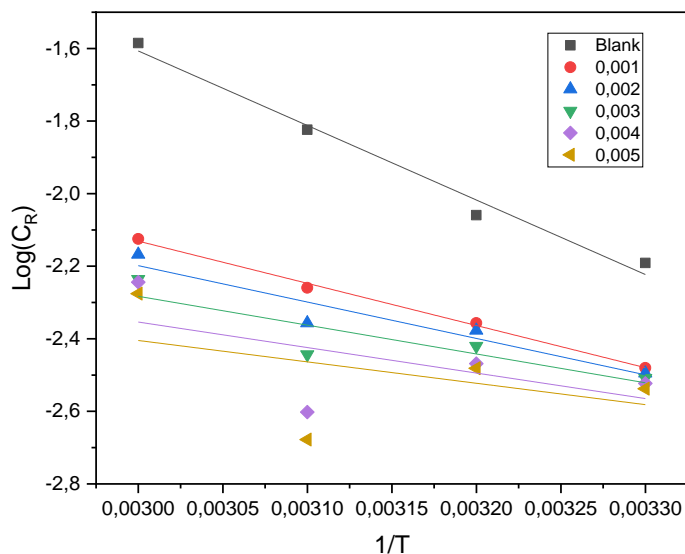


**Figure 4. 44:** Arrhenius plots for zinc metal corrosion in 1.5 M HCl solution in the absence and presence of a different concentration of EBDMDG as an inhibitor

The values of  $E_a$  are recorded in Tables 4.11 and 4.12 and were calculated from the slopes and intercepts of Arrhenius plots shown in figures 4.41-42. It was clear that the  $E_a$  values in the presence of EMDA inhibitor are higher than in the blank, the values of  $E_a$  increase with the increase in the concentration of EMDA inhibitor on zinc metal as is shown in table 4.11. The activation energy of the corrosion inhibition process is changed from 39.32 to 52.34, 52.33, 51.80, 56.00, and 56.55 kJ/mol<sup>1</sup> In the presence of EBMDA, EBDA and EBDMDG activation energy values were lower than in the blank solution. The energy values of EBMDA in Table 4.11 decrease from 39.32kJ/mol<sup>1</sup> to 21.63, 20.18, 21.13, 22.06, and 20.22 kJ/mol<sup>1</sup>. In Table 4.12 it shows the energy values of EBDA and EBDMDG which also decrease from that of blank, it decreases with an increase in inhibitor concentration. This indicates the stability of the adsorbed organic film on the metal surface<sup>99</sup>.

The unchanged or lower activation energy in the presence of inhibitor molecules from the blank solution is often an aspect of the chemisorption process. While physical adsorption is when the energy values are higher<sup>100,101</sup>.

**Table 4.12:** Arrhenius and transition parameters for the adsorption of different concentration of EMDA, EBMDA, EBDA, and EBDMDG in 1.5M HCl on zinc metal

Inhibitor	Inhibitor concentration (M)	$E_a$ (kJ.mol <sup>-1</sup> )	$\Delta H^*$ (kJ.mol <sup>-1</sup> )	$\Delta S^*$ (JK <sup>-1</sup> mol <sup>-1</sup> )
EMDA	Blank	39.32	36.70	-193.803
	1×10 <sup>-4</sup>	52.34	49.69	-189.71
	2×10 <sup>-4</sup>	52.33	49.69	-189.79
	3×10 <sup>-4</sup>	51.80	49.16	-190.13
	4×10 <sup>-4</sup>	56.00	53.38	-188.65
	5×10 <sup>-4</sup>	56.55	53.93	-188.59
EBMDA	Blank	39.32	36.70	-193.80
	1×10 <sup>-4</sup>	21.63	19.01	399.26
	2×10 <sup>-4</sup>	20.18	17.56	399.85
	3×10 <sup>-4</sup>	21.13	18.42	399.56
	4×10 <sup>-4</sup>	22.06	19.23	399.34
	5×10 <sup>-4</sup>	20.22	17.61	400.05
EBDA	Blank	39.32	36.70	-193.80
	1×10 <sup>-3</sup>	29.71	27.09	198.22
	2×10 <sup>-3</sup>	29.65	26.92	198.33
	3×10 <sup>-3</sup>	26.61	23.98	199.49
	4×10 <sup>-3</sup>	25.03	22.41	200.12
	5×10 <sup>-3</sup>	18.13	15.51	202.82
EBDMDG	Blank	39.32	36.70	-193.80
	1×10 <sup>-3</sup>	22.26	19.67	194.39
	2×10 <sup>-3</sup>	19.20	16.56	202.90
	3×10 <sup>-3</sup>	15.21	12.56	204.54
	4×10 <sup>-3</sup>	13.46	10.85	205.32
	5×10 <sup>-3</sup>	11.29	8.68	206.22

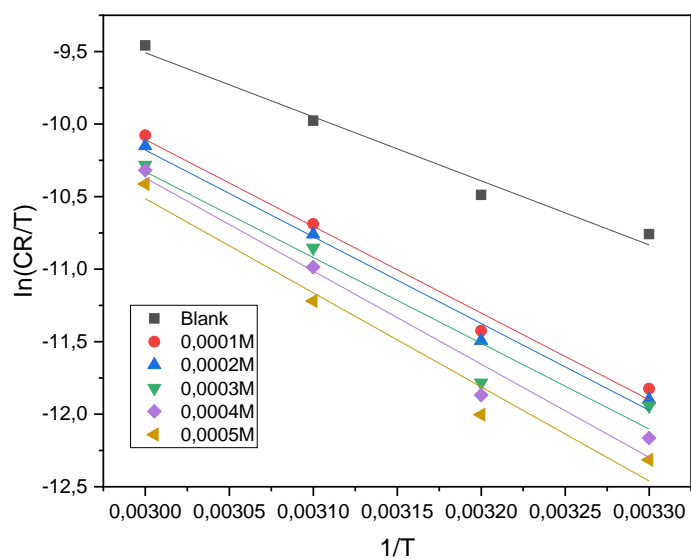


**Figure 4. 45:** Transition state plots at different concentration of EMDA

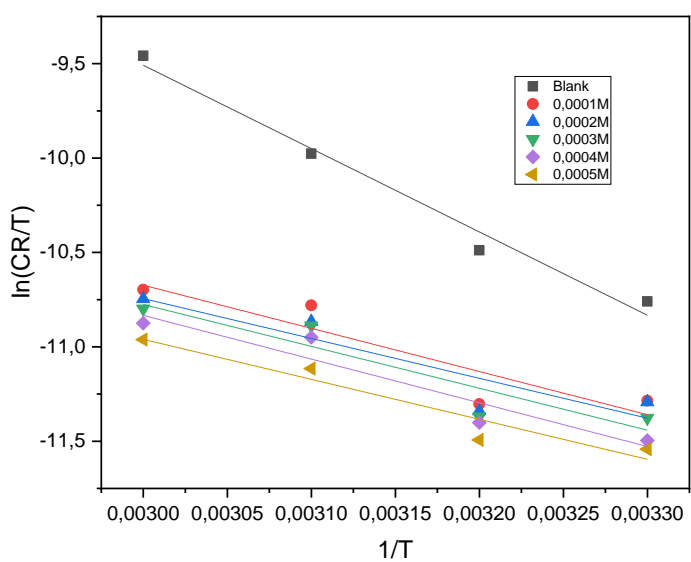


**Figure 4. 46:** Transition state plots at different concentration of EBMDA

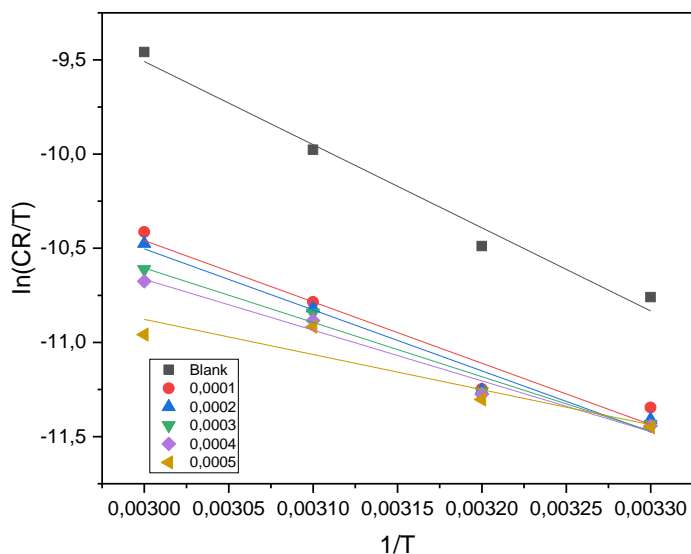


**Figure 4. 47:** Transition state plots at different concentration of EBDA

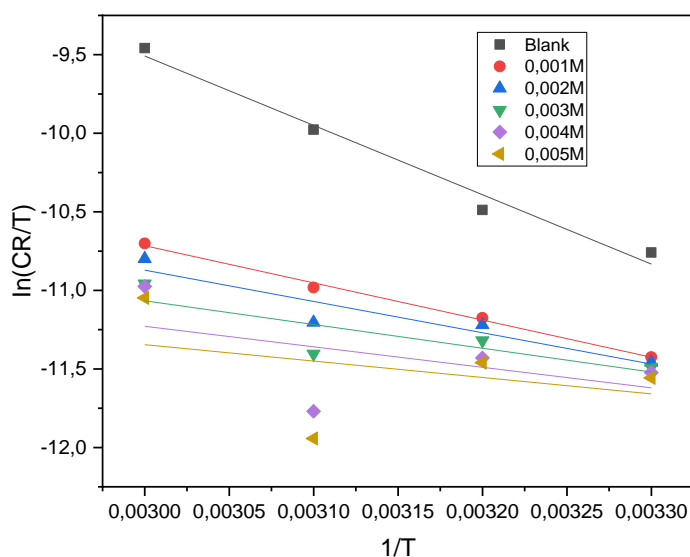


**Figure 4. 48:** Transition state plots at different concentration of EBDMDG

The values of  $\Delta H^*$  and  $\Delta S^*$  were obtained from the slope (slope =  $-\Delta H^*/2.303R$ ) and intercept ( $\ln(k_B/h) + \Delta S^*/R$ ) of the transition state plots, respectively. The values of  $\Delta H^*$  and  $\Delta S^*$  were tabulated above in Tables 4.11-12. The values of change in enthalpy in the presence and absence of inhibitors are positive. The positive values of enthalpy reflect the endothermic nature of the zinc dissolution process which is attributed to chemisorption<sup>102</sup>. From the tables above, it can be observed that when the concentration of EMDA inhibitor increases, the enthalpy also increases. The enthalpy at 0.0001M was 49.69kJ.mol<sup>-1</sup> and increase to 53.93kJ.mol<sup>-1</sup> at 0.0005M.

The values of entropy are negative in the absence and presence of EMDA inhibitor and positive in the Presence of EBMDA, EBDA, and EBDMDG inhibitors. The positive entropy in the presence of EBMDA, EBDA, and EBDMDG inhibitors is due to the disorderly adsorption of molecules by replacing the water molecules from the zinc surface. The tables above indicate that when the inhibitors are present the entropy increases compare to the ones with the absence of inhibitors. An increase in entropy implies that an increase in disordering takes place on going from reactants to the activated complex.

#### 4.4.2. Aluminium metal

The Arrhenius plots ( $\log C_R$  vs.  $1/T$ ) and the transition state plots ( $\log (C_R/T)$  vs.  $1/T$ ) for aluminium corrosion in 1.5 M HCl without and with various concentrations of the inhibitors are shown in figures 4.49-56.

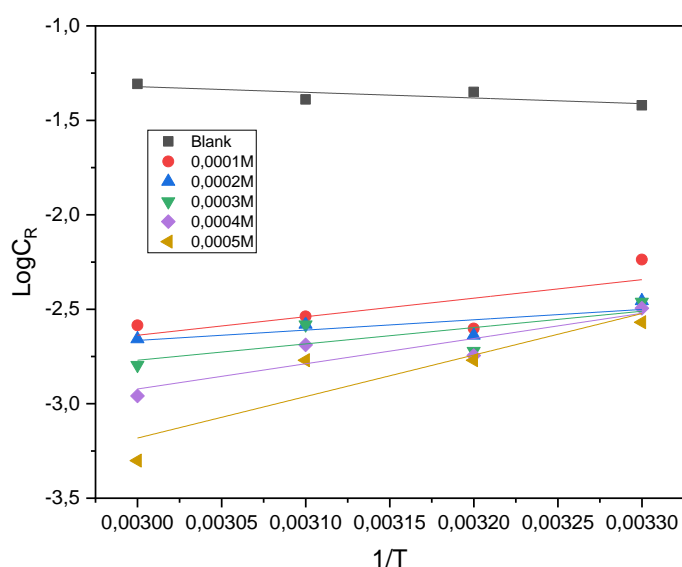


**Figure 4. 49:** Arrhenius plots for aluminium metal corrosion in 1.5 M HCl solution in the absence and presence of a different concentration of EMDA as an inhibitor

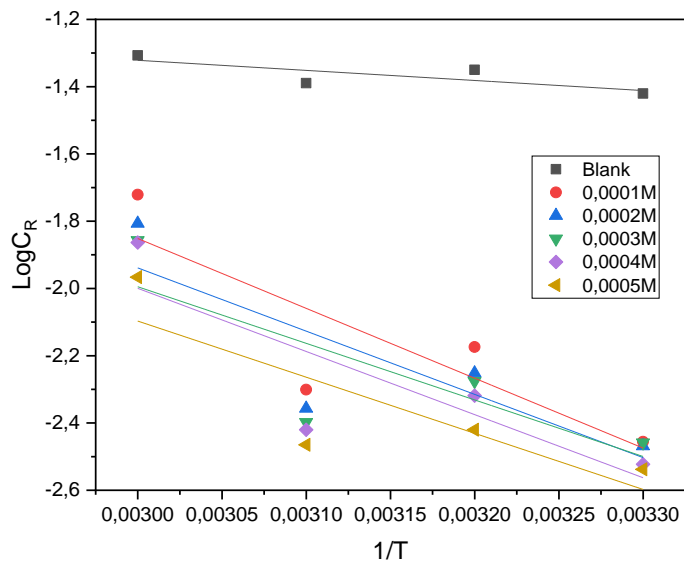


**Figure 4. 50:** Arrhenius plots for aluminium metal corrosion in 1.5 M HCl solution in the absence and presence of a different concentration of EBMDA as an inhibitor

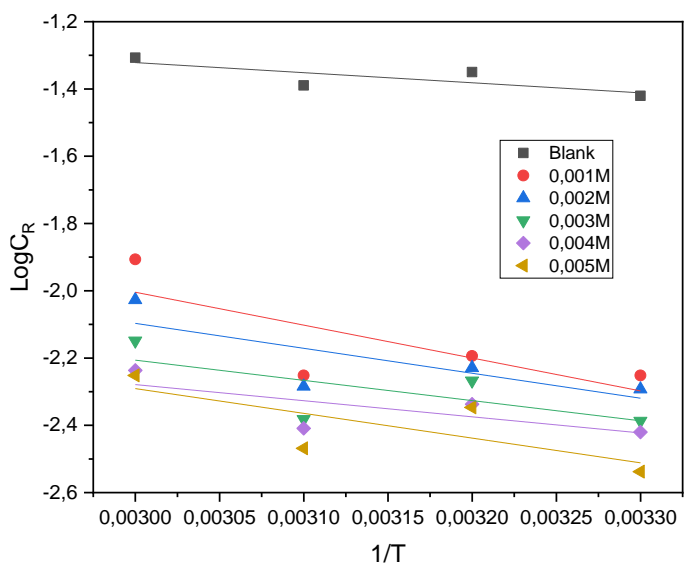


**Figure 4. 51:** Arrhenius plots for aluminium metal corrosion in 1.5 M HCl solution in the absence and presence of a different concentration of EBDA as an inhibitor

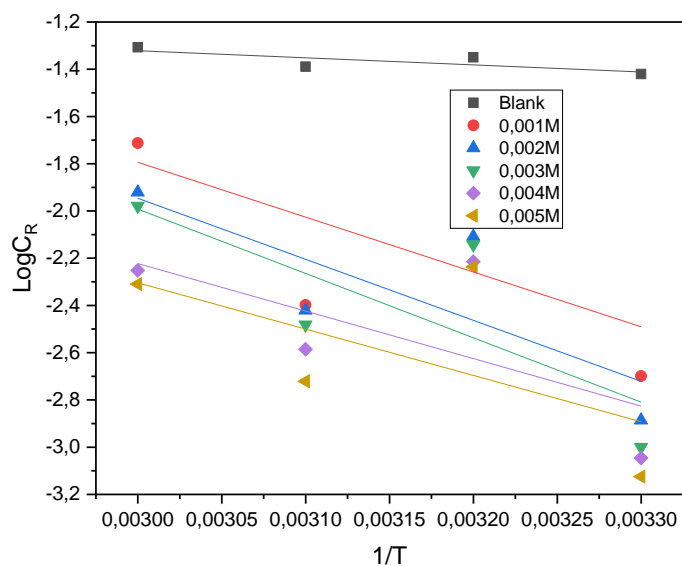


**Figure 4. 52:** Arrhenius plots for aluminium metal corrosion in 1.5 M HCl solution in the absence and presence of a different concentration of EBDMDG as an inhibitor

The value of activation energy was obtained from the Arrhenius plots slope shown in figures 4.49-52. It can be seen that for all four inhibitors the activation energy is lower than that without an inhibitor. It can be concluded that the type of process occurring on aluminium is the chemisorption process.

**Table 4.13:** Arrhenius and transition parameters for the adsorption of different concentrations of EMDA, EBMDA, EBDA and EBDMDG in 1.5M HCl on aluminium metal.

Inhibitor	Inhibitor concentration (M)	$E_a$ (kJ.mol <sup>-1</sup> )	$\Delta H^*$ (kJ.mol <sup>1</sup> )	$-\Delta S^*$ (JK <sup>-1</sup> mol <sup>1</sup> )
EMDA	Blank	57.42	4.64	204
	1×10 <sup>-4</sup>	18.78	23.84	218.07
	2×10 <sup>-4</sup>	10.47	15.30	215.04
	3×10 <sup>-4</sup>	16.55	24.52	218.67
	4×10 <sup>-4</sup>	25.54	30.35	221.07
	5×10 <sup>-4</sup>	42.07	44.69	226.80
EBMDA	Blank	57.42	4.64	204
	1×10 <sup>-4</sup>	39.76	42.03	192.35
	2×10 <sup>-4</sup>	36.00	37.38	194.25
	3×10 <sup>-4</sup>	31.56	37.15	194.43
	4×10 <sup>-4</sup>	35.85	38.17	194.12
	5×10 <sup>-4</sup>	31.95	31.04	196.94
	Blank	57.42	4.64	204



EBDA	$1 \times 10^{-3}$	18.72	18.33	201
	$2 \times 10^{-3}$	14.20	13.68	203
	$3 \times 10^{-3}$	11.51	13.28	203.56
	$4 \times 10^{-3}$	9.18	9.30	205.19
	$5 \times 10^{-3}$	14.08	16.14	202.71
EBDMDG	Blank	57.42	4.64	204
	$1 \times 10^{-3}$	44.45	66.29	183.12
	$2 \times 10^{-3}$	49.46	58.80	186.39
	$3 \times 10^{-3}$	52.17	62.50	185.15
	$4 \times 10^{-3}$	38.51	50.08	190.14
	$5 \times 10^{-3}$	44.77	53.46	189.03

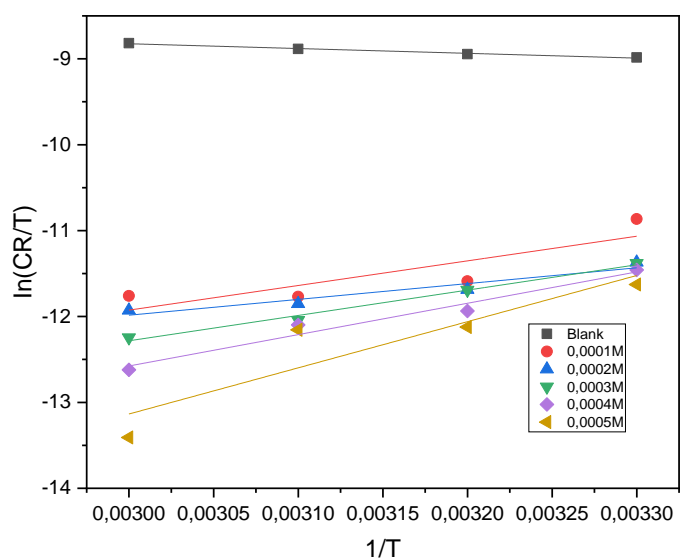


**Figure 4. 53:** Transition state plots at different concentration of EMDA

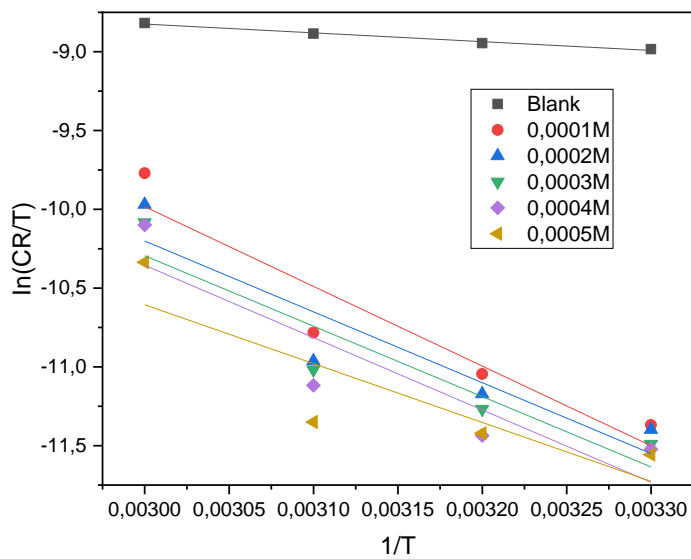


**Figure 4. 54:** Transition state plots at different concentration of EBMDA

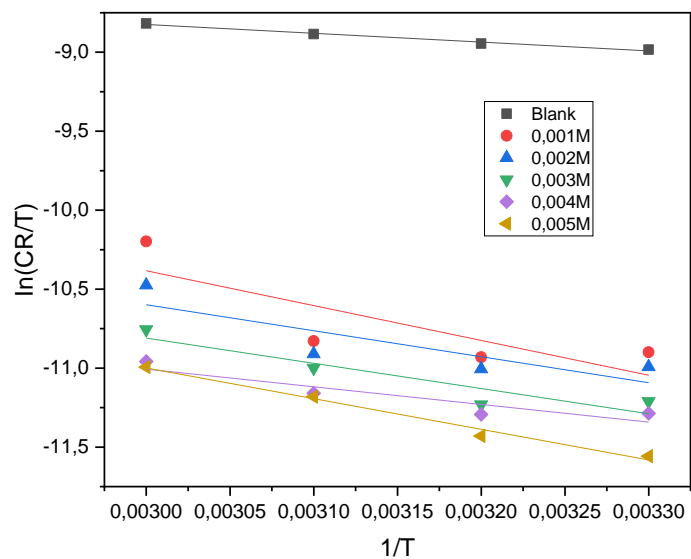


**Figure 4. 55:** Transition state plots at different concentration of EBDA

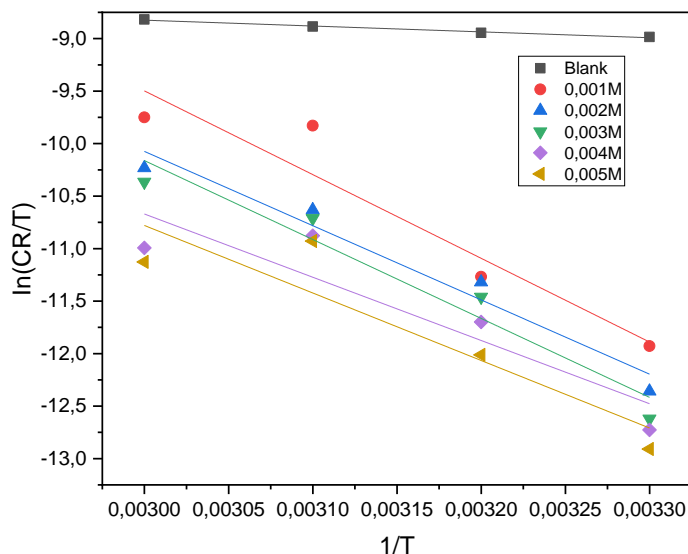


**Figure 4. 56:** Transition state plots at different concentration of EBDMDG

Tables 4.13-14 indicate the values of  $\Delta H^*$  and  $\Delta S^*$  were obtained from the slope (slope =  $-\Delta H^*/2.303R$ ) and intercept ( $\ln(k_B/h) + \Delta S^*/R$ ) of the transition state plots. The values of change in enthalpy in the presence and absence of inhibitors are positive. The positive values of enthalpy reflect the endothermic nature of the aluminium dissolution process which is attributed to the chemisorption process. The positive entropy in the presence of EBMDA, EBDA, and EBDMDG inhibitors is due to the disorderly adsorption of molecules by replacing the water molecules from the zinc surface.

#### 4.4. Electrochemical Impedance Spectroscopy (EIS)

The corrosion behavior of zinc and aluminium in 1.5M HCl absence and presence of inhibitors was carried out by the EIS method. EIS has been successfully applied to corrosion studies or many years and proven to be a powerful and accurate method for measuring corrosion rates. From the process, Nyquist plots of metals in 1.5M HCl in the absence and presence of various concentrations of EMDA, EBMDA, EBDA, and EBDMDA inhibitors were composed and presented in the below figures.

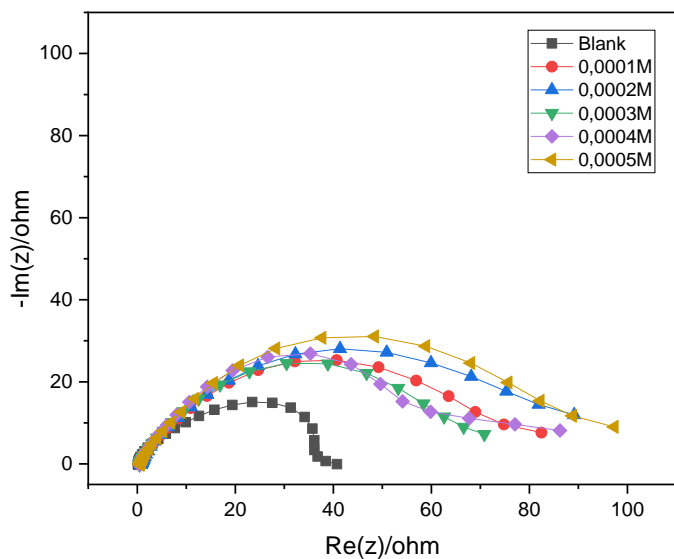


**Figure 4. 57:** Nyquist plot of zinc in 1.5M HCl in the absence and presence of different concentrations of EMDA

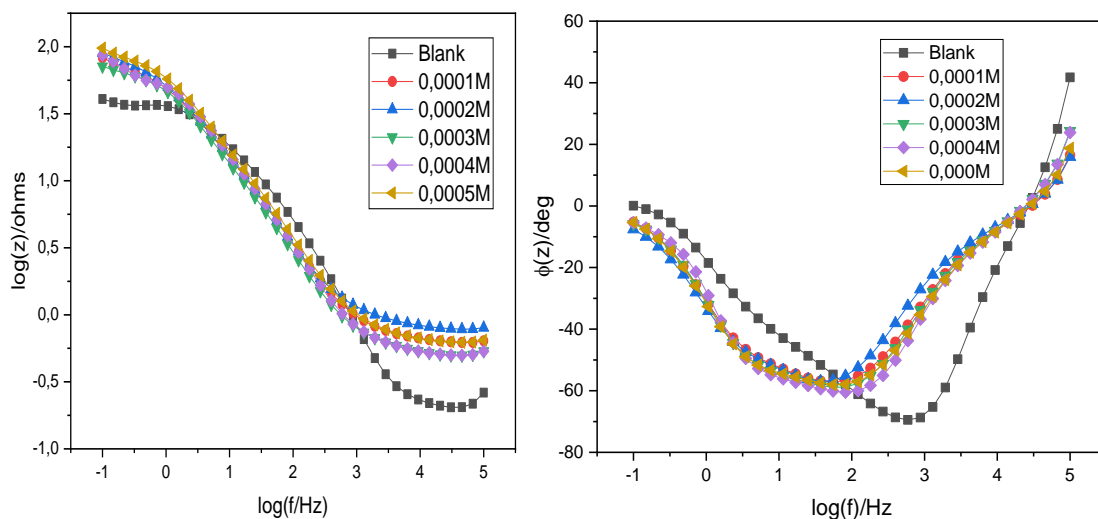


**Figure 4. 58:** Bode plots of mild steel in 1.5M HCl in the absence and presence of different concentrations of EMDA

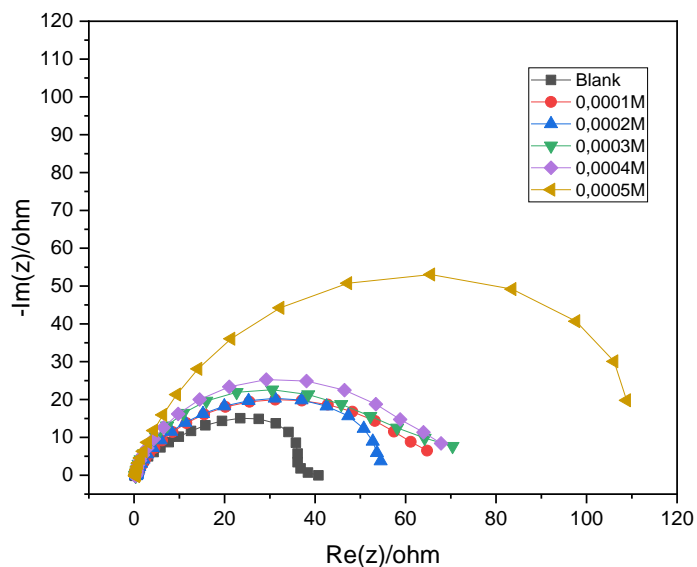


**Figure 4. 59:** Nyquist plot of zinc in 1.5M HCl in the absence and presence of different concentrations of EBMDA

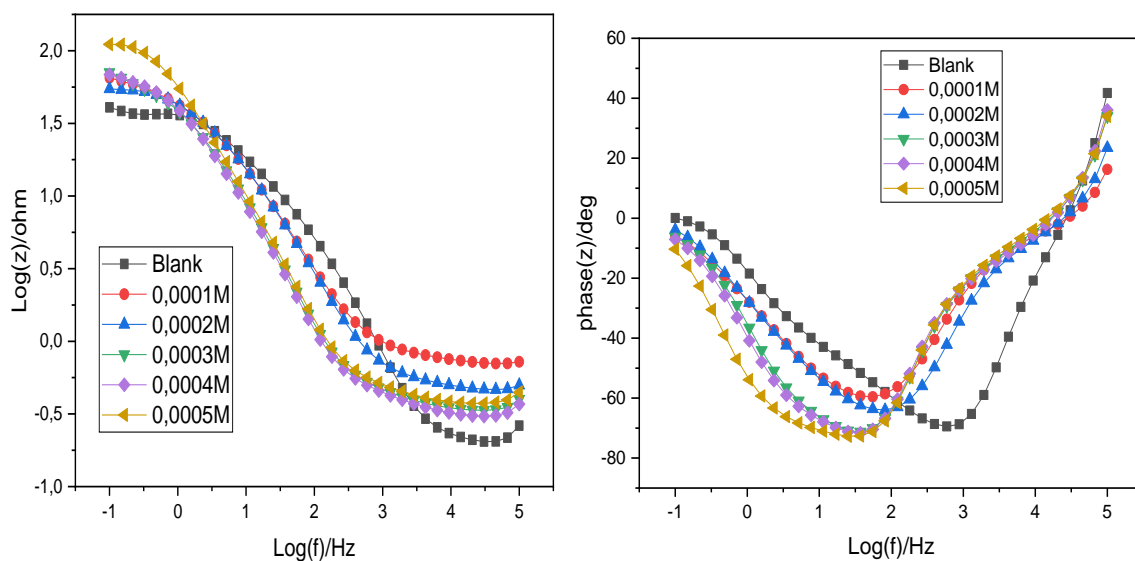


**Figure 4. 60:** Bode plots of mild steel in 1.5M HCl in the absence and presence of different concentrations of EBMDA

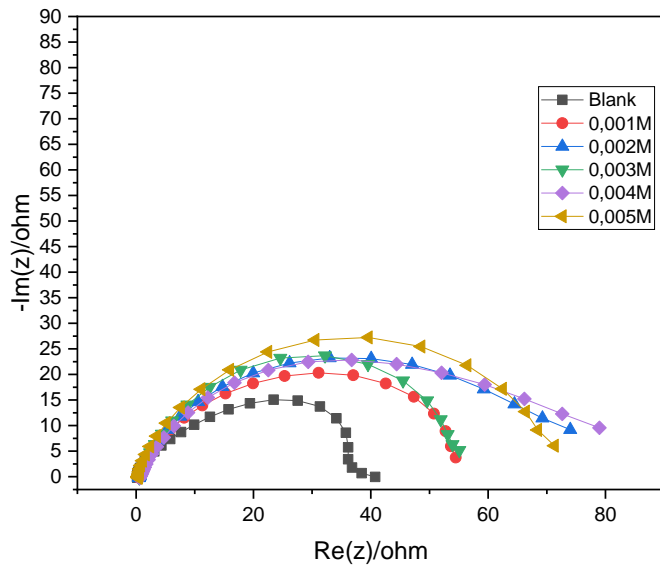


**Figure 4. 61:** Nyquist plot of zinc in 1.5M HCl in the absence and presence of different concentrations of EBDA

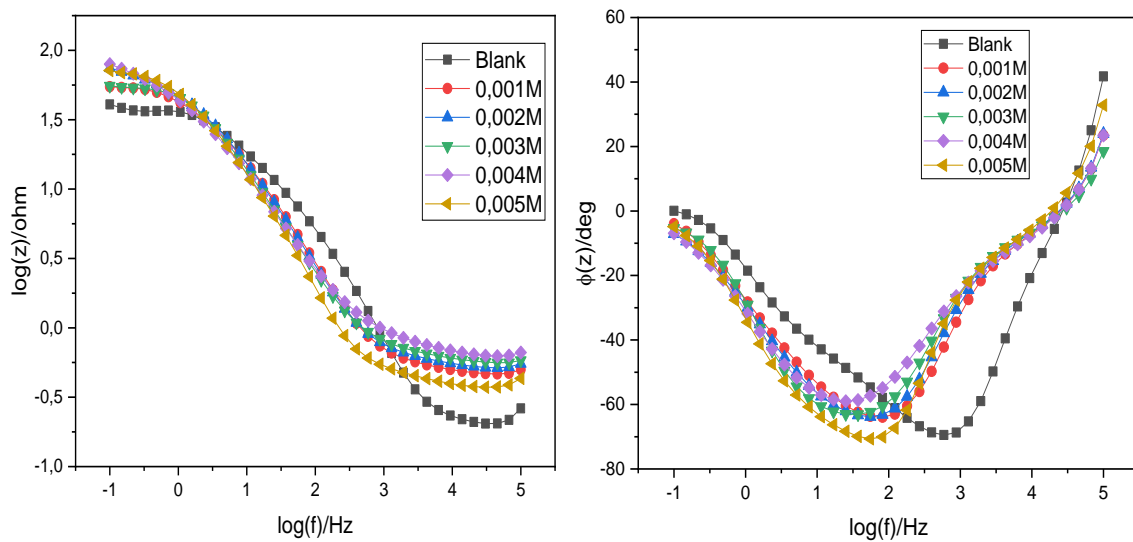


**Figure 4. 62:** Bode plots of mild steel in 1.5M HCl in the absence and presence of different concentrations of EBDA

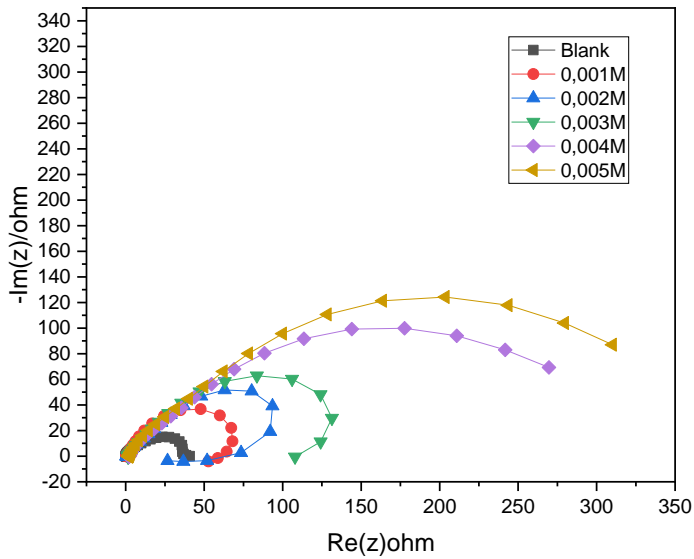


**Figure 4. 63:** Nyquist plot of zinc in 1.5M HCl in the absence and presence of different concentrations of EBDMDG

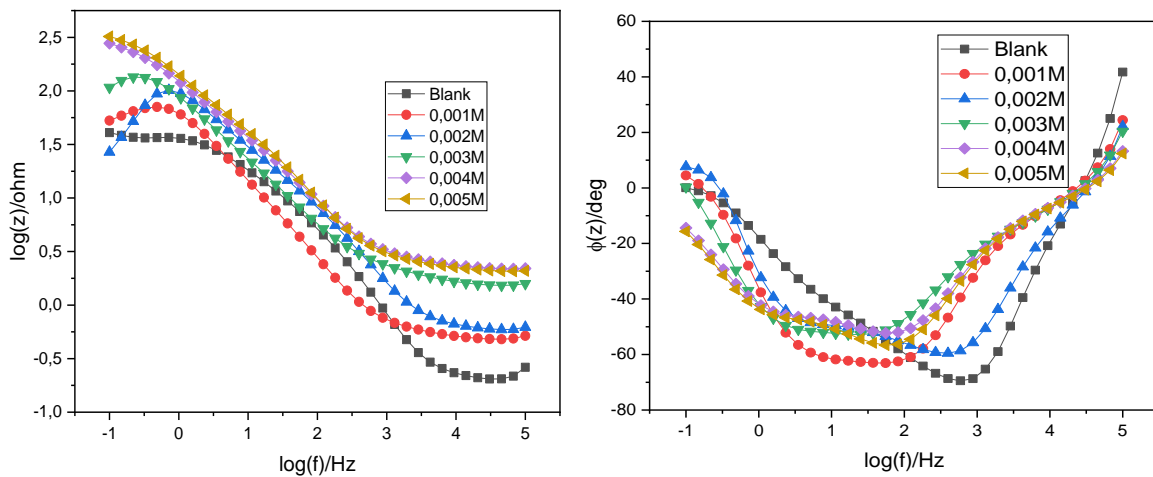


**Figure 4. 64:** Bode plots of mild steel in 1.5M HCl in the absence and presence of different concentrations of EBDMDG.

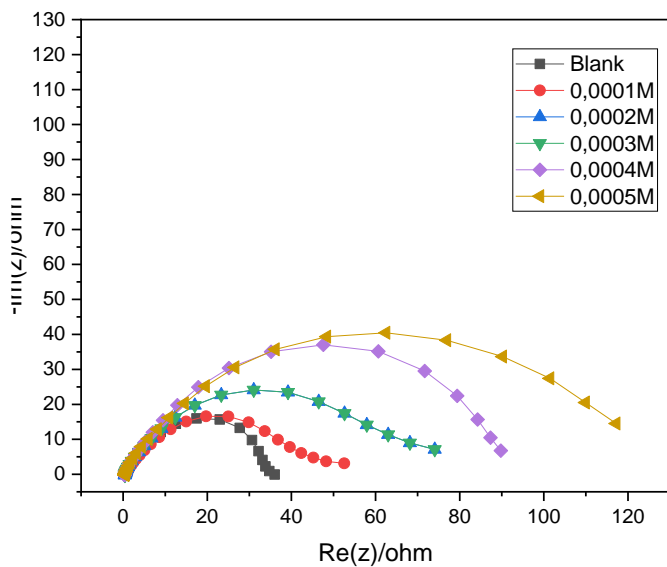


**Figure 4. 65:** Nyquist plot of zinc in 1.5M HCl in the absence and presence of different concentrations of EBDMDG.

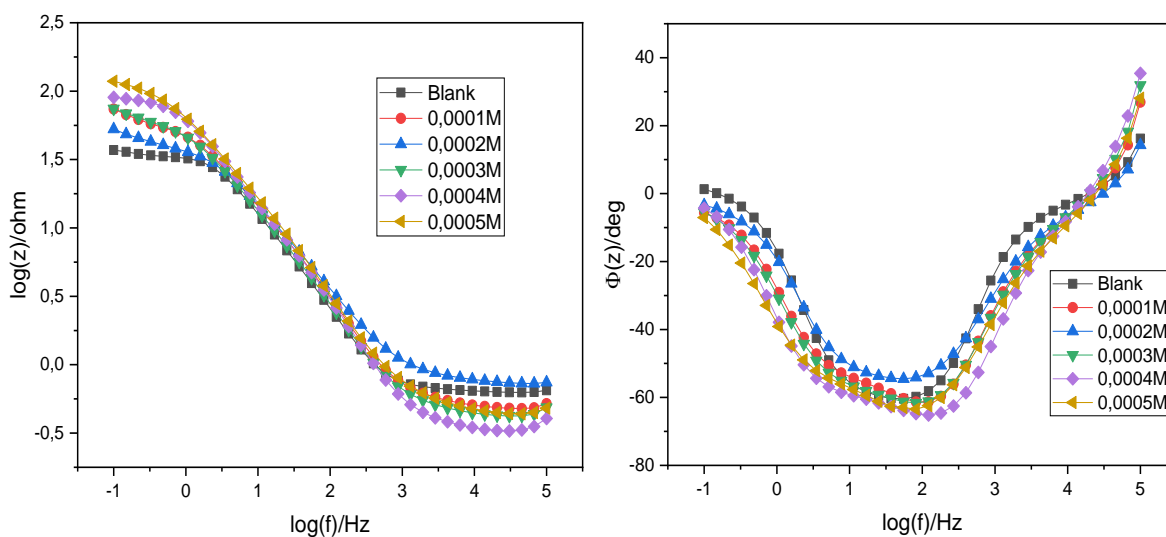


**Figure 4. 66:** Bode plots of zinc in 1.5M HCl in the absence and presence of different concentrations of EBDMDG.



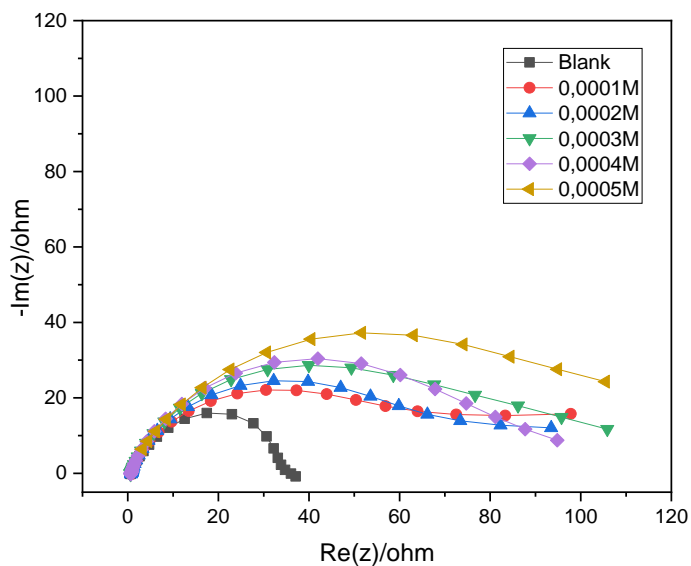


**Figure 4. 67:** Nyquist plot of aluminium in 1.5M HCl in the absence and presence of different concentrations of EMDA.

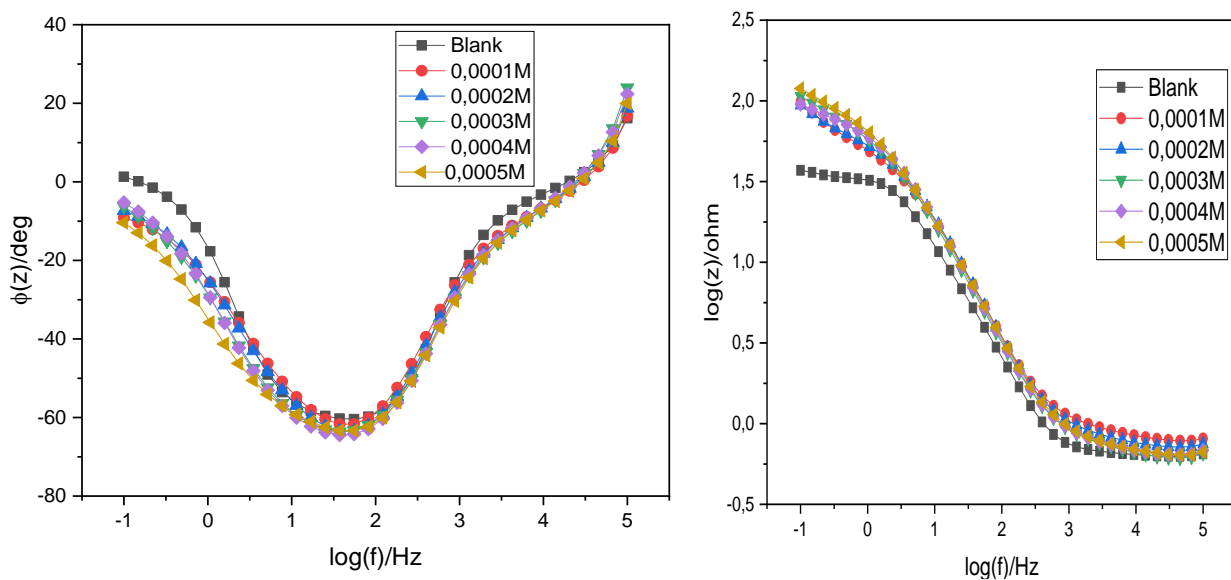


**Figure 4. 68:** Bode plots of aluminium in 1.5M HCl in the absence and presence of different concentrations of EMDA.

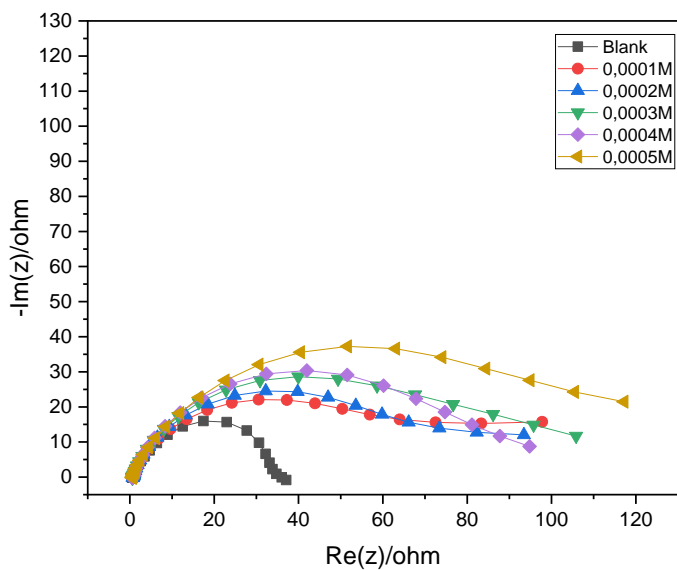


**Figure 4. 69:** Nyquist plot of aluminium in 1.5M HCl in the absence and presence of different concentrations of EBMDA.

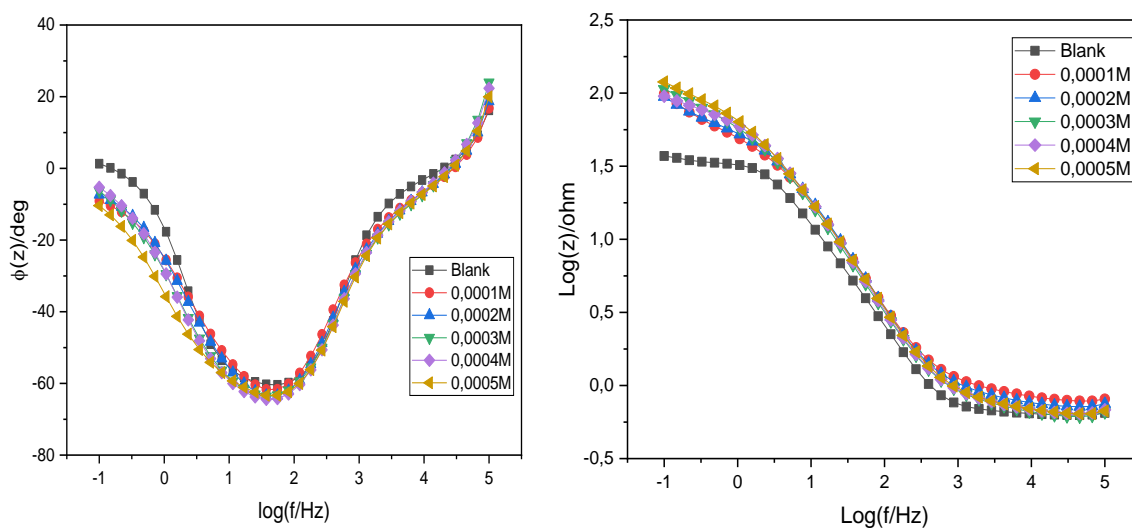


**Figure 4. 70:** Bode plots of aluminium in 1.5M HCl in the absence and presence of different concentrations of EBMDA.

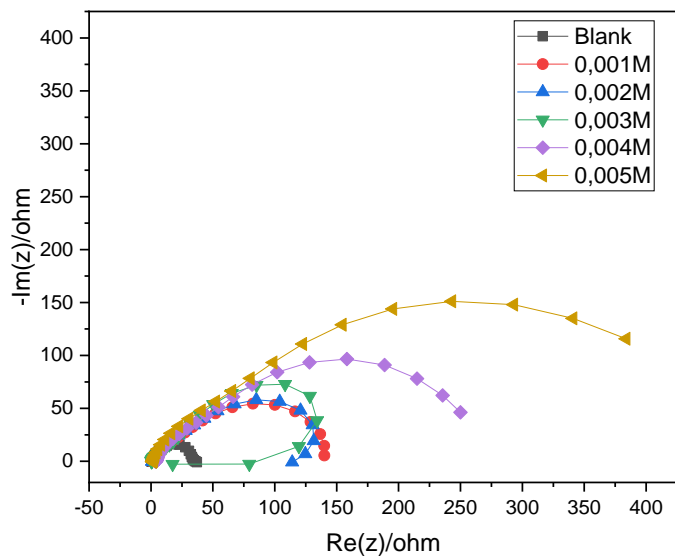


**Figure 4. 71:** Nyquist plot of aluminium in 1.5M HCl in the absence and presence of different concentrations of EBDA.

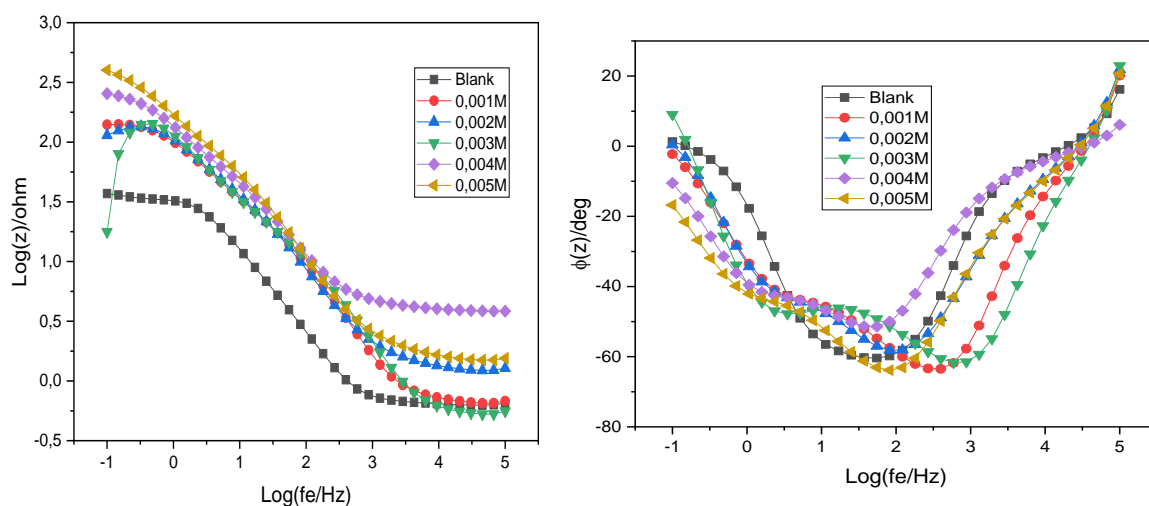


**Figure 4. 72:** Bode plots of aluminium in 1.5M HCl in the absence and presence of different concentrations of EBDA.

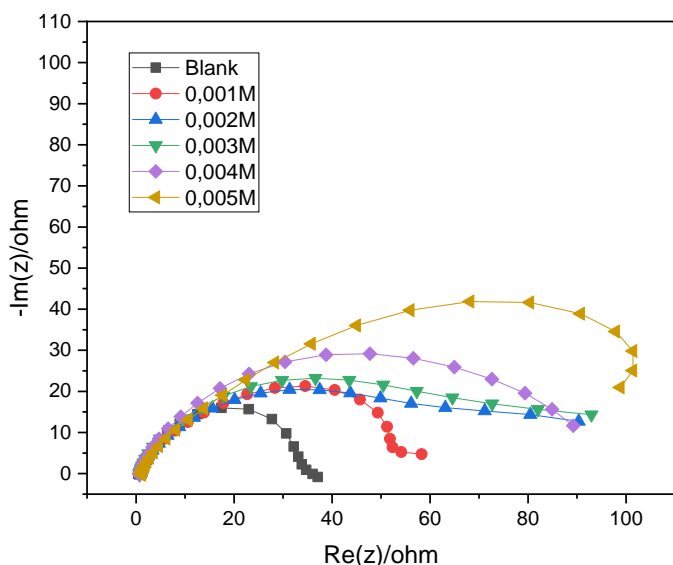


**Figure 4. 73:** Nyquist plot of aluminium in 1.5M HCl in the absence and presence of different concentrations of EBDMDG.

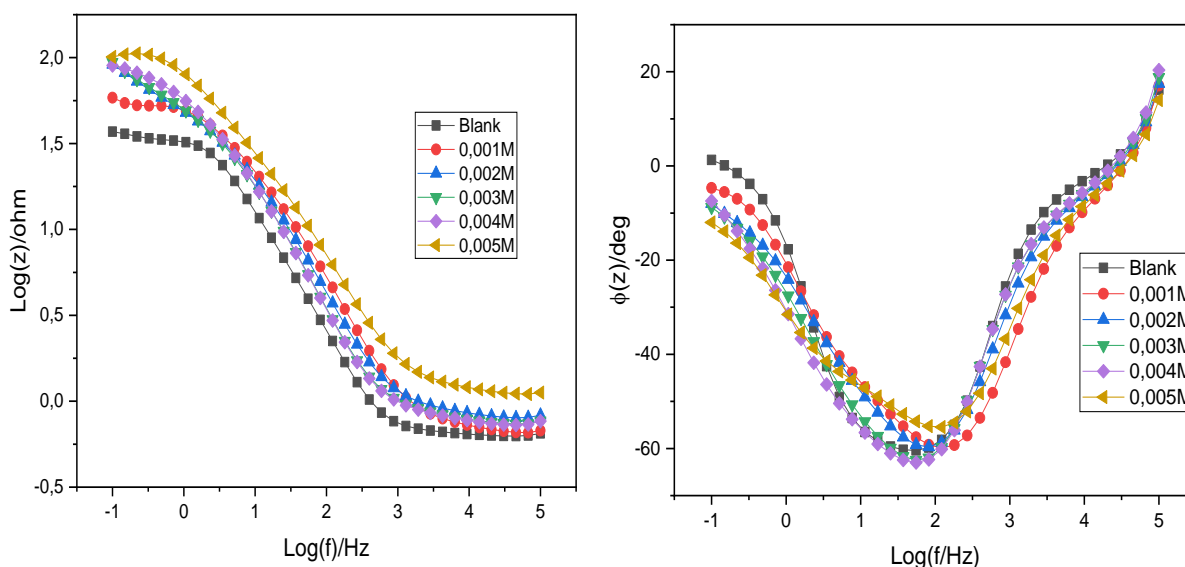


**Figure 4. 74:** Bode plots of aluminium in 1.5M HCl in the absence and presence of different concentrations of EBDMDG.

Nyquist plots for all metals are similar in shape and differ in diameter for different inhibitor concentrations. The addition of inhibitors medium leads to an increase in diameter of semicircles compared to a blank solution, indicating the adsorption of inhibitors molecule on the surface of zinc and aluminium. The formation of the organic film becomes thicker and more protective to the metals with an increase in inhibitor concentration<sup>103</sup>. The results obtained reveal that each impedance diagram consists of a large capacitive loop with a low-frequency dispersion. The Nyquist plots described in the above figures were

fitted using electrode-equivalent circuits (EEC) to equivalent circuit model in figures 4.75-77 which include charge transfer resistance ( $R_1$ ), solution resistance ( $R_2$ ), inductor ( $L_4$ ), constant phase element ( $Q_1$ ), and Capacitor ( $C_2$ ). From impedance measurements, inhibition efficiencies were calculated using equation (19).

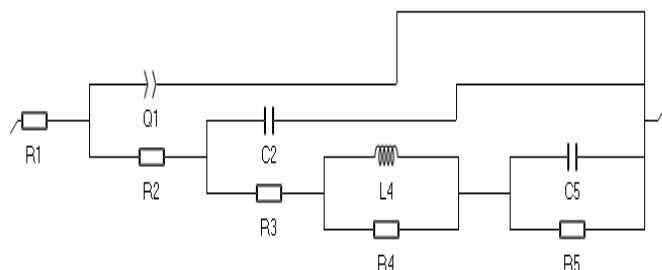


**Figure 4. 75:** Equivalent circuit used to fit the impedance spectra obtained for zinc corrosion in 1.5 M HCl in the absence and presence of EMDA, EBMDA, and EBDMDG.

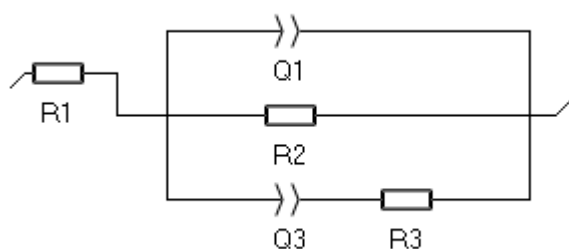


**Figure 4. 76:** Equivalent circuit used to fit the impedance spectra obtained for zinc corrosion in 1.5 M HCl in the presence of EBDA.

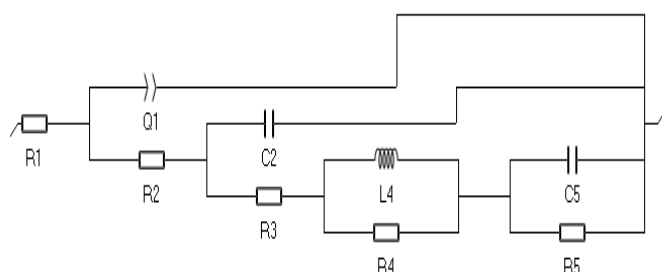


**Figure 4. 77:** Equivalent circuit used to fit the impedance spectra obtained for aluminium corrosion in 1.5 M HCl in the absence of inhibitor.

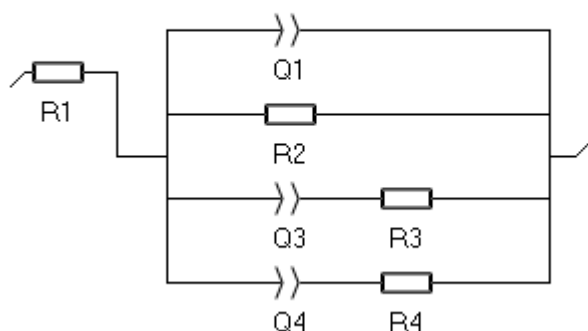


**Figure 4. 78:** Equivalent circuit used to fit the impedance spectra obtained for aluminium corrosion in 1.5 M HCl in the presence of inhibitors.

**Table 4. 14:** Corrosion inhibition efficiencies calculated from EIS data for zinc.

Inhibitor	Inhibitor concentration (M)	$R_s$ (ohm)	$R_{ct}$ (ohm)	N	% $I_{EIS}$
EMDA	Blank	0.202	13.79	0.934	0
	$1 \times 10^{-4}$	0.6256	39.68	0.7713	65.25
	$2 \times 10^{-4}$	0.7936	58.91	0.7523	76.59
	$3 \times 10^{-4}$	0.4927	70.1	0.7515	80.33
	$4 \times 10^{-4}$	0.4942	70.48	0.7715	80.43
	$5 \times 10^{-4}$	0.6106	95.3	0.7396	85.53
EBMDA	Blank	0.202	13.79	0.934	0
	$1 \times 10^{-4}$	0.7172	47.86	0.7946	71.19
	$2 \times 10^{-4}$	0.4642	55.36	0.7988	75.09
	$3 \times 10^{-4}$	0.3488	62.25	0.8585	77.85
	$4 \times 10^{-4}$	0.3322	66.44	0.8481	79.24
	$5 \times 10^{-4}$	0.3873	123.7	0.8685	88.85
EBDA	Blank	0.202	13.79	0.934	0.202
	$1 \times 10^{-3}$	8.62	73.08	-	81.13
	$2 \times 10^{-3}$	18.64	73.12	-	81.14
	$3 \times 10^{-3}$	16.15	88.16	-	84.00
	$4 \times 10^{-3}$	0.5998	123.8	-	88.86
	$5 \times 10^{-3}$	4.29	132.3	-	89.5
EBDMDG	Blank	0.202	13.79	0.934	0
	$1 \times 10^{-3}$	0.4756	37.29	0.8395	63.02
	$2 \times 10^{-3}$	0.5283	54.42	0.8204	74.67
	$3 \times 10^{-3}$	0.5813	58.94	0.8097	76.60
	$4 \times 10^{-3}$	0.3846	69.91	0.8568	
	$5 \times 10^{-3}$	0.7431	76.58	0.7431	81.99

**Table 4. 15:** Corrosion inhibition efficiencies calculated from EIS data for aluminium.

Inhibitor	Inhibitor concentration (M)	$R_s$ (ohm)	$R_{ct}$ (ohm)	%IE <sub>EIS</sub>
EMDA	Blank	0.6325	5.103	0
	$1 \times 10^{-4}$	16.52	26.75	80.92
	$2 \times 10^{-4}$	19.46	17.4	70.67
	$3 \times 10^{-4}$	18.55	31.02	83.57
	$4 \times 10^{-4}$	21.93	39.8	87.00
	$5 \times 10^{-4}$	21.93	39.8	87.18
EBMDA	Blank	0.6325	5.103	0
	$1 \times 10^{-4}$	13.14	15.51	67.09
	$2 \times 10^{-4}$	18.11	13.91	63.31
	$3 \times 10^{-4}$	19.02	19.42	73.72
	$4 \times 10^{-4}$	19.94	25.88	80.28
	$5 \times 10^{-4}$	20.10	31.65	83.87
EBDA	Blank	0.6325	5.103	0
	$1 \times 10^{-3}$	17.8	8.97	43.15
	$2 \times 10^{-3}$	17.51	9.75	47.66
	$3 \times 10^{-3}$	21.01	9.837	48.12
	$4 \times 10^{-3}$	18.01	10.02	49.07
	$5 \times 10^{-3}$	16.30	11.85	56.94
EBDMDG	Blank	0.6325	5.103	0
	$1 \times 10^{-3}$	18.37	12.99	60.72
	$2 \times 10^{-3}$	20.04	26.82	80.97
	$3 \times 10^{-3}$	23.43	48.53	89.48
	$4 \times 10^{-3}$	19.28	57.74	90.32
	$5 \times 10^{-3}$	26.01	58.45	91.69

In Tables 4.15-16 it shown that the values of  $R_{ct}$  increase with an increase in all four inhibitors which then lead to an increase in %IE<sub>EIS</sub>. For example, at a lower concentration ( $1 \times 10^{-4}$  M) of EMDA, the  $R_{ct}$  was 66.88 ohm when the concentration of inhibitor increase to a higher concentration of  $1 \times 10^{-4}$  M the  $R_{ct}$  increase to 95.3 for zinc metal. The same trend was observed on aluminium metal at a lower concentration of EMDA the %IE<sub>EIS</sub> was 80% and increase to 87.18%.

#### 4.5. Potentiodynamic Polarization (PDP)

Potentiodynamic polarization methods are often used for corrosion testing because they provide useful information about corrosion mechanisms. In this study, PDP is used to describe the characteristic of the corrosion system. Figures 4.79-87 show PDP curves of zinc and aluminium in 1.5M HCl in the absence and presence of EMDA, EBMDA, EBDA, and EBDMDG inhibitors. From the Tafel plot, the related electrochemical parameters such as corrosion potential ( $E_{corr}$ ), corrosion current ( $I_{corr}$ ), cathodic Tafel slope ( $b_c$ ), and anodic Tafel slope ( $b_a$ ) were obtained and calculated from EC-Lab software<sup>83</sup>. % $I_{PDP}$  was calculated from the polarization measurement according to equation (18) and given in table 4.17.

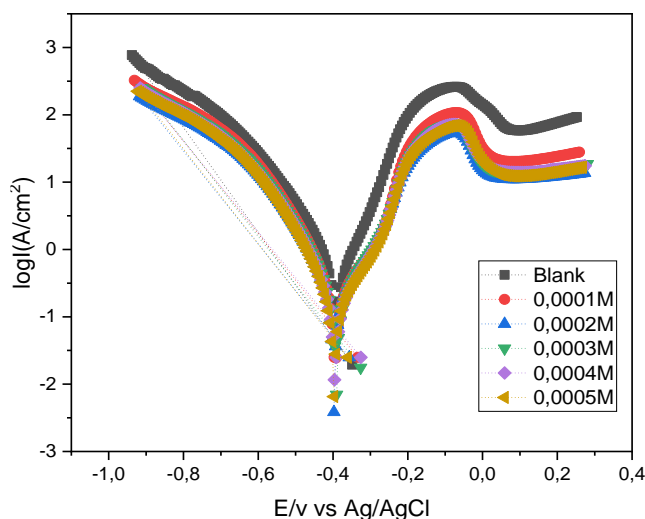


**Figure 4. 79:** Tafel plots for zinc in 1.5 M HCl in the absence and presence of different concentrations of EMDA

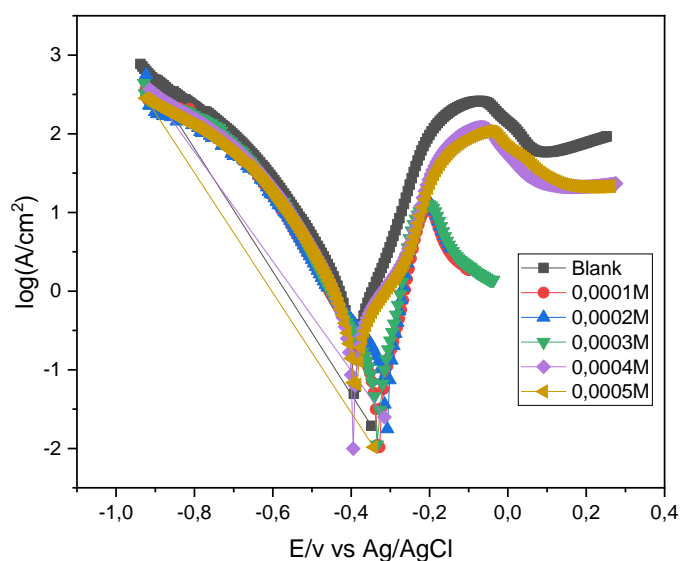




**Figure 4. 80:** Tafel plots for zinc in 1.5 M HCl in the absence and presence of different concentrations of EBMDA

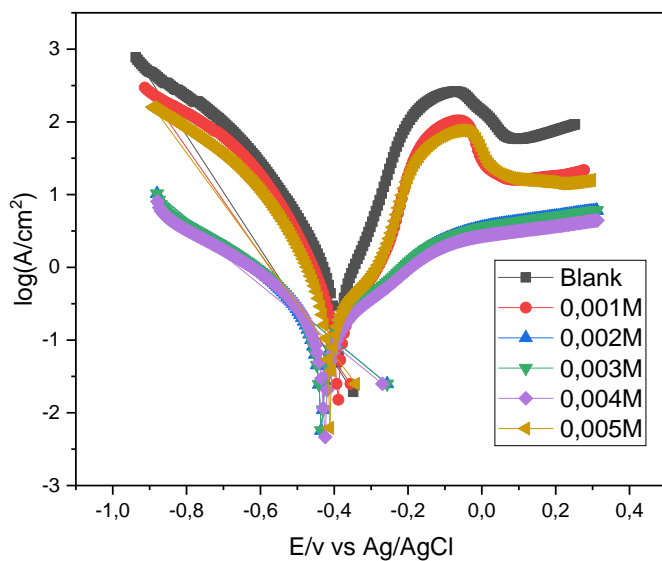


**Figure 4. 81:** Tafel plots for zinc in 1.5 M HCl in the absence and presence of different concentrations of EBDA

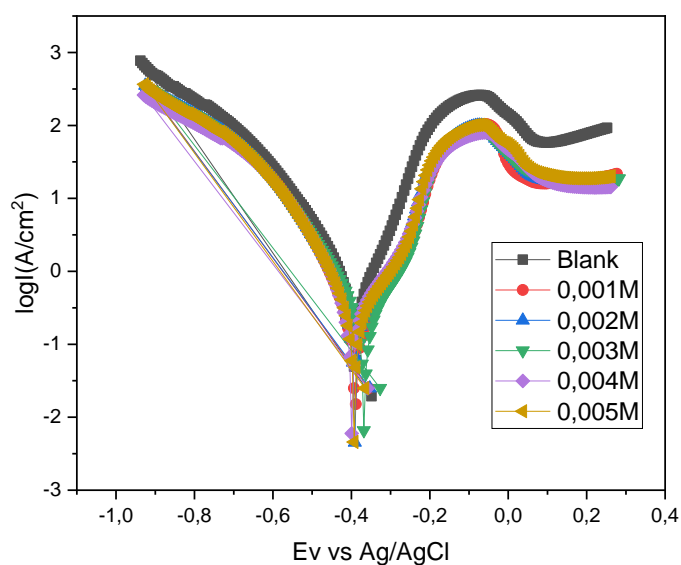


**Figure 4. 82:** Tafel plots for zinc in 1.5 M HCl in the absence and presence of different concentrations of EBDMDG

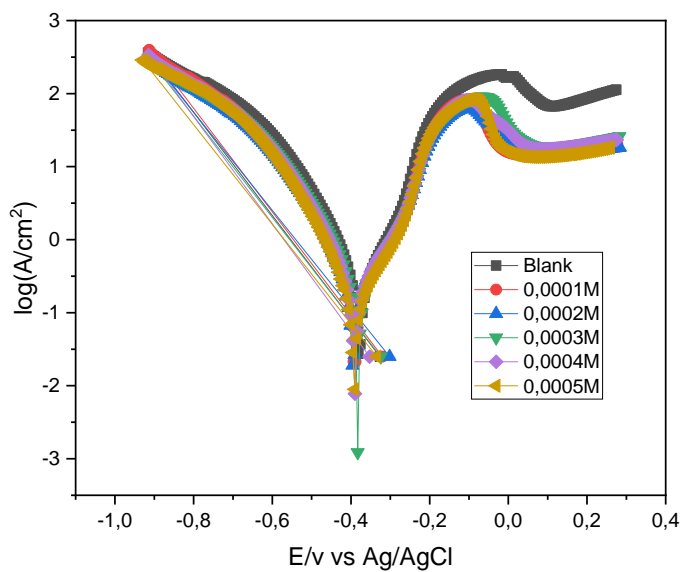


**Figure 4. 83:** Tafel plots for aluminium in 1.5 M HCl in the absence and presence of different concentrations of EMDA

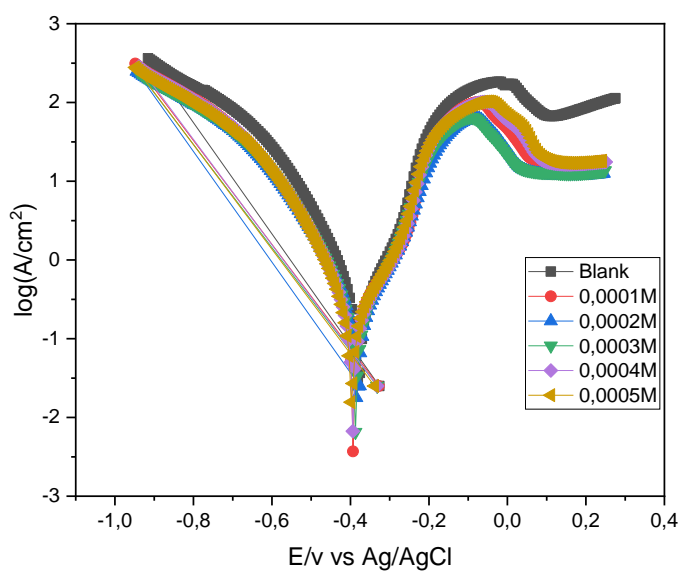


**Figure 4. 84:** Tafel plots for aluminium in 1.5 M HCl in the absence and presence of different concentrations of EBMDA

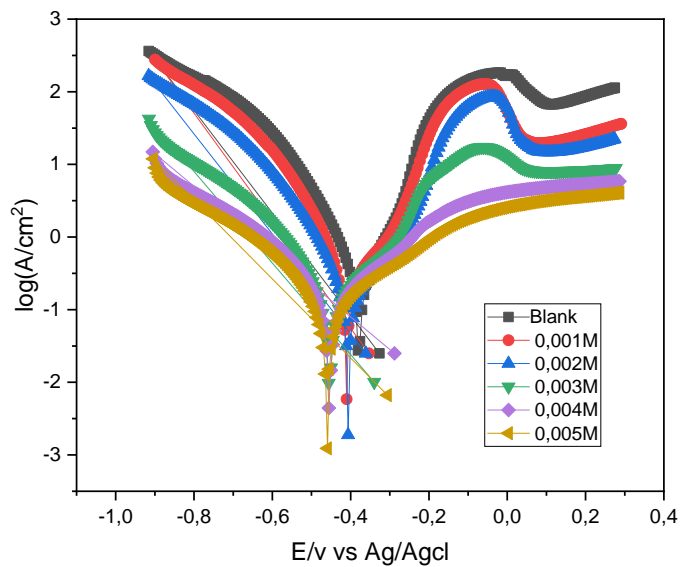


**Figure 4. 85:** Tafel plots for aluminium in 1.5 M HCl in the absence and presence of different concentrations of EBDA

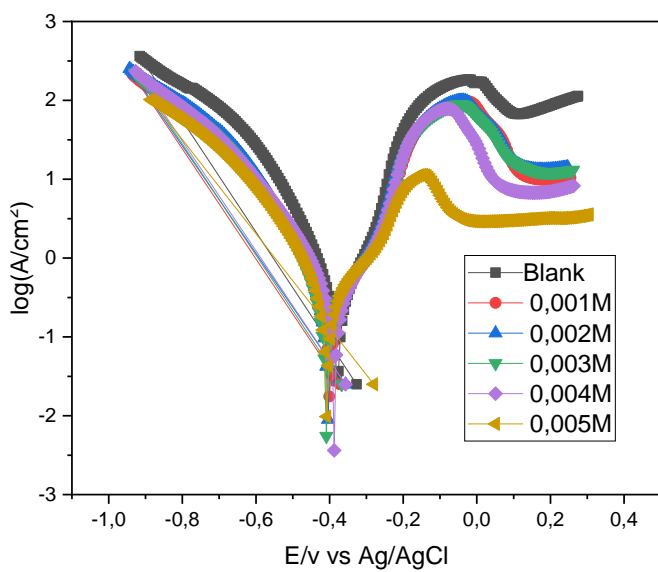


**Figure 4. 86:** Tafel plots for aluminium in 1.5 M HCl in the absence and presence of different concentrations of EBDMDG

**Table 4. 16:** Potentiodynamic polarization (PDP) parameters such as corrosion potential ( $E_{\text{corr}}$ ), corrosion current density ( $i_{\text{corr}}$ ), and anodic and cathodic Tafel slopes ( $b_a$  and  $b_c$ ) using different inhibitors on zinc metal.

Inhibitor	Inhibitor con.(M)	$-E_{\text{corr}}$ (mV) With Ag/AgCl	$i_{\text{corr}}$ (mA.cm <sup>-2</sup> )	$b_a$ (mV.dec <sup>-1</sup> )	$b_c$ (mV.dec <sup>-1</sup> )	% $I_{\text{PDP}}$	% $I_{\text{EWL}}$
EMDA	Blank	390.251	351.88	102.70	77.70	0	0
	$1 \times 10^{-4}$	364.67	99.61	96.60	77.20	71.69	65.53
	$2 \times 10^{-4}$	305.42	88.15	137.20	40.10	74.95	68.01
	$3 \times 10^{-4}$	330.27	79.78	102.00	101.80	77.33	69.41
	$4 \times 10^{-4}$	390.251	351.88	102.70	77.70	0	0
	$5 \times 10^{-4}$	364.67	99.61	96.60	77.20	71.69	65.53
EBMDA	Blank	390.251	351.88	102.70	77.70	0	0
	$1 \times 10^{-4}$	362.00	122.838	103.90	80.20	65.01	40.94
	$2 \times 10^{-4}$	342.19	96.37	109.60	58.10	72.61	41.34
	$3 \times 10^{-4}$	305.33	91.71	139.10	36.70	73.94	46.12
	$4 \times 10^{-4}$	331.69	80.46	110.80	54.00	77.14	52.16
	$5 \times 10^{-4}$	332.26	78.24	109.60	51.30	77.76	54.31
EBDA	Blank	390.251	351.88	102.70	77.70	0	0
	$1 \times 10^{-3}$	372.66	199.282	96.6	88.6	43.36	44.4
	$2 \times 10^{-3}$	375.429	186.49	106.2	87.8	47.00	47.84
	$3 \times 10^{-3}$	359.12	186.05	105.3	94.5	47.13	49.13
	$4 \times 10^{-3}$	386.132	178.493	96.2	97.8	49.27	49.57
	$5 \times 10^{-3}$	362.01	122.84	103.9	80.2	65.01	50
EBDMDG	Blank	390.251	351.88	102.70	77.70	0	0
	$1 \times 10^{-3}$	396.05	140.72	100.6	113.2	60.01	48.76
	$2 \times 10^{-3}$	374.619	113.214	94.0	86.6	62.14	50.31
	$3 \times 10^{-3}$	450.83	126.09	147.2	199.8	64.17	51.86
	$4 \times 10^{-3}$	407.446	124.653	247.5	237.0	64.57	53.42
	$5 \times 10^{-3}$	423.106	120.03	218.06	232.40	65.90	54.97

**Table 4. 17:** Potentiodynamic polarization (PDP) parameters such as corrosion potential ( $E_{corr}$ ), corrosion current density ( $i_{corr}$ ), and anodic and cathodic Tafel slopes ( $b_a$  and  $b_c$ ) using different inhibitors on Aluminium metal.

Inhibitor	Inhibitor con.(M)	$-E_{corr}$ (mV) With Ag/AgCl	$i_{corr}$ (mA.cm <sup>-2</sup> )	$b_a$ (mV.dec <sup>-1</sup> )	$b_c$ (mV.dec <sup>-1</sup> )	% $I_{E_{PDP}}$	% $I_{E_{WL}}$
EMDA	Blank	349.11	250.02	118.40	68.00	0	0
	$1 \times 10^{-4}$	396.52	92.71	44.20	87.40	62.92	84.74
	$2 \times 10^{-4}$	398.54	87.21	46.10	86.50	65.12	90.79
	$3 \times 10^{-4}$	384.62	83.09	46.4	66.0	66.77	90.89
	$4 \times 10^{-4}$	392.95	82.09	59.5	94.1	67.17	91.58
	$5 \times 10^{-4}$	394.49	76.05	43.2	76.4	69.58	92.89
EBMDA	Blank	349.11	250.02	118.40	68.00	0	0
	$1 \times 10^{-4}$	384.76	119.49	76.4	100.90	52.20	90.79
	$2 \times 10^{-4}$	386.79	100.237	70.4	89.2	59.90	91.05
	$3 \times 10^{-4}$	406.132	102.85	50.40	84.70	58.86	91.84
	$4 \times 10^{-4}$	384.61	93.30	70.40	82.20	62.68	92.11
	$5 \times 10^{-4}$	406.55	84.89	54.90	62.20	66.04	92.37
EBDA	Blank	349.11	250.02	118.40	68.00	0	0
	$1 \times 10^{-3}$	389.28	93.341	85.4	60.10	62.70	85.26
	$2 \times 10^{-3}$	398.46	85.70	64.2	84.60	65.72	86.57
	$3 \times 10^{-3}$	392.91	86.72	56.1	71.40	65.31	89.21
	$4 \times 10^{-3}$	396.59	80.75	49.80	82.80	67.70	90.00
	$5 \times 10^{-3}$	383.92	69.01	47.10	59.70	72.36	92.37
EBDMDG	Blank	349.11	250.02	118.40	68.00	0	0
	$1 \times 10^{-3}$	411.04	95.31	68.20	139.9	61.88	94.74
	$2 \times 10^{-3}$	463.19	74.12	156.70	220.9	70.36	96.58
	$3 \times 10^{-3}$	469.68	68.45	117.40	168.00	72.62	97.37
	$4 \times 10^{-3}$	457.302	67.940	155.70	200.10	72.83	97.63
	$5 \times 10^{-3}$	459.53	63.93	122.90	65.30	74.43	97.89

From Tables 7.17 and 7.18 it can be observed that  $I_{corr}$  decrease with an increase in all four inhibitors concentration, when  $I_{corr}$  decreases this means that the rate of electrochemical reaction was reduced due to the formation of a barrier layer over zinc and aluminium surface through the adsorption of inhibitors. % $I_{E_{PDP}}$  increases with the decrease in  $I_{corr}$ , it expresses the same trend as % $I_{E_{WL}}$  increases with an increase in the concentration of inhibitors. The  $E_{corr}$  in the blank is lower than when inhibitor is introduced. If cathodic and anodic reactions are affected by the inhibitor, the inhibitor is considered a mixed type corrosion inhibitor but if the shift in  $E_{corr}$  in the presence of inhibitor is greater

than 85mV with respect to that of blank it is classified as a cathodic or anodic inhibitor<sup>83</sup>. In this study, all four inhibitors are mixed-type inhibitors. In table 7.17 the highest corrosion inhibition efficiency obtained in PDP was 83.47% which was composed of EMDA inhibitor, same as in gravimetric analysis. For aluminum in table 7.18 the highest %IE<sub>PDP</sub> was 74.43% for EBDMDA inhibitor.

# CHAPTER 5

## CONCLUSIONS

## 5.1. Conclusions

The aim of this study was achieved. The TZD derivatives namely EMDA, EBMDA, EBDA, and EBDMDG were successfully synthesized and characterized. The synthesised compounds were tested for corrosion as corrosion inhibitors of Zn and Al in 1.5M HCl at different temperatures. From the gravimetric analysis, the highest corrosion inhibition efficiency was obtained at the highest concentration for all four inhibitors. The ideal time for obtaining highest %IE for Zn was 6 hours and Al was for 3hours. An increase in temperature in temperature is known as the factor that leads to corrosion of materials, the effect of temperature on %IE for Zn and Al was studied and the results obtained indicate the different trend of %IE. %IE for Zn in the presence of EBMDA, EBDA, and EBDMDG increases with an increase in temperature while in the presence of EMDA act inversely proportional to temperature. For Al, the %IE for both four inhibitors acts opposite to that of Zn metal.

Thermodynamic and kinetics results obtained for corrosion and corrosion inhibition for Zn and Al revealed that the action of adsorption of both inhibitors for Zn indicates physisorption process and for aluminium in the presence of EMDA inhibitors indicates chemisorption process while in the presence of EBMDA, EBDA, and EBDMDG revealed physisorption process. Kinetics study revealed that the activation energy in the presence of EMDA is higher than that without the inhibitor, in the presence of EBMDA, EBDA, and EBDMDG the activation energy for zinc is lower than that in the blank. While the activation energy of both inhibitors for aluminum is lower than that in the blank.

Electrochemical studies (EIS and PDP) were used to characterize the inhibitory action. EIS fit was used to analyze the data, Nyquist and Bode plots were achieved and an electrical circuit model was developed to explain the inhibition action of the inhibitors. Charge transfer resistance is directly proportional to the concentration of the inhibitors. PDP Tafel systems bring about the behaviour on anodic and cathodic sides on zinc and aluminum sheets. The rate of electrochemical reaction was reduced due to the formation of a barrier layer over zinc and aluminium surface through the adsorption of inhibitors, this is because the corrosion current obtained decreases with an increase in concentration inhibitors.



## 5.2. RECOMMENDATIONS

The research presented in this dissertation advocates the use of thiazolidinediones derivatives as corrosion inhibitors of zinc and aluminium in 1.5M HCl. It recommends that the surface morphology interface interaction between the inhibitors and metal surface should be studied. For future work, it can also be recommended that quantum chemical studies be done using the same compounds that are employed in this study.

## REFERENCES

1. Shreir, L.L. ed. *Corrosion: metal/environment reactions*. Newnes, 2013.
2. Uhug, H.H. "Why Metals Corrode." *Corrosion* 5.6 (1949): 169-174.
3. Li, W.H., He, Q., Zhang, S.T., Pei, C.L. and Hou, B.R. "Some new triazole derivatives as inhibitors for mild steel corrosion in acidic medium." *Journal of Applied Electrochemistry* 38.3 (2008): 289-295.
4. Oki, M. and Anawe, P.A. "A review of corrosion in agricultural industries." *Physical Science International Journal* (2015): 216-222.
5. Eker, B., and Yuksel, E. "Solutions to corrosion caused by agricultural chemicals." *Trakia Journal of Sciences* 3.7 (2005): 1-6.
6. Koch, G., Varney, J., Thompson, N., Moghissi, O., Gould, M. and Payer, J International Measures of Prevention, Application, and Economics of Corrosion Technologies Study. NACE Int. 2016.
7. Verma, C., Olasunkanmi, L.O., Ebenso, E.E. and Quraishi, M.A. "Substituents effect on corrosion inhibition performance of organic compounds in aggressive ionic solutions: a review." *Journal of Molecular Liquids* 251 (2018): 100-118.
8. Dearnley, P.A. and Aldrich-Smith, G. "Corrosion–wear mechanisms of hard coated austenitic 316L stainless steels." *Wear* 256.5 (2004): 491-499.
9. Revie, R. Winston. *Corrosion and corrosion control: an introduction to corrosion science and engineering*. John Wiley & Sons, 2008.
10. Sastri, Vedula S. *Corrosion inhibitors: principles and applications*. No. Sirsi) i9780471976080. New York: Wiley, 1998.
11. Hart, E. *Corrosion Inhibitors: Principles, Mechanisms and Applications*. Corrosion.Inhibitor.Principle.Mechanism.Appliction. (2016):367–373.
12. Loto, C. A., Loto, R.T. and Popoola, A.P.I. "Corrosion inhibition of thiourea and thiadiazole derivatives: a review." *Journal of Materials and Environmental Science* 3.5 (2012): 885-894

13. Obot, I. B., Obi-Egbedi, N.O. and Umoren, S.A. "Adsorption characteristics and corrosion inhibitive properties of clotrimazole for aluminium corrosion in hydrochloric acid." *International Journal Electrochemical of Science* 4.6 (2009): 863-877.
14. Stupnišek-Lisac, E., Podbršček, S. and Sorić, T. "Non-toxic organic zinc corrosion inhibitors in hydrochloric acid." *Journal of Applied Electrochemistry* 24.8 (1994): 779-784.
15. Raps, D., Hack, T., Wehr, J., Zheludkevich, M.L, Bastos, A.C, Ferreira, M. G. S and Nuyken, O. J. C. S. "Electrochemical study of inhibitor-containing organic-inorganic hybrid coatings on AA2024." *Corrosion Science* 51.5 (2009): 1012-1021.
16. Gaidis, J.M. "Chemistry of corrosion inhibitors." *Cement and Concrete Composites* 26.3 (2004): 181-189.
17. Parham, H., Zargar, B and Shiralipour, R. "Fast and efficient removal of mercury from water samples using magnetic iron oxide nanoparticles modified with 2-mercaptobenzothiazole." *Journal of hazardous materials* 205 (2012): 94-100.
18. Najjar, Yousef SH. "Gaseous pollutants formation and their harmful effects on health and environment." *Innovative energy policies* 1 (2011): 1-9.
19. Popov, B.N. *Corrosion engineering: principles and solved problems*. Elsevier, 2015.
20. Shaw, B.A. and Kelly, R.G. "What is corrosion?." *Interface-Electrochemical Society* 15.1 (2006): 24-27.
21. Trethewey, K. R., and Chamberlain, J. "Corrosion for science and engineering." (1995).
22. Tang, Z. "A review of corrosion inhibitors for rust preventative fluids." *Current Opinion in Solid State and Materials Science* 23.4 (2019): 100759.
23. Saha, S.K., Ghosh, P., Hens, A., Murmu, N.C. and Banerjee, P. "Density functional theory and molecular dynamics simulation study on corrosion inhibition performance of mild steel by mercapto-quinoline Schiff base corrosion inhibitor." *Physica E: Low-dimensional systems and nanostructures* 66 (2015): 332-341.

24. Zhang, J., Hosemann, P. and Maloy, S. "Models of liquid metal corrosion." *Journal of Nuclear Materials* 404.1 (2010): 82-96.
25. Zelinka, S. L., and Stone, D.S. "Corrosion of metals in wood: Comparing the results of a rapid test method with long-term exposure tests across six wood treatments." *Corrosion Science* 53.5 (2011): 1708-1714
26. Haridas, V., Sankaran S. "Corrosion by other gas." *Journal of Solid State Chemistry* 262: 2016.
27. De Rosa, L., Tomachuk, C. R. Springer, J., Mitton, D. B. Saiello, S. and Bellucci, F. "The wet corrosion of molybdenum thin film— Part I: Behavior at 25° C." *Materials and corrosion* 55.8 (2004): 602-609.
28. Kamimura, T., Nasu, S., Segi, T., Tazaki, T., Morimoto, S. and Miyuki, H. "Corrosion behavior of steel under wet and dry cycles containing Cr<sup>3+</sup> ion." *Corrosion science* 45.8 (2003): 1863-1879.
29. Bushman, J.B. and Engineer, P.P. "Calculation of Corrosion Rate from Corrosion Current (Faraday's Law)." *Bushman & Associates Inc* (2000).
30. Gonzalez, J. A., Andrade, C., Alonso, C. and Feliu, S. "Comparison of rates of general corrosion and maximum pitting penetration on concrete embedded steel reinforcement." *Cement and concrete research* 25.2 (1995): 257-264.
31. Jia, J.X., Song, G. and Atrens, A. "Influence of geometry on galvanic corrosion of AZ91D coupled to steel." *Corrosion Science* 48.8 (2006): 2133-2153.
32. Perez, N. *Electrochemistry and corrosion science*. Vol. 412. Boston: Kluwer academic publishers, 2004.
33. Robineau, M., Romaine, A., Sabot, R., Jeannin, M., Deydier, V., Necib, S. and Refait, P. "Galvanic corrosion of carbon steel in anoxic conditions at 80° C associated with a heterogeneous magnetite (Fe<sub>3</sub>O<sub>4</sub>)/mackinawite (FeS) layer." *Electrochimica Acta* 255 (2017): 274-285.

34. Hernandez, S., Hassani, S. and Nassef, A.S. "Erosion–corrosion." *Trends in Oil and Gas Corrosion Research and Technologies* (2017): 341-362.
35. Rajahram, S. S., Harvey, T.J. and Wood, R.J.K. "Erosion–corrosion resistance of engineering materials in various test conditions." *Wear* 267.1-4 (2009): 244-254.
36. Toor, I.U., Irshad, H.M., Badr, H.M. and Samad, M.A. "The effect of impingement velocity and angle variation on the erosion corrosion performance of API 5L-X65 carbon steel in a flow loop." *Metals* 8.6 (2018): 402.
37. Makhoulouf, A.S.H. "Intelligent stannate-based coatings of self-healing functionality for magnesium alloys." *Intelligent Coatings for Corrosion Control*. Butterworth-Heinemann, (2015): 537-555.
38. Boag, A., E. Hughes, A. M. Glenn, T. H. Muster, and D. McCulloch. "Corrosion of AA2024-T3 Part I: Localised corrosion of isolated IM particles." *Corrosion Science* 53.1 (2011): 17-26.
39. Hribšek, U. "Introduction to corrosion." *The Electrochemical Society Interface* (2014).
40. Wharton, J.A. and Stokes, K.R. "The influence of nickel–aluminium bronze microstructure and crevice solution on the initiation of crevice corrosion." *Electrochimica Acta* 53.5 (2008): 2463-2473.
41. Jung, J.Y., Park, S.Y., Won, H.J., Choi, W.K., Moon, J.K. and Park, S.J. "Crevice Corrosion Properties of PWR Structure Materials Under Reductive Decontamination Conditions." *Journal of Nuclear Fuel Cycle and Waste Technology (JNFCWT)* 12.3 (2014): 199-209.
42. Yepez, O., Obeyesekere, N. and Wylde, J. "On the Anodic reaction of the CO<sub>2</sub> corrosion process." *NACE International Corrosion Conference Proceedings*. NACE International, 2019.
43. Electric Power Research Institute, et al. *Cost of corrosion in the electric power industry*. Electric Power Research Institute, 2001.

44. Syrett, B.C. and Gorman, J.A. "Cost of corrosion in the electric power industry: An update." *Materials performance* 42.2 (2003): 32-38.
45. Foka, F.E.T., Yah, C.S. and Agbortabot Bissong, M.E. "Physico-chemical properties and microbiological quality of borehole water in four crowded areas of Benin City, Nigeria, during rainfalls." *Shiraz E-Medical Journal* 19.11 (2018).
46. Salgar Chaparro, Silvia Juliana. *Understanding of Microbiologically Influenced Corrosion in Carbon Steel Pipelines: Towards Developing a Methodology to Assess Probability of Failure*. Diss. Curtin University, 2020.
47. Hope, B.B., Page, J.A. and Ip, A.K. "Corrosion rates of steel in concrete." *Cement and Concrete Research* 16.5 (1986): 771-781.
48. McGowan, J.G., Hyers, R.W., Sullivan, K.L., Manwell, J.F., Nair, S.V., McNiff, B. and Syrett, B.C. "A review of materials degradation in utility scale wind turbines." *Energy Materials* 2.1 (2007): 41-64.
49. Roberge, Pierre R. *Corrosion engineering*. McGraw-Hill Education, 2008.
50. Shreir, L.L. ed. *Corrosion: metal/environment reactions*. Newnes, 2013.
51. Angst, Ueli M., Mette R. Geiker, Maria Cruz Alonso, Rob Polder, O. Burkan Isgor, Bernhard Elsener, Hong Wong. "The effect of the steel–concrete interface on chloride-induced corrosion initiation in concrete: a critical review by RILEM TC 262-SCI." *Materials and Structures* 52.4 (2019): 1-25.
52. Altwaiq, A.M. and Abdel-Rahem, R.A. "Reaction between Zinc and Hydrochloric Acid in Solutions Containing Alkyltrimethylammonium Bromide CnTAB (n= 8, 10, and 12) Cationic Surfactants: Influence of Surfactant Chain Length." *Journal of Surfactants and Detergents* 22.4 (2019): 845-853.
53. Mingo, B., Arrabal, R., Mohedano, M., Llamazares, Y., Matykina, E., Yerokhin, A. and Pardo, A. "Influence of sealing post-treatments on the corrosion resistance of PEO coated AZ91 magnesium alloy." *Applied Surface Science* 433 (2018): 653-667.

54. Wang, Y., Liu, M., Liu, F., Zhao, C., Zhao, D., Han, F. and Liu, C. "Research on the effect of wall corrosion and rim seal on the withdrawal loss for a floating roof tank." *Environmental Science and Pollution Research* 25.19 (2018): 18434-18442.
55. Abdel-Gaber, A.M., Abd-El Nabey, B.A., Sidahmed, I.M., El-Zayady, A.M. and Saadawy, M. "Effect of temperature on inhibitive action of damsissa extract on the corrosion of steel in acidic media." *Corrosion* 62.4 (2006): 293-299.
56. Gupta, A., Anand, Y., Tyagi, S.K. and Anand, S. "Economic and thermodynamic study of different cooling options: A review." *Renewable and Sustainable Energy Reviews* 62 (2016): 164-194.
57. Piippo, J., Laitinen, T. and Sirkiä, P. "Corrosion behaviour of zinc and aluminium in simulated nuclear accident environments." (1997).
58. Yuan Ma, F. "Corrosive effects of chlorides on metals." *Pitting Corrosion. China: In Technology.* (2012).
59. Nwanonenyi, S.C., Obasi, H.C., Oguzie, E.E., Chukwujike, I.C. and Anyiam, C.K. "Inhibition and adsorption of polyvinyl acetate (PVAc) on the corrosion of aluminium in sulphuric and hydrochloric acid environment." *Journal of Bio-and Tribo-Corrosion* 3.4 (2017): 1-13.
60. Ambat, R., Davenport, A.J., Scamans, G.M. and Afseth, A. "Effect of iron-containing intermetallic particles on the corrosion behaviour of aluminium." *Corrosion science* 48.11 (2006): 3455-3471.
61. Huang, C.S., Wu, J.Y., Ding, M., Xu, H.W., Zhang, M., Chen, M., Xue, M., Zhang, X.G. and Tian, K.P. "Study on Corrosion of Zinc Metal in Acid Environment." *2018 7th International Conference on Energy and Environmental Protection (ICEEP 2018).* Atlantis Press, 2018.
62. Thomas, S., Birbilis, N., Venkatraman, M.S. and Cole, I.S. "Corrosion of zinc as a function of pH." *Corrosion, The Journal of Science and Engineering* 68.1 (2012): 015009-1.



63. Neufeld, A.K., Cole, I.S., Bond, A.M. and Furman, S.A. "The initiation mechanism of corrosion of zinc by sodium chloride particle deposition." *Corrosion Science* 44.3 (2002): 555-572.
64. Thim, G.P., Oliveira, M.A., Oliveira, E.D. and Melo, F.C. "Sol-gel silica film preparation from aqueous solutions for corrosion protection." *Journal of non-crystalline solids* 273.1-3 (2000): 124-128.
65. De Damborenea, J., A. Conde, and M. A. Arenas. "Corrosion inhibition with rare earth metal compounds in aqueous solutions." *Rare Earth-based Corrosion Inhibitors*. Woodhead Publishing, 2014. 84-116.
66. Grundmeier, Guido, W. Schmidt, and M. J. E. A. Stratmann. "Corrosion protection by organic coatings: electrochemical mechanism and novel methods of investigation." *Electrochimica Acta* 45.15-16 (2000): 2515-2533.
67. Hammache, H., L. Makhloufi, and B. Saidani. "Corrosion protection of iron by polypyrrole modified by copper using the cementation process." *Corrosion science* 45.9 (2003): 2031-2042.
68. Zaarei, D., Sarabi, A.A., Sharif, F. and Kassiriha, S.M. "Structure, properties and corrosion resistivity of polymeric nanocomposite coatings based on layered silicates." *Journal of Coatings Technology and Research* 5.2 (2008): 241-249.
69. Bertolini, L., Bolzoni, F., Pedferri, P., Lazzari, L. and Pastore, T. "Cathodic protection and cathodic prevention in concrete: principles and applications." *Journal of applied Electrochemistry* 28.12 (1998): 1321-1331.
70. Zhu, J.H., Su, M.N., Huang, J.Y., Ueda, T. and Xing, F. "The ICCP-SS technique for retrofitting reinforced concrete compressive members subjected to corrosion." *Construction and Building Materials* 167 (2018): 669-679.
71. Olasunkanmi, L.O., Obot, I.B., Kabanda, M.M. and Ebenso, E.E. "Some quinoxalin-6-yl derivatives as corrosion inhibitors for mild steel in hydrochloric acid: experimental and theoretical studies." *The Journal of Physical Chemistry C* 119.28 (2015): 16004-16019.

72. Papavinasam, S., Revie, R.W., Attard, M., Demoz, A. and Michaelian, K. "Comparison of laboratory methodologies to evaluate corrosion inhibitors for oil and gas pipelines." *Corrosion* 59.10 (2003).
73. Murulana, L.C., Kabanda, M.M. and Ebenso, E.E. Experimental and theoretical studies on the corrosion inhibition of mild steel by some sulphonamides in aqueous HCl. *RSC Advances*, 5(36) (2015): 22-26.
74. Nanjan, M.J., Mohammed, M., Kumar, B.P. and Chandrasekar, M.J.N. "Thiazolidinediones as antidiabetic agents: a critical review." *Bioorganic chemistry* 77 (2018): 548-567.
75. Guja, C. and Miulescu, R.D. "Heart failure in type 2 diabetes—the “forgotten” complication." *Romanian Journal of Diabetes Nutrition and Metabolic Diseases* 25.2 (2018): 123-130.
76. Jerry, R., and Chisholm, D.J. "Thiazolidinediones-mechanisms of action." *Australia Prescriber* 27 (2004): 67-70.
77. Vellalacheruvu, R., Leela, R.S. and Ravindranath, L.K. "Novel Route for Synthesis of Thiozolidine-2, 4-Dione Derivatives as a Mannich Base." *International Journal of Organic Chemistry* 7.3 (2017): 269-283.
78. Mendoza G., Hernández, H., Quintero, L., Sosa-Rivadeneira, M., Bernes, S., Sansinenea, E. and Ortiz, A. "Synthesis of N-substituted 2, 4-thiazolidinediones from oxazolidinethiones." *Tetrahedron letters* 46.46 (2005): 7867-7870.
79. Mudaliar, S. and Henry, R.R. "New oral therapies for type 2 diabetes mellitus: the glitazones or insulin sensitizers." *Annual review of medicine* 52.1 (2001): 239-257.
80. Abdallah, M., I. A. Zaafarany, and B. A. Al Jahdaly. "Corrosion inhibition of zinc in hydrochloric acid using some antibiotic drugs." *Journal. Mater Environment. Science* 7.4 (2016): 1107-1118.
81. Langill, T. J., in *ASM Handbook*, Vol. 13A, Corrosion: Fundamentals, Testing, and Protection, ASM International, Materials Park, OH, (2003). 801.

82. Alapafuja, S.O., Nikas, S.P., Shukla, V.G., Papanastasiou, I. and Makriyannis, A. "Microwave-assisted synthesis of sodium sulfonates precursors of sulfonyl chlorides and fluorides." *Tetrahedron letters* 50.50 (2009): 7028-7031.
83. Ghazoui, A., Bencaht, N., Al-Deyab, S.S., Zarrouk, A., Hammouti, B., Ramdani, M. and Guenbour, M. "An Investigation of two novel pyridazine derivatives as corrosion inhibitor for C38 steel in 1.0 M HCl." *Interntional.Journal.Electrochemical.Science* 8. (2013).
84. Meng, G., Zheng, M., Dong, M., Gao, Y., Zheng, A., Li, Z. and Hu, R "Synthetic optimization of rosiglitazone and related intermediates for industrial purposes." *Research on Chemical Intermediates* 42.3 (2016): 2023-2033.
85. Swathi, N., Ramu, Y., Subrahmanyam, C.V.S. and Satyanarayana, K "Synthesis, quantum mechanical calculation and biological evaluation of 5-(4-substituted aryl/hetero aryl methyldene)-1, 3-thiazolidine-2, 4-diones." *Interntional. Journal. Pharmacy. Sci* 4 (2012): 561-566.
86. Tshiluka, N.R. *Synthesis of Glitazone Analogues as Anti-Diabetic Drugs*. Msc Dissertation, submitted to University of Venda. 2018.
87. Fones, W.S., Marguerite L. "Hydrolysis of N-acyl derivatives of alanine and phenylalanine by acylase I and carboxypeptidase." *Journal of Biological Chemistry* 201.2 (1953): 847-856.
88. Patil, V., Tilekar, K., Mehendale-Munj, S., Mohan, R. and Ramaa, C.S. "Synthesis and primary cytotoxicity evaluation of new 5-benzylidene-2, 4-thiazolidinedione derivatives." *European journal of medicinal chemistry* 45.10 (2010): 4539-4544.
89. Pasupathy, A., Nirmala, S., Sakthivel, P., Abirami, G. and Raja, M. "Diphenyl Sulphide as Corrosion Inhibitor for Zinc Metal in Acid Solutions." *International Journal of Scientific and Research Publications* (2014): 497.
90. Li, X., Deng, S. and Fu, H. "Inhibition of the corrosion of steel in HCl, H<sub>2</sub>SO<sub>4</sub> solutions by bamboo leaf extract." *Corrosion Science* 62 (2012): 163-175.

91. Ismaily Alaoui, K., El Hajjaji, F., Azaroual, M., Taleb, M., Chetouani, A., Hammouti, B., Abridgach, F., Khoutoul, M., Abboud, Y., Aouniti, A. and Touzani, R. "Experimental and quantum chemical studies on corrosion inhibition performance of pyrazolic derivatives for mild steel in hydrochloric acid medium, correlation between electronic structure and inhibition efficiency." *Journal of Chemical and Pharmaceutical Research* 6.7 (2014): 63-81.
92. Hmamou, D.B., Salghi, R., Zarrouk, A., Zarrok, H., Al-Deyab, S.S., Benali, O. and Hammouti, B. "The inhibited effect of phenolphthalein towards the corrosion of C38 steel in hydrochloric acid." *International. Journal. Electrochemical. Science.* 7 (2012): 8988-9003.
93. Singh, A. K., Quraishi, M. A. "Adsorption properties and inhibition of mild steel corrosion in hydrochloric acid solution by ceftobiprole." *Journal of Applied Electrochemistry* 41.1 (2011): 7-18.
94. Lee, S., Ford, A.K., Mangubhai, S., Wild, C. and Ferse, S.C. "Effects of sandfish (*Holothuria scabra*) removal on shallow-water sediments in Fiji." *PeerJ* 6 (2018): e4773.
95. Nmai, Charles K. "Multi-functional organic corrosion inhibitor." *Cement and Concrete Composites* 26.3 (2004): 199-207.
96. Ormellese, M., Lazzari, L., Goidanich, S., Fumagalli, G. and Brenna, A. "A study of organic substances as inhibitors for chloride-induced corrosion in concrete." *Corrosion Science* 51.12 (2009): 2959-2968.
97. Kuznetsov, Yurii I., J. G. N. Thomas, and A. D. Mercer. *Organic inhibitors of corrosion of metals*. Springer Science & Business Media, 1996.
98. Kumari, P.P., Shetty, P. and Rao, S.A. "Electrochemical measurements for the corrosion inhibition of mild steel in 1 M hydrochloric acid by using an aromatic hydrazide derivative." *Arabian Journal of Chemistry* 10.5 (2017): 653-663.

99. Hamdy, AS, El-Shenawy E, El-Bitar. "Electrochemical impedance spectroscopy study of the corrosion behavior of some niobium bearing stainless steels in 3.5% NaCl." *International Journal of Electrochemical Science* 1.4 (2006): 171-180.
100. Cui, Z, Wang, L., Zhong, M., Ge, F., Gao, H., Man, C., Liu, C. and Wang, X "Electrochemical behavior and surface characteristics of pure titanium during corrosion in simulated desulfurized flue gas condensates." *Journal of The Electrochemical Society* 165.9 (2018):542.
101. Tebbji, K., Hammouti, B., Oudda, H., Ramdani, A. and Benkadour, M. "The inhibitive effect of bipyrazolic derivatives on the corrosion of steel in hydrochloric acid solution." *Applied surface science* 252.5 (2005): 1378-1385.
102. Manamela, K.M., Murulana, L.C., Kabanda, M.M. and Ebenso, E.E. "Adsorptive and DFT studies of some imidazolium based ionic liquids as corrosion inhibitors for zinc in acidic medium." *International Journal of Electrochemical Science* 9 (2014): 3029-3046.
103. Zarrouk, A., Warad, I., Hammouti, B., Dafali, A., Al-Deyab, S.S. and Benchat, N. "The effect of temperature on the corrosion of Cu/HNO<sub>3</sub> in the presence of organic inhibitor: part-2." *International Journal of Electrochemical Science* 5.10 (2010): 1516-26.